



City Research Online

City, University of London Institutional Repository

Citation: Vita, Vasiliki (2016). Electricity distribution networks' analysis with particular references to distributed generation and protection. (Unpublished Doctoral thesis, City University London)

This is the accepted version of the paper.

This version of the publication may differ from the final published version.

Permanent repository link: <https://openaccess.city.ac.uk/id/eprint/15180/>

Link to published version:

Copyright: City Research Online aims to make research outputs of City, University of London available to a wider audience. Copyright and Moral Rights remain with the author(s) and/or copyright holders. URLs from City Research Online may be freely distributed and linked to.

Reuse: Copies of full items can be used for personal research or study, educational, or not-for-profit purposes without prior permission or charge. Provided that the authors, title and full bibliographic details are credited, a hyperlink and/or URL is given for the original metadata page and the content is not changed in any way.

City Research Online:

<http://openaccess.city.ac.uk/>

publications@city.ac.uk



**Electricity distribution networks' analysis
with particular references to distributed
generation and protection**

A thesis submitted to
CITY UNIVERSITY LONDON
for the Degree of
DOCTOR OF PHILOSOPHY

By

Vasiliki Vita

School of Engineering and Mathematical Sciences
Department of Electrical and Electronic Engineering

City University
London EC1V 0HB
United Kingdom

May 2016

Table of Contents

| | |
|--|-----------|
| Table of Contents | 2 |
| Acknowledgments | 5 |
| List of Abbreviations | 6 |
| List of Figures | 7 |
| List of Tables | 13 |
| Copyright Declaration | 14 |
| Abstract | 15 |
| 1. Introduction | 16 |
| 1.1 Background | 16 |
| 1.2 Thesis Objectives | 17 |
| 1.3 Outline of the Thesis | 18 |
| 1.4 Contribution | 20 |
| 1.5 List of Author's Publications | 21 |
| 2. Electricity Distribution Networks | 23 |
| 2.1 Introduction | 23 |
| 2.2 Electric Power Systems | 23 |
| 2.3 Distribution Networks | 26 |
| 2.3.1 Radial Distribution Configuration | 26 |
| 2.3.2 Loop Distribution Configuration | 27 |
| 2.3.3 Network Distribution Configuration | 28 |
| 2.3.4 Power Losses | 28 |
| 2.3.5 Voltage Drop | 29 |
| 2.4 Distributed Generation | 29 |
| 2.4.1 DG definition | 32 |
| 2.4.2 Distributed Generation Benefits | 33 |
| 2.4.3 Distributed Generation Drawbacks | 34 |
| 2.4.4 Issues arising from Distributed Generation use | 35 |
| 2.5 Conclusions | 37 |
| 2.6 References | 37 |

| | |
|--|-----------|
| 3. Voltage Profiles and Power Losses in Distribution Networks with Distributed Generation | 39 |
| 3.1 Introduction | 39 |
| 3.2 Literature Review | 39 |
| 3.3 The Impact of Distributed Generation in Voltage Profile and Power Losses | 43 |
| 3.3.1 Voltage Profile | 43 |
| 3.3.2 Power Losses | 43 |
| 3.4 Voltage Profile and Power Losses Studies on Distribution Networks with Distributed Generation | 44 |
| 3.4.1 Simulation Process | 44 |
| 3.4.2 IEEE 14-Bus Network System | 45 |
| 3.4.2.1 System Description | 45 |
| 3.4.2.2 Simulation Results | 47 |
| 3.4.3 IEEE 33-Bus Radial Distribution System | 55 |
| 3.4.3.1 System Description | 55 |
| 3.4.3.2 Simulation Results | 56 |
| 3.5 Development of a Decision Making Algorithm for the Optimum Size and Placement of DG in Distribution Networks | 69 |
| 3.6 Conclusions | 71 |
| 3.7 References | 71 |
| 4. Syntactic Pattern Recognition of Power System Signals | 73 |
| 4.1 Introduction | 73 |
| 4.2 Research Incentives | 73 |
| 4.3 Literature Review | 76 |
| 4.3.1 Languages and Grammars | 76 |
| 4.3.1.1 Context Free Grammars | 76 |
| 4.3.1.2 Augmenting Context Free Grammars | 77 |
| 4.3.2 Parsing Algorithms and Implementations | 77 |
| 4.3.2.1 Earley's Parsing Algorithm | 79 |
| 4.3.2.2 Hardware Implementations | 80 |

| | | |
|-----------|---|------------|
| 4.4 | The Syntactic Approach in Power System Signals | 81 |
| 4.4.1 | Primitive Pattern Selection | 81 |
| 4.4.2 | Linguistic Representation | 83 |
| 4.4.3 | Pattern Grammar AG_{PSW} | 83 |
| 4.5 | System Description | 85 |
| 4.5.1 | The Combinatorial Parser | 87 |
| 4.5.2 | Extended Parallel Parser | 88 |
| 4.6 | Results | 97 |
| 4.7 | Conclusions | 101 |
| 4.8 | References | 101 |
| 5. | Lightning Protection of Modern Distribution Networks | 104 |
| 5.1 | Introduction | 104 |
| 5.2 | Literature Review | 105 |
| 5.3 | Modern Distribution Network Configuration | 108 |
| 5.3.1 | Distribution Lines | 108 |
| 5.3.2 | Shield Wires | 111 |
| 5.3.3 | Metal Oxide Surge Arresters | 111 |
| 5.3.4 | Distributed Generation Units | 115 |
| 5.4 | Lightning Protection Studies for Modern Distribution Networks | 116 |
| 5.4.1 | System Configuration | 116 |
| 5.4.2 | Sensitivity Analysis for Lightning Strike Hit Position | 118 |
| 5.4.3 | Sensitivity Analysis for Lightning Current Peak Magnitude | 125 |
| 5.4.4 | Sensitivity Analysis for Surge Arresters Models | 130 |
| 5.4.5 | Sensitivity Analysis for Distributed Generation Sizes | 134 |
| 5.5 | Conclusions | 141 |
| 5.6 | References | 142 |
| 6. | Conclusions | 145 |
| 6.1 | Conclusions | 145 |
| 6.2 | Contribution | 146 |
| 6.3 | Further Work | 149 |

Acknowledgments

The completion of this thesis would not have been possible without the support of my supervisor, who guided and encouraged me, the City University London, providing me with the financial means to complete this research, my family and friends, who endured this long process with me, always offering support and love.

List of Abbreviations

| | |
|------|---|
| AG | Attribute Grammars |
| CFG | Context Free Grammars |
| CNF | Chomsky Normal Form |
| CT | Current Transformer |
| CVT | Capacitor Voltage Transformer |
| CYK | Cocke-Younger-Kasami |
| DECC | Department of Energy and Climate Change |
| DG | Distributed Generation |
| ECG | ElectroCardioGram |
| EHV | Extra-High Voltage |
| EPRI | Electric Power Research Institute |
| FPGA | Field Programmable Gate Arrays |
| FSM | Finite State Machine |
| HDL | Hardware Description Language |
| HV | High Voltage |
| IPTO | Independent Power Transmission Operator |
| LHS | Left Hand Side |
| lhss | left hand side symbol |
| PV | Photovoltaic |
| RHS | Right Hand Side |
| rhss | right hand side symbols |
| SCFG | Stochastic Context Free Grammar |
| SPR | Syntactic Pattern Recognition |
| UHV | Ultra-High Voltage |

List of Figures

- Figure 2.1:** Electric power system.
- Figure 2.2:** The radial distribution configuration.
- Figure 2.3:** The loop distribution configuration.
- Figure 2.4:** The network distribution configuration.
- Figure 2.5:** DG technologies.
- Figure 2.6:** Traditional and current electric power systems.
- Figure 3.1:** Single line diagram of the IEEE 14-Bus Network System.
- Figure 3.2:** Single line diagram of the IEEE 14-Bus Network System in NEPLAN.
- Figure 3.3:** Voltage profiles of the 13.8 kV buses when a DG PV unit has been connected at bus 6.
- Figure 3.4:** Voltage profiles of the 13.8 kV buses when a DG PV unit has been connected at bus 12.
- Figure 3.5:** Voltage profiles of the 13.8 kV buses when a DG wind generator unit has been connected at bus 6.
- Figure 3.6:** Voltage profiles of the 13.8 kV buses when a DG wind generator unit has been connected at bus 12.
- Figure 3.7:** Total network real power losses when DG PV units have been connected at different buses.
- Figure 3.8:** Total network reactive power losses when DG PV units have been connected at different buses.
- Figure 3.9:** Total network apparent power losses when DG PV units have been connected at different buses.
- Figure 3.10:** Total network real power losses when DG wind generator units have been connected at different buses.

Figure 3.11: Total network reactive power losses when DG wind generator units have been connected at different buses.

Figure 3.12: Total network apparent power losses when DG wind generator units have been connected at different buses.

Figure 3.13: Single line diagram of the IEEE 33-bus radial distribution system.

Figure 3.14: Single line diagram of IEEE 33-bus radial distribution system in NEPLAN.

Figure 3.15: Voltage profiles of network buses when a DG PV unit has been connected at bus 6.

Figure 3.16: Voltage profiles of network buses when a DG PV unit has been connected at bus 18.

Figure 3.17: Voltage profiles of network buses when a DG PV unit has been connected at bus 33.

Figure 3.18: Voltage profiles of network buses when a DG wind generator unit has been connected at bus 6.

Figure 3.19: Voltage profiles of network buses when a DG wind generator unit has been connected at bus 18.

Figure 3.20: Voltage profiles of network buses when a DG wind generator unit has been connected at bus 33.

Figure 3.21: Total network real power losses when DG PV units have been connected at different buses.

Figure 3.22: Total network reactive power losses when DG PV units have been connected at different buses.

Figure 3.23: Total network apparent power losses when DG PV units have been connected at different buses.

Figure 3.24: Total network real power losses when DG wind generator units have been connected at different buses.

Figure 3.25: Total network reactive power losses when DG wind generator units have been connected at different buses.

Figure 3.26: Total network apparent power losses when DG wind generator units have been connected at different buses.

Figure 3.27: The flow chart of the proposed decision making algorithm.

Figure 4.1: Positive and negative peak patterns.

Figure 4.2: Main tasks of the proposed system.

Figure 4.3: Parsing architecture presented in [21] for $n=3$.

Figure 4.4: Abstract implementation of the combinational circuit C_{\otimes} architecture.

Figure 4.5: Flow chart of the parse tree construction algorithm.

Figure 4.6: Parse tree traversal.

Figure 4.7: Semantic Evaluator architecture.

Figure 4.8: Subset of data provided by IPTO.

Figure 4.9: Examined waveform subset.

Figure 4.10: Parse tree for input string pnpnpnpn.

Figure 4.11: Noise (error) evaluation by gradually recognizing substrings.

Figure 4.12: Performance evaluation of recognizing 50 peaks.

Figure 5.1: The PI model.

Figure 5.2: Two-port equivalent circuit model of a line.

Figure 5.3: Metal oxide surge arrester cut (1: electrodes, 2: fiber glass, 3: varistor column, 4: external insulator).

Figure 5.4: The IEEE model.

Figure 5.5: The Pinceti-Gianettoni model.

Figure 5.6: The Fernandez-Diaz model.

Figure 5.7: Unshielded wooden pole of a typical 20 kV distribution line.

Figure 5.8: Simulation model of unshielded distribution network with DGs.

Figure 5.9: Simulation model of distribution line with DG that is hit in position A.

Figure 5.10: Developed overvoltage at position A, for lightning hit at position A, in relation to grounding resistance.

Figure 5.11: Developed overvoltage at position B, for lightning hit at position A, in relation to grounding resistance.

Figure 5.12: Developed overvoltage at position C, for lightning hit at position A in relation to grounding resistance.

Figure 5.13: Developed overvoltage at position D, for lightning hit at position A, in relation to grounding resistance.

Figure 5.14: Developed overvoltage at position E, for lightning hit at position A, in relation to grounding resistance.

Figure 5.15: Simulation model of distribution line with DG that is hit in position C.

Figure 5.16: Developed overvoltage at position A, for lightning hit at position C, in relation to grounding resistance.

Figure 5.17: Developed overvoltage at position B, for lightning hit at position C, in relation to grounding resistance.

Figure 5.18 Developed overvoltage at position C, for lightning hit at position C in relation to grounding resistance.

Figure 5.19: Developed overvoltage at position D, for lightning hit at position C, in relation to grounding resistance.

Figure 5.20: Developed overvoltage at position E, for lightning hit at position C, in relation to grounding resistance.

Figure 5.21: Developed overvoltages at position A for different peak lightning current magnitudes in relation to grounding resistance (no DG).

Figure 5.22 Developed overvoltages at position B for different peak lightning current magnitudes in relation to grounding resistance (no DG).

Figure 5.23: Developed overvoltages at position C for different peak lightning current magnitudes in relation to grounding resistance (no DG).

Figure 5.24: Developed overvoltages at position D for different peak lightning current magnitudes in relation to grounding resistance (no DG).

Figure 5.25: Developed overvoltages at position E for different peak lightning current magnitudes in relation to grounding resistance (no DG).

Figure 5.26: Developed overvoltages at position A for different peak lightning current magnitudes in relation to grounding resistance (with DG).

Figure 5.27: Developed overvoltages at position B for different peak lightning current magnitudes in relation to grounding resistance (with DG).

Figure 5.28: Developed overvoltages at position C for different peak lightning current magnitudes in relation to grounding resistance (with DG).

Figure 5.29: Developed overvoltages at position D for different peak lightning current magnitudes in relation to grounding resistance (with DG).

Figure 5.30: Developed overvoltages at position E for different peak lightning current magnitudes in relation to grounding resistance (with DG).

Figure 5.31: Developed overvoltages at position A for different surge arresters models in relation to grounding resistance (no DG).

Figure 5.32: Developed overvoltages at position B for different surge arresters models in relation to grounding resistance (no DG).

Figure 5.33: Developed overvoltages at position C for different surge arresters models in relation to grounding resistance (no DG).

Figure 5.34: Developed overvoltages at position A for different surge arresters models in relation to grounding resistance (with DG).

Figure 5.35: Developed overvoltages at position B for different surge arresters models in relation to grounding resistance (with DG).

Figure 5.36: Developed overvoltages at position C for different surge arresters models in relation to grounding resistance (with DG).

Figure 5.37: Developed overvoltage at position A, for lightning hit at position A, in relation to grounding resistance for DG sizes 500 kW - 500 kW - 500 kW.

Figure 5.38: Developed overvoltage at position A, for lightning hit at position A, in relation to grounding resistance for DG sizes 500 kW - 1 MW - 500 kW.

Figure 5.39: Developed overvoltage at position A, for lightning hit at position A, in relation to grounding resistance for DG sizes 1 MW - 500 kW - 1 MW.

Figure 5.40: Developed overvoltage at position A, for lightning hit at position A, in relation to grounding resistance for DG sizes 1 MW - 1 MW - 1 MW.

Figure 5.41: Developed overvoltage at position C, for lightning hit at position A, in relation to grounding resistance for DG sizes 500 kW - 500 kW - 500 kW.

Figure 5.42: Developed overvoltage at position C, for lightning hit at position A, in relation to grounding resistance for DG sizes 500 kW - 1 MW - 500 kW.

Figure 5.43: Developed overvoltage at position C, for lightning hit at position A, in relation to grounding resistance for DG sizes 1 MW - 500 kW - 1 MW.

Figure 5.44: Developed overvoltage at position C, for lightning hit at position A, in relation to grounding resistance for DG sizes 1 MW - 1 MW - 1 MW.

Figure 5.45: Developed overvoltage at position E, for lightning hit at position A, in relation to grounding resistance for DG sizes 500 kW - 500 kW - 500 kW.

Figure 5.46: Developed overvoltage at position E, for lightning hit at position A, in relation to grounding resistance for DG sizes 500 kW - 1 MW - 500 kW.

Figure 5.47: Developed overvoltage at position E, for lightning hit at position A, in relation to grounding resistance for DG sizes 1 MW - 500 kW - 1 MW.

Figure 5.48: Developed overvoltage at position E, for lightning hit at position A, in relation to grounding resistance for DG sizes 1 MW - 1 MW - 1 MW.

List of Tables

- Table 2.1:** Different terms for DG and their description.
- Table 2.2:** Ratings categories of DG.
- Table 3.1:** The sizes of the DG units used in the simulation studies.
- Table 3.2:** Load data of the IEEE 14-Bus Network System.
- Table 3.3:** Line data of the IEEE 14-Bus Network System.
- Table 3.4:** Base case voltage profiles of IEEE 14-Bus Network System (with no DG).
- Table 3.5:** Base case power losses of IEEE 14-Bus Network System (with no DG).
- Table 3.6:** Load data of the IEEE 33-Bus Radial Distribution System.
- Table 3.7:** Line data of the IEEE 33-Bus Radial Distribution System.
- Table 3.8:** Base case voltage profiles of IEEE 33-Bus Radial Distribution System (no DG).
- Table 3.9:** Base case power losses of IEEE 33-Bus Radial Distribution System (no DG).
- Table 4.1:** Syntactic and semantic Rules of AG_{PS} .
- Table 4.2:** Extended start rule of AG_{PSW} .
- Table 4.3:** Syntactic and semantic Rules of AG_{PSW} .
- Table 5.1:** Surge arrester characteristics.
- Table 5.2:** Simulation scenarios.

Copyright Declaration

The author hereby grants powers of discretion to the librarian of City University London, to allow this thesis to be copied in whole or in part without further reference to the author. This permission covers only single copies made for study purposes, subject to normal conditions of acknowledgement.

Vasiliki VITA

May 2016

Abstract

Electric power systems have served well the consumers need for continuous, uninterrupted power supply of good quality and at the minimum possible cost. However, nowadays, the worldwide increasing demand on electric power, coupled with governmental policy changes towards “green” energy and emissions reduction have led to significant changes in the electric power generation. These changes have introduced many serious issues and problems to the electric power systems and although they have been efficiently addressed in the past years, now they need to be restudied and reanalysed taking into consideration all new developments.

Distributed generation (DG), constitutes one of the most important developments in modern electric power systems and introduced many benefits as well as drawbacks. DG units are connected to the electric power system near load centres, thus, directly to the distribution network. DG units are larger in number than the more massive conventional power stations and are linked to the introduction of bidirectional power flow. As a result, the configuration of the traditional electric power systems and the networks’ operation have been prominently altered over the last years as soon as DG was introduced into the electric network. This progress has offered many challenges that need to be addressed such as those in terms of control and protection of electric power systems and particularly of distribution networks.

The current PhD Thesis attempts to offer a contribution to the electricity distribution networks’ studies with particular reference to distributed generation and protection. In particular, the problems and the issues arising from the installation of DG units in distribution networks are studied. Research on the methods for improving voltage profiles and for reducing real and reactive power losses in distribution networks caused by DGs installation is conducted. Moreover, a decision making algorithm is developed and proposed for selecting the optimum size and location of DG in distribution networks. Furthermore, a new technique based on syntactic pattern recognition for the identification of power system signals used by protective relays is developed in an effort to contribute in the deterrence and reduction of faults. Finally, extensive studies in a distribution network have been conducted, with and without DGs, which aimed to identify the influence of several important parameters in the network’s lightning performance and with its main goal the limitation of lightning faults.

Chapter 1

Introduction

1.1 Background

Electric energy plays a vital role in everyday people's life and in society in general as it is accountable for development, economic growth and wealth. Everyday new and more applications are invented and new procedures are adopted which necessitate electric power for their operation and use. For more than seven decades, electric power systems have served this increasing need for electric power adequately, having succeeded to provide consumers with continuous, uninterrupted, of good quality and at the minimum possible cost power supply. However, nowadays, the worldwide increasing demand for electric power, coupled with governmental policy for "green" energy and emissions reduction – responsible for the greenhouse effect – have led to significant modifications in the electric power generation. These changes have introduced many serious issues and problems to the electric power systems and although they have been efficiently addressed in the past years, now they need to be restudied and reanalysed taking into consideration all new developments.

Distributed generation (DG) – i.e., small scale generation units that mainly use renewable sources- constitutes one of the most important developments in modern electric power systems and introduced many benefits as well as drawbacks. DG units are interconnected with the electric power system near load centres, thus, directly to the distribution network. DG units are larger in number than the more massive conventional power stations (typically located closer to an energy source) and are linked to the introduction of bidirectional power flow, mainly in distribution network, but in transmission network as well. As a result, the overall perspective, the configuration of the traditional electric power systems and the networks' operation have been considerably reformed over the last years once DG was introduced into the

electric network construction. All the above have resulted to many challenges that must be addressed such as control and protection of electric power systems and more specifically of distribution networks.

The current PhD Thesis attempts to contribute in the analyses that are conducted for the electricity distribution networks with particular references to distributed generation and protection. More specifically, the problems and the issues that arise from the installation of DG units in distribution networks are studied. Then research is carried out on both a network and a radial distribution system in terms of the improvement of voltage profiles and of real and reactive power losses reduction in distribution networks affected by the installation of DGs. A decision making algorithm is developed and proposed for the optimum size and location selection of a new DG in existing distribution networks. Furthermore, a new technique is developed to be used by protective relays, which is based on syntactic pattern recognition in order to identify power system signals. This newly proposed technique can be applied both in distribution and transmission networks and could contribute in the prevention and reduction of faults. Finally, extensive studies have been conducted in a distribution network, with and without DGs connected, in an effort to identify the influence of several important parameters in the network's lightning performance with ultimate goal the reduction of lightning faults.

1.2 Thesis Objectives

The PhD Thesis objectives of this research are summarized to the following:

- a) Study of different problems and issues that arise from the increasing installation of distributed generation units in the existing distribution networks.
- b) Analysis of the impact of distributed generation in voltage profiles and in real and reactive power losses of distribution networks.
- c) Development of an algorithm for deciding the optimum size and placement of new DG in distribution networks.

- d) Development of a novel technique to be executed on a dedicated embedded system, for the syntactic pattern recognition of power system signals' faults in an effort to design distribution and transmission networks' protection in a more efficient way.
- e) Analysis on the lightning performance and protection of modern distribution networks (with distributed generation), taking into consideration significant parameters such as: grounding resistance, lightning current peak magnitude, position of lightning hit, different models of surge arresters and different sizes of DGs.

1.3 Outline of the Thesis

The current PhD Thesis is divided into the following six chapters.

This first chapter introduces the objectives of this research work, as well as the outline of the Thesis. Furthermore, the contribution of this Thesis is described briefly and a list is provided with the up today author's publications that were produced based on the research presented in this Thesis.

In the second chapter, a brief analysis of electric power systems' structure is presented with special attention to the role of electricity distribution networks. Following, different distribution networks' configurations and main issues are described. Thereafter, the concept of distributed generation (DG) is presented with the connections to the distribution networks to be trending upwards. Detailed information of the variety in DG sizes, the categories and the technologies used and being reported worldwide is provided. Finally, the advantages and disadvantages accruing from the DG's application, are presented, combined with a discussion on different issues that have emerged from the installation of distributed generation in existing distribution networks most of which constitute risks and threats that will deteriorate in the near future as the electricity production from distributed generation increases.

The third chapter consists of the studies conducted on distribution networks with the aim to identify the impact of distributed generation in voltage profiles and real and reactive power losses. After the studies, a novel methodology has been developed and applied on two well-known distribution test systems, i.e., the IEEE 14-bus network

system, and the IEEE 33-bus radial distribution system. Several simulations have been conducted on both under study distribution networks, with two different units and sizes of the most commonly used DG types (PV and wind generator), implemented in NEPLAN, one of the most reliable power systems software. As a final point, a decision making algorithm has been proposed for the optimum size and placement of new DG in existing distribution networks. Useful inferences have been conducted, which can assist in the future in the implementation and development of distribution networks with distributed generation, resulting in a more efficient and productive power system.

In chapter four, a novel approach for the recognition and analysis of power systems' signals applied on protective relays is proposed, in an effort to prevent distribution and transmission lines' faults in a more efficient way, thus avoiding and/or eliminating safety problems and financial losses. A hardware implementation for the real-time syntactic pattern recognition of power system waveforms has been performed. The application of the syntactic methods aiming to analyze power system signals and to measure its parameters is thoroughly studied, as the sub problems of primitive pattern selection, linguistic representation, and pattern grammar formulation are tackled with. The proposed (dedicated embedded) system was coded in Verilog hardware description language (HDL), simulated for validation, implemented and tested on an XILINX FPGA board system using waveforms and data provided by the Independent Power Transmission Operator (IPTO) in Greece.

The fifth chapter consists of numerous sensitivity studies conducted on modern distribution networks (with DG) in an effort to support lightning protection in a more efficient way. A selected distribution network was modelled and then a series of simulations have been conducted, with and without the presence of DG units (of different sizes), calculating the developed overvoltages triggered from lightning hits of different lightning current peak magnitudes and on different positions of the distribution network. Furthermore, the impact of grounding resistance in the scale of the produced overvoltages and the more effective protection of the networks using different models of surge arresters have been examined. The outcome of these studies could contribute significantly in the way that new electric utilities are designed and

could assist engineers in the development of new protection schemes for the modern distribution networks.

In conclusion, chapter six, summarizes the conclusions that have been extracted and highlights the contribution of this PhD Thesis in the analysis of electricity distribution networks' with particular reference to distributed generation and protection, proposing areas and topics where attention should be driven and further and add hoc research should be conducted.

1.4 Contribution

The contribution of the PhD Thesis can be briefly summarized in the following:

- A contribution to the improvement of distribution networks' voltage profiles linked with different types of distributed generation has been conducted.
- A contribution to the reduction of both real and reactive power losses of distribution networks with different types of distributed generation has been conducted.
- A decision making algorithm for the optimum size and placement of DG in distribution networks has been developed.
- A linguistic representation of power system waveforms has been defined.
- An attribute grammar capable of modelling power system waveforms has been presented.
- An attribute grammar evaluator based on a parallel parsing algorithm has been designed.
- A system for the real-time syntactic pattern recognition of power system waveforms has been implemented on a FPGA reconfigurable board designed to be applied on a protective relay.
- The influence of distributed generation in the lightning performance of distribution networks has been analyzed.
- Sensitivity analyses of significant parameters affecting the lightning performance of distribution networks, such as grounding resistance, lightning

current peak magnitude, position of lightning strike hit, different models of surge arresters and different DG sizes, have been conducted.

1.5 List of Author's Publications

The following publications based on the work presented in this Thesis have been produced.

Journal Publications

1. V. Vita, L. Ekonomou, C.A. Christodoulou, The impact of distributed generation to the lightning protection of modern distribution lines, *Energy Systems*, Vol. 7, No. 2, (DOI) 10.1007/s12667-015-0175-3, 2016, pp. 357-364.
1. V. Vita, T.I. Maris, Sensitivity analyses of parameters that affect the lightning performance of distribution networks with distributed generation, *Journal of Multidisciplinary Engineering Science Studies*, 2016 (Accepted, In Press).
2. C. Pavlatos, V. Vita, A.C. Dimopoulos, An efficient embedded system for the fault recognition of power system signals, *IET Science, Measurement and Technology*, (Under Review).
3. V. Vita, S. Agamah, L. Ekonomou, An optimization algorithm for the optimum size and placement of distributed generation in distribution networks, *Simulation Modelling Practice and Theory*, (Under Review).

Conference Publications

1. C. Pavlatos, V. Vita, L. Ekonomou, Syntactic pattern recognition of power system signals, 19th WSEAS International Conference on Systems (part of CSCC '15), Zakynthos Island, Greece, pp. 73-77, 2015.
2. V. Vita, T. Alimardan, L. Ekonomou, The impact of distributed generation in the distribution networks' voltage profile and energy losses, 9th IEEE European Modelling Symposium on Mathematical Modelling and Computer Simulation, Madrid, Spain, pp. 260-265, 2015.

Book Chapters

1. C. Pavlatos, V. Vita, Linguistic representation of power system signals, Electricity Distribution, Energy Systems Series, Springer-Verlag Berlin Heidelberg, pp. 285-295, 2016, DOI 10.1007/978-3-662-49434-9_12.

Chapter 2

Electricity Distribution Networks

2.1 Introduction

This chapter provides a brief illustration of electric power systems' configuration with special attention paid in the miscellaneous configurations of electricity distribution networks (radial, loop and network). Issues such as power loss and voltage drop, are discussed. Furthermore, the concept of distributed generation (DG) is presented, providing information for a number of DG sizes, categories and technologies that have been reported worldwide and are connected to the distribution networks. Benefits and drawbacks related to DGs are also presented, while problems and issues arising from constant and increasing installation of distributed generation in distribution networks are described in detail.

2.2 Electric Power Systems

The structure of a traditional electric power system consists of three main sections: generation, transmission and distribution that are clearly distinguished by either stepping-up or stepping-down power transformers. Figure 2.1 presents the structure of a typical electric power system.

Generation consists of large power stations, which have a typical size of higher than 500 MW power, produced at around 20 kV. The biggest share of the electricity generation is produced by a small number of large fossil fuel fired power stations where high temperature is used to produce high pressure steam in boilers used to drive the turbines which in turn rotate the large generators' shafts. There are a few countries around the world that possess nuclear power stations for generating electricity (the required high pressure steam is produced by nuclear fission instead of burning fossil

fuels), while almost all countries possess generating units that are using renewable energy sources (solar, wind, geothermal, biomass, etc.), since these technologies are considered more environmentally friendly than the traditional sources (coal, oil and natural gas).

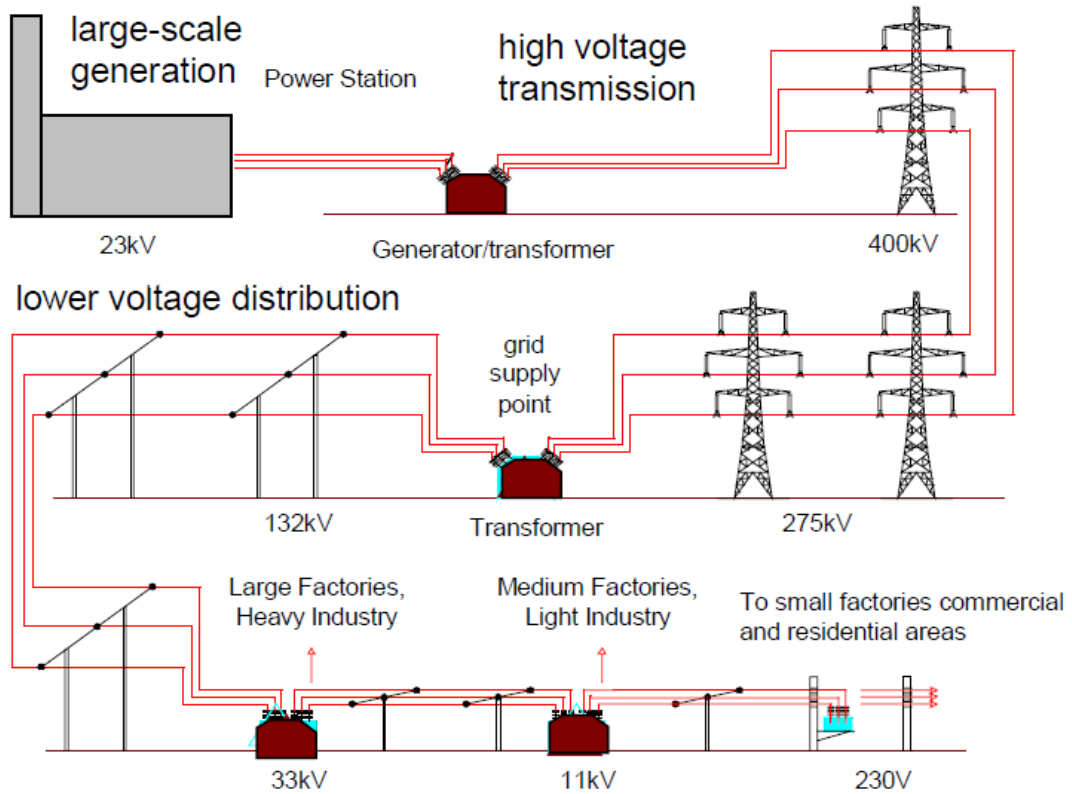


Figure 2.1: Electric power system [1].

Transmission consists mainly of an overhead transmission network (the percentage of underground and submarine cables is relative low) that transfers the electric power from generating units to distribution, which eventually supplies the load [2]. The transmission network is also interconnected with neighbouring transmission networks for exchanging electric power due to both financial (electric power trading) and practical reasons (maintenance scheduling, sharing of generation reserves and emergencies, i.e., lack of sufficient electric power, assistance in the grid stability, etc.). Stepping-up transformers are used to raise the voltage of the generated power in order to transmission it to long distances. This has a result the reduction of current for a specific amount of transferred electric power, resulting in the reduction of power losses and in the more cost-effective construction of transmission network's infrastructure (size of conductors, type of towers, etc.).

Based on the international standards transmission voltage networks operate at 132 kV or higher voltage. The transmission networks up to 230 kV are usually referred as high voltage (HV) transmission networks, while transmission voltages above 230 kV are usually referred to as extra-high voltage (EHV). Finally voltages above 1000 kV are referred to as ultra-high voltages (UHV). The United Kingdom possesses the following EHV and HV networks: 400 kV and 275 kV in England and Wales, 400 kV, 275 kV and 132 kV in Scotland, and 275 kV and 110 kV in Northern Ireland.

Distribution consists of distribution networks and stepping-down transformers that distribute electricity to different consumers. The distribution network links the distribution transformers to the consumers' service-entrance equipment. The primary distribution lines range from 4 to 34.5 kV and supply the load in a well-defined geographical area. Some industrial customers are served directly by the primary feeders. The secondary distribution network reduces the voltage for utilization by commercial and residential consumers. It serves most of the customers at levels of 230 V (Europe)/120 V (North America), single-phase, and 400 V (Europe)/208 V (North America), three-phase.

Distribution networks make use of both overhead conductors/cables and underground cables. The growth of underground distribution has been extremely rapid and up to 70% of new residential construction in North America and Europe is via underground systems [2].

The model that has been presented in this section and is called the centralized model, has served well during the past decades its ultimate goal for uninterrupted power supply to consumers at the best achievable quality. The main characteristic of the centralized model is the unidirectional power flow from higher to lower voltage levels. However, the electric power system structure has undergone through major changes worldwide when privatization took place in the early nineties, resulting to the separation of generation from transmission and distribution. According to the Parliamentary Office of Science and Technology [1], the main goal of such a movement was to accommodate competition in the electricity industry, to deliver better services for customers, decrease in electricity rates, and to improve efficiency. There were also significant environmental motives and the need exploit alternative energy sources. As a

result, the electric power system has evolved from the centralized to the decentralized model, broadly observed and implemented nowadays, which consists of small scale distributed power stations, located closer to load centres. This new decentralized model has introduced the bidirectional power flow, mainly in the distribution networks, but in the transmission networks as well, altering the philosophy and operation of networks and introducing many significant problems that need to be further studied and analysed.

2.3 Distribution Networks

As it has already been mentioned in section 2.2, the distribution network is a very important part of the electric power system. Electric power is transferred through this network to consumers. The distribution network consists of many different elements such as: bus bars, overhead lines, underground cables, switches, circuit breakers and transformers. As electricity demand increases continuously over the past years, the distribution network is constantly expanding, causing its congestion. Distribution networks have been initially designed to serve an unidirectional power flow from higher to lower voltage levels. In the majority of the cases, distribution networks have been designed in a radial configuration, although there other configurations as well. There are three different configurations, i.e., radial, loop and network configurations. Each configuration forms a distinct feeder arrangement and unique type of connection.

2.3.1 Radial Distribution Configuration

The radial configuration is widely used especially for the supply of low-load consumers and remote areas. The main advantages of this configuration are the simplicity in operation and design and the reduced construction cost in contrast to the loop and network configurations. The main disadvantage of the radial configuration is its low reliability since in the case of a fault, downstream buses (nodes) will be isolated (buses are only supplied from one side). In order to reduce the duration of interruptions, overhead feeders can be protected by automatic devices located at the substation or at other locations on the feeder. These devices reenergize the feeder in cases of temporary faults [3]. A radial configuration of a distribution network is shown in Figure 2.2.

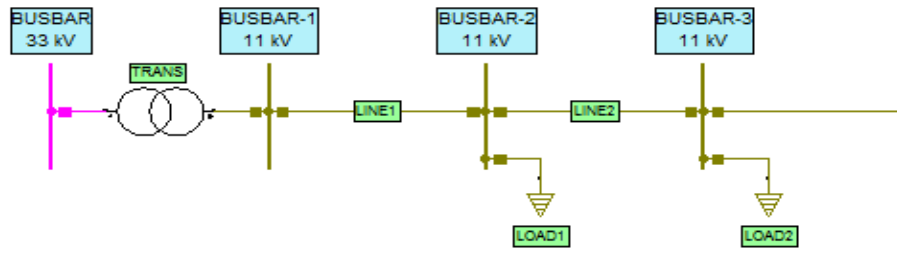


Figure 2.2: The radial distribution configuration.

2.3.2 Loop Distribution Configuration

The loop system is used where a higher level of service reliability and continuity of supply is necessary. Two primary feeders form a closed loop, in order all buses and loads to be supplied from one feeder or another in the event of a fault. One or more additional feeders along separate routes may be implemented for critical loads that cannot tolerate extended interruptions. Switching from one feeder to an alternative can be accomplished either manually or automatically with the help of circuit breakers and/or electrical interlocks, used to prevent the connection of a functional feeder with a faulted one [3]. The main disadvantages of this configuration are the higher cost and augmented complexity compared to the radial configuration. A loop configuration of a distribution network is shown in Figure 2.3.

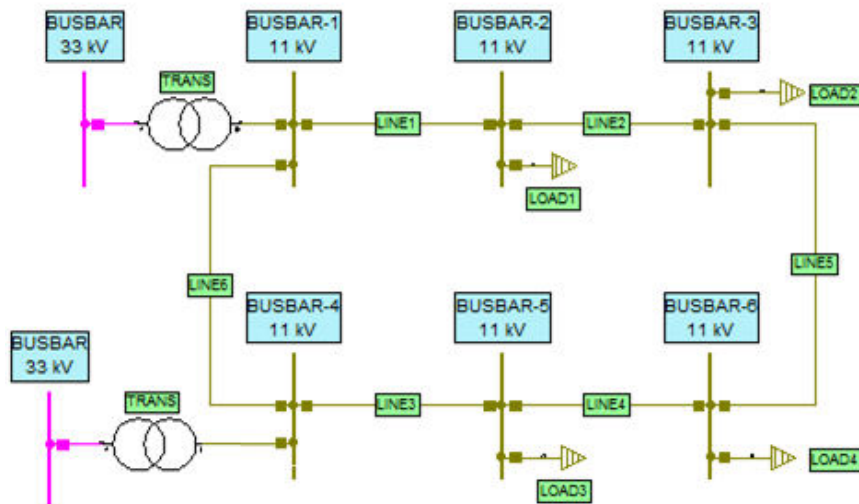


Figure 2.3: The loop distribution configuration.

2.3.3 Network Distribution Configuration

A group of radial and loop systems or the expansion of one of them will result in a network configuration distribution network. Network configuration is used to supply high-density load areas in downtown sections of cities, where the highest degree of reliability is needed. Such networks are supplied by two or more primary feeders through network transformers. These transformers are protected by devices that open to disconnect the transformer from the network if the transformer or supply feeder is faulted. Special current-limiting devices are also used at various locations to keep problems from spreading [3]. A network configuration of a distribution network is shown in Figure 2.4.

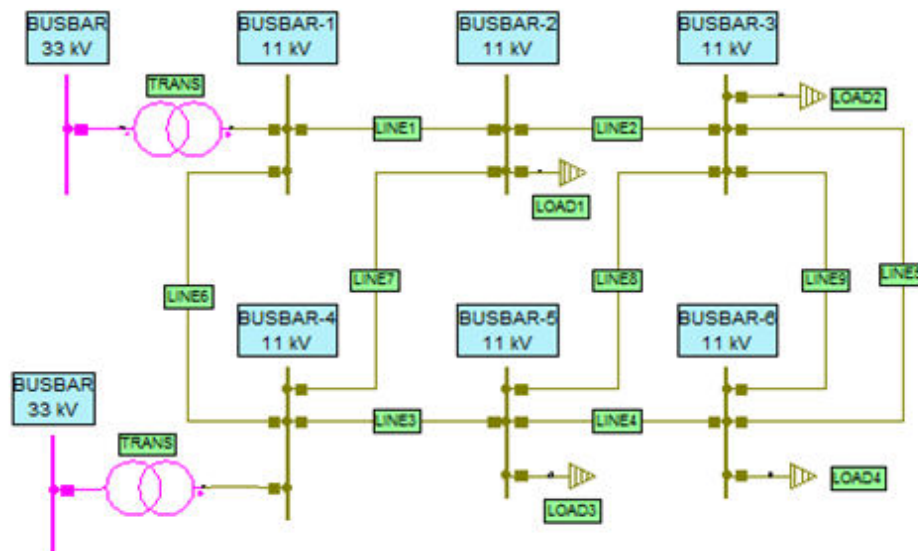


Figure 2.4: The network distribution configuration.

2.3.4 Power Losses

Electric energy passes from generation to transmission and distribution networks through overhead lines and underground cables. Losses are unavoidable as long as power is flowing in the power system. According to the UK Department of Energy and Climate Change (DECC) [4], an increase of 0.2 % in losses has occurred, from 7.5 % in 2011 to 7.7 % in 2012, represented as percentage of electricity demand. Three types of losses have been recorded by the DECC: a) 23 % in the transmission network, which

accounts for 6.8 TWh, b) 73 % in the distribution network, which accounts for 21.1TWh, and c) 4 % as theft which accounts for 1TWh.

Hence, the distribution network's losses constitute the largest share of power losses within the electric power system. This is because it is constructed from many components such as lines, transformers, substations, capacitors, switches, circuit breakers. Furthermore, the existence of different load capacities at different load profiles contributes significantly to these power losses.

Distribution networks present two types of energy losses, i.e., losses in the conductors due to the magnitude of the current and transformer core losses that are independent of current. Current related losses are equal to the current squared times the resistance of the conductor (I^2R). Accompanying these losses are reactive losses, which are related to the reactance of the conductor and are given by (I^2X). The core losses result from the energy used in transformer cores as a result of hysteresis and eddy currents. These losses depend on the magnetic material used in the core [2].

2.3.5 Voltage Drop

Voltage drops in distribution networks are a common occurrence when different loads are connected to bus bars and across long distance lines. As the length of a line increases, its inductive reactance increases, and there is an increase in inductive reactive power. However, as inductive reactive power increases, the voltage drop across the line also increases and the voltage at the far or receiving end of the line drops. To reduce the voltage drop and support the voltage at the receiving end, more capacitive reactive power is needed to offset the inductive effect. The equipment that is usually used to regulate and provide voltage support is voltage regulators and capacitors. The recent years has been also observed that distributed generation has the potential to improve voltage if optimally is placed and sized in a distribution network.

2.4 Distributed Generation (DG)

The Electric Power Research Institute (EPRI) makes clear that the origin of distributed generation is dated back to the early twentieth century, thus it is not a new concept [5]. However, the continuous increasing demand for electricity, the environmental

concerns and the government policies have now made it an attractive option. In addition, technological advancement has made it possible to shift from large central generation stations powered by fossil fuels, or nuclear power (as is the case in some countries), to smaller generators most of which are connected to the distribution system. Such generator technologies can be based on alternative energy sources, with a concentration on renewable sources such as: wind and solar energy and on non-renewable sources such as: diesel and gas generator. Figure 2.5 presents an illustration of DG's diverse range of technologies [6]. The classification of these technologies has been made based on DG's output power, categorising the DG units into “dispatchable” (generating units that can be turned on or off, or can adjust their power output on demand) and “non-dispatchable” units.

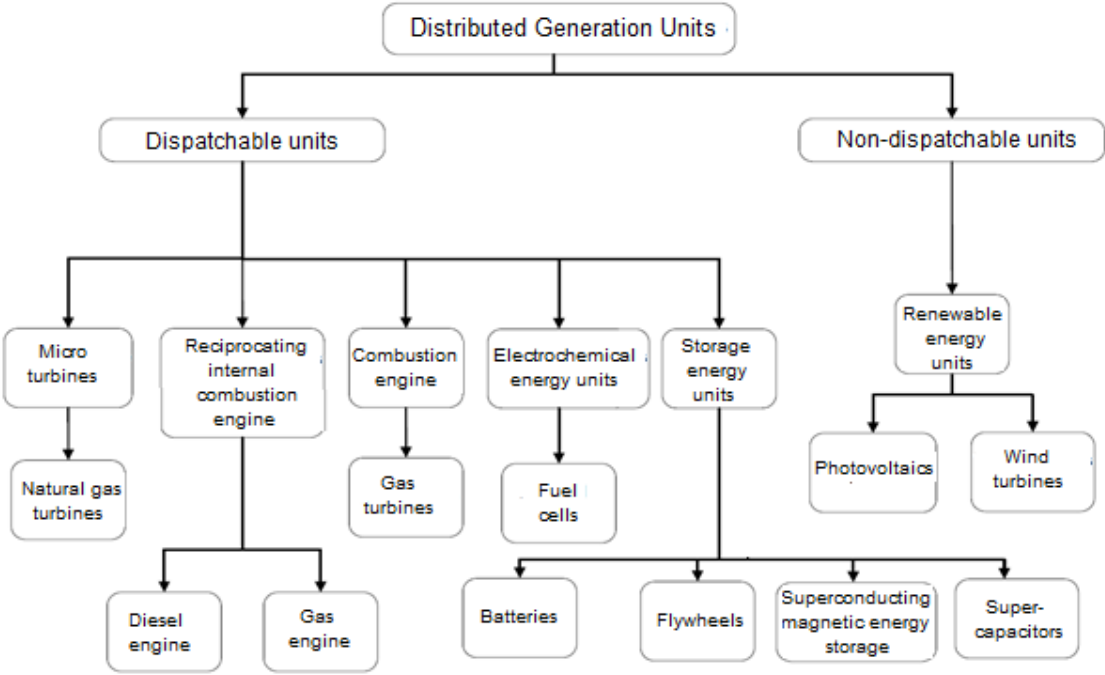
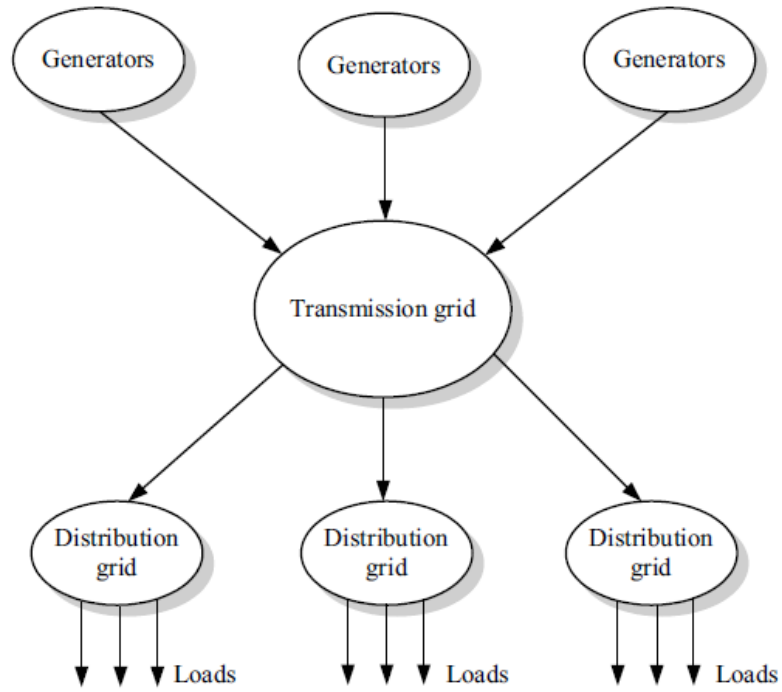
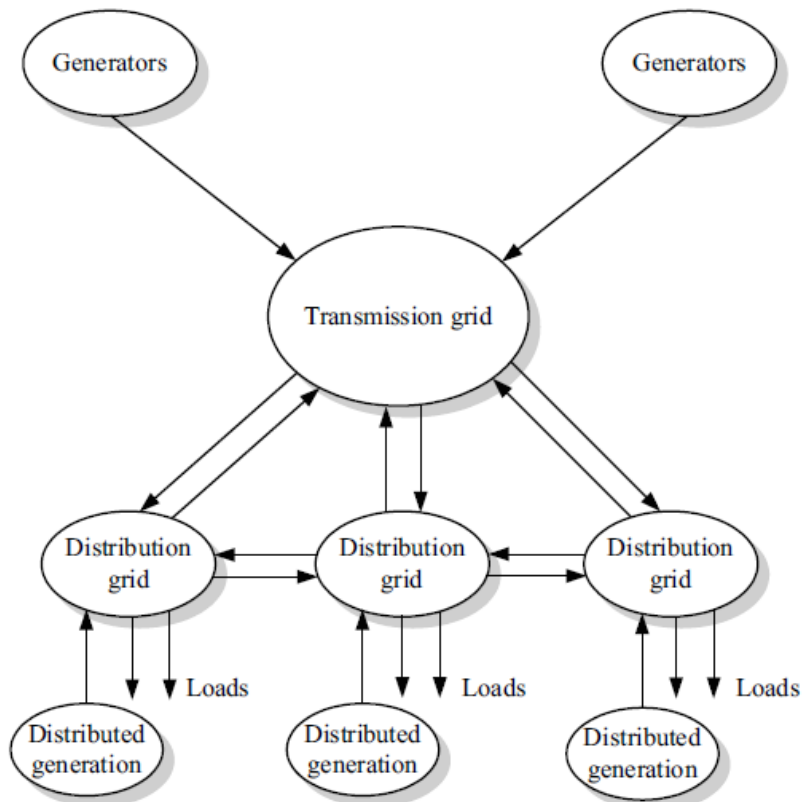


Figure 2.5: DG technologies [6].

DG units can be used either in an isolated way, supplying power only for serving the consumer’s local demand, or in an integrated way, supplying power to the electric power system. In distribution systems, DG offer many advantages for both consumers and electric utilities, especially in cases where central generation is not feasible or in cases where there are serious issues/problems with the transmission network [7]. Figure 2.6 presents traditional and current (with DG) electric power systems.



Traditional power systems



Current power systems

Figure 2.6: Traditional and current electric power systems.

2.4.1 DG definition

In general, there is no consensus among countries or researchers on the term “distributed generation” (DG) or its definition. In some countries it may be referred as “embedded generation”, while in others it is known as “dispersed generation” or “decentralized generation”. The International Energy Agency has introduced all existing different terms in order to describe DG providing also their relevant descriptions (Table 2.1) [8].

Table 2.1: Different terms for DG and their description.

| Term | Description |
|------------------------------|---|
| Distributed generation | DG technologies connected close to load centres with the exception of wind turbines |
| Dispersed generation | DG including wind turbines (stand alone or grid connected) |
| Distributed power | DG and energy storage |
| Distributed energy resources | DG and demand side management |
| Decentralised power | DG connected to the distribution system |

In the same way a variety of definitions may be found in the literature that relate to size, location or the underlying technology. Ackermann et al. in [9] approached this problem by reviewing a number of different issues so that a more subtle definition for DG could be reached. The issues were: location, technology, purpose, mode of operation, ownership, size, power delivery area, DG penetration and environmental impact. Their definition for DG was: “DG can be defined as an electric power generation source connected directly to the distribution network or on the customer site of the meter”. Table 2.2 below shows Ackermann’s et al classification for DG based on the size [9].

Distributed generation units can be owned and operated by either electric utilities or consumers and in general provide a variety of benefits to both their owners and the broader electric power system. The large DG units are typically dispatchable and communicate with system operators with the same way as traditional central generating plants do. On the other hand neither electric utilities nor system operators typically

monitor or control the operation of small DG units (mainly the renewables) and especially those in residential applications.

Table 2.2: Ratings categories of DG.

| Ratings | Categories |
|----------------|-------------------------------|
| 1W < 5kW | Micro-distributed generation |
| 5kW < 5MW | Small distributed generation |
| 5MW < 50MW | Medium distributed generation |
| 50MW < 300MW | Large distributed generation |

2.4.2 Distributed Generation Benefits

The installation of distributed generation units promises several potential economic and technical benefits. The major benefits of the integration of DG units in electricity distribution networks can be summarized as follows [10-13]:

- a) DG units are usually installed near the load site on the radial distribution networks. Thus, part of the transmission power is replaced by the injected DG power, causing a reduction in transmission and distribution line losses, which minimizes costs related to loss.
- b) The injection of real power and the injection or consumption of reactive power by DG units improve system voltage profiles and the load factor, which minimizes the number of required voltage regulators, capacitors and their ratings and maintenance costs. It must be mentioned that the amount of improvement depends on the sitting and sizing of DG units.
- c) The increasing power demands, due to load growth, can be covered by DG units without the need to increase existing traditional generation capacity. This has also as a result the reduction or delay for building new transmission and distribution lines and for upgrading the present power systems.
- d) DGs are flexible devices that can be installed at load centres rather than at substations, where difficulties due geographical constraints or scarcity of land availability may occur. In addition, DG locations are not restricted by the government's choice for potential locations, as is the case when selecting new substation locations.

- e) DG technology is available in a wide capacity range (i.e., from 3 kW up to 50 MW), giving the possibility to DG units to be easily installed on distribution networks, both medium and low voltage.
- f) DG units require a short period of time to install and pose less of an investment risk due to their modular characteristics, which enables them to be easily assembled anywhere. Each DG unit is totally independent of the others, can generate electricity immediately after its installation and cannot be affected by other units' operation failure.
- g) DG technologies produce electric power with few emissions (and sometimes zero emissions). This feature makes them more environmentally friendly compared to traditional power plants.
- h) DGs can contribute significantly in the reliability and service continuity since there many different generation plants across the power system in contrast to the very few large centralized generation units. This can be extremely useful for consumers that require the highest possible reliability no matter if they have to pay for higher service costs.

2.4.3 Distributed Generation Drawbacks

The integrating of DG units into electrical distribution systems may also lead to negative impacts, especially for large scale installations if they are not optimally handled. The main drawbacks of DG are summarized as follows:

- a) The continuous connection of DGs results to a more complex power system. The control, operation, protection and security of the system changes that result the need for the conduction of new studies and the development of new techniques.
- b) DGs inject harmonics into the system due to the fact that are connected to the system using power converters.
- c) The connection of DGs could cause overvoltages and disturbances to the system's voltage profile, mainly due to mismatched synchronisation with the electrical supply utilities.

- d) Although the use of DGs results in the reduction of power losses, there are cases where power losses are increased due to network configurations and nature of DGs technology.
- e) Modifications in the distribution networks' protection schemes must be done when DG units are connected, e.g., altering relay settings due to dissimilar short circuit levels. Disconnection for any reason of the DG units requires that the distribution networks' protection schemes settings retrace to their previous state, i.e. before the connection of DG units.

2.4.4 Issues arising from Distributed Generation use

The impact that the increasing connection of distributed generation (DG) plants has in the electric power systems, can be summarized in the following issues:

- a) **Regulation and balancing issues.** Larger penetration of renewable energy sources, in the form of DG, from the strictly technical point of view, depends on two major issues: i) grid connection issues, and ii) power system regulation issues. The first issue addresses the need for network reinforcements, which is more a question of feasibility and economics, while the second relates to complex balancing issues. Regulation and balancing issues can only be addressed in coordination between all power system players on a national and international (interconnection) level.
- b) **Selective protection coordination issues.** The connection of DG increases the complexity of selective protection coordination. From a technical point of view, the DG presence in distribution networks may result to conflicts in the normal operation of the current networks. This is mainly because, unlike the meshed transmission system, the distribution system is designed as a “passive” radial system, without generators operating in parallel, or power flow control. In addition, the connection of DG can alter the fault current during a grid disturbance, which leads to incorrect operation of the protective system and causes fault detection problems and selectivity problems.
- c) **Distribution grid stability.** Stability issues are important for DG installations. The DG should be able to remain synchronized after a major fault. Furthermore, a massive implementation of DG leads to the inertia of the entire system to decrease. Unless fast

acting primary control is applied, the system frequency will become significantly sensitive to disturbances.

d) **Islanding effect.** When the main line of a utility system, which contains DG is disconnected, more than one DG continue to operate in the isolated section (island), thus leading to the islanding effect. Unintended islanding is of paramount importance for the general public, maintenance personnel and installed equipment, since the distribution lines remain energized.

e) **Distribution system reliability performance.** DG affects significantly the reliability and operational indices of existing distribution networks. The operation of DG in parallel with the transmission supply system and its performance during abnormal conditions, such as power supply outages must be taken into account.

f) **Management of micro-grids in the new market environment.** The micro-grid is a low voltage network which usually operates interconnected with the main medium voltage network. In case of emergency the micro-grid can run autonomously being a solution to the structure for the coordination of the DG units. The investigation of control approaches, possible configurations and security issues related to the micro-grids operation is of high importance.

g) **Optimum sitting and sizing of DG.** Today there is no specific plan, neither for the sitting nor for the sizing of DG units, in almost all electric power systems worldwide. This can result voltage fluctuations, causing currents that exceed the line's thermal limit, harmonic problems and instability of the voltage profile of some electricity consumers. In addition, the bi-directional power flows can lead to voltage profile fluctuation and change the short circuit levels sufficiently to cause fuse-breaker discoordination. Studies have shown that the installation of DG units in distribution networks can improve the voltage profiles and contribute significantly in the minimization of both real and reactive power losses. The specific location and size of DG units play an important role in both voltage profile and power losses, since significant penetration of DGs has been shown that it may cause overvoltages or undervoltages [14].

h) **Lightning performance and protection.** The installation of DGs affects significantly the lightning performance and the lightning protection of distribution networks, resulting in an increase of lightning faults and consequently an increase of the fault reimbursement costs for Distribution System Operators. Detailed lightning studies must be conducted in distribution networks with DG in an effort to evaluate the influence of DGs and the efficiency of existing lightning protection methods and to develop and propose new protection schemes that will consider the existence of DGs in the modern electric power systems.

2.5 Conclusions

In this chapter, the essential theoretical background for the acquisition of this PhD Thesis has been presented. The structure of electric power systems has been examined paying special attention to the structure of the distribution network, to the distribution configurations and their complications in terms of power losses and voltage drop. Moreover, the general idea of distributed generation has been described in detail and all the advantages and disadvantages triggered by their installation in distribution networks have been enlightened. Finally, issues arising from the increasing number of DGs installation and operation in modern electric power systems have been discussed.

2.6 References

- [1] The Parliamentary Office of Science and Technology, UK electricity networks, POST, no. 163, 2001.
- [2] El Hawary ME, Introduction to electrical power systems, John Wiley & Sons, Inc., Hoboken, New Jersey, 2008.
- [3] Casazza J, Delea F, Understanding electric power systems, 2nd edition, John Wiley & Sons, Inc., Hoboken, New Jersey, 2010.
- [4] Department of Energy and Climate Change, UK renewable energy roadmap update 2013, https://www.gov.uk/government/uploads/system/uploads/attachment_data/file/255182/.
- [5] Electric Power Research Institute, <http://www.epri.com/>.

- [6] Al-Abri R, Voltage stability analysis with high distributed generation (DG) penetration, PhD Thesis, University of Waterloo, Waterloo, Ontario, Canada, 2012.
- [7] Viral R, Khatod DK, Optimal planning of distributed generation systems in distribution system: A review, *Renewable and Sustainable Energy Reviews*, vol. 16, pp. 5146-5165, 2012.
- [8] International Energy Agency, Distributed generation in liberalised electricity markets, IEA Publications, 2002.
- [9] Ackermann T, Andersson G, Soder L, Distributed generation: a definition, *Electric Power Systems Research*, vol. 57, pp. 195-204, 2001.
- [10] El-Khattam W, Salama MMA, Distributed generation technologies, definitions and benefits, *Electric Power Systems Research*, vol. 71, no. 2, pp. 119-128, 2004.
- [11] El-Khattam W, Salama MMA, Distribution system planning using distributed generation, *Electrical and Computer Engineering, IEEE CCECE 2003*, vol. 1, pp. 579-582, 2003.
- [12] Chiradeja P, Ramakumar R, An approach to quantify the technical benefits of distributed generation, *IEEE Transactions on Energy Conversion*, vol. 19, no. 4, pp. 764-773, 2004.
- [13] Celli G, Pilo F, Optimal distributed generation allocation in MV distribution networks, *Power Industry Computer Applications, 22nd IEEE Power Engineering Society International Conference on Innovative Computing for Power - Electric Energy Meets the Market*, pp. 81-86, 2001.
- [14] Viral R, Khatod DK, Optimal planning of distributed generation systems in distribution system: A review, *Renewable and Sustainable Energy Reviews*, vol. 16, pp. 5146-5165, 2012.

Chapter 3

Voltage Profiles and Power Losses in Distribution Networks with Distributed Generation

3.1 Introduction

This chapter presents studies that have been conducted on distribution networks in order to identify the impact of distributed generation (DG) in voltage profiles and real and reactive power losses. Related research works published in the technical literature are described and the concepts of voltage profiles and power losses are analysed. A methodology has been applied in order to serve the studies that have been conducted. Simulations have been carried out using the power systems software NEPLAN. Two well-known distribution test systems have been used in the studies. The first one was the IEEE 14-bus network system, and the second one was the IEEE 33-bus radial distribution system. Finally an optimization algorithm for the optimum size and placement of DG in distribution networks has been developed. Useful conclusions have been extracted that can assist the future development of distribution networks with distributed generation resulting in the more efficient and productive use of it.

3.2 Literature Review

The worldwide continuous integration of distributed generation in the electric power systems is a result of electricity markets' privatisation, of environment protection from emissions and of technological progression. The unadvised and uncontrolled installation of DGs in the distribution network during the past two decades brought in serious problems and challenges to the distribution networks. Such problems are the inevitable bidirectional power flow in the modern distribution networks, in contrast to unidirectional power flow from higher to lower voltages, and the very important

problems of voltage drop and power losses. Researchers from all over world are studying the former mentioned problems and have featured various techniques and methodologies for selecting the optimum sitting and sizing of DGs in an effort to improve voltage profiles and minimize or even eliminate power losses of modern distribution networks with distributed generation. Subsequent is a presentation of the most important latest studies published in the technical literature.

A new particle swarm optimization method has been proposed in [1] aiming to improve the power quality and the reliability of a distribution system by identifying the optimal number of DGs that must be connected and their suitable locations in the system. The proposed method was tested on the IEEE 30-bus system, producing results that have shown considerable reduction in the total power loss of the system and improvement in voltage profiles of the buses and in reliability.

Jamian et al. in [2] used multiple types of optimization techniques to regulate the DG's output in order to compute its optimal size. Comparative studies of a new proposed rank evolutionary particle swarm optimization method with evolutionary particle swarm optimization and traditional particle swarm optimization were conducted. The implementation of evolutionary programming and particle swarm optimization allowed the entire particles to move toward the optimal value more rapidly. Their applied technique has shown a reduction in power losses which can be achieved when an optimal DG size is selected. Another conclusion made, was that evolutionary particle swarm optimization showed better results than the conventional particle swarm optimization due to its reduced iteration numbers and minor consumed computing time.

A study conducted by Kotb et al. [3] used genetic algorithms to optimize the location and size of different DG units. Three main objectives have been selected, i.e., voltage, real and reactive power losses, and DG size, aiming to reduce the total power losses and improve the voltage profiles. A 69-bus radial distribution test system has been used in their study for testing and verification purposes. The proposed methodology suggested that the installation of three DG units of the same size in three different positions of the 69-bus radial distribution test system, resulted in the reduction of power losses and in voltage profiles enhancement.

A similar technique that combines a genetic algorithm with particle swarm optimisation method for the siting and sizing of DGs in distribution networks has been proposed in [4]. The suggested technique aimed at voltage improvement, voltage stabilisation and power loss reduction in radial systems. The genetic algorithm has been used in order to locate the optimum place for DG installation while the particle swarm optimisation method has been used so as to compute the DG's optimum size. A 33-bus radial system and a 69-bus radial system were used in order to test the proposed technique.

Correspondingly in [5], genetic and particle swarm optimization algorithms have been exploited for optimal placement and sizing of both a DG and a capacitor. The performance of these algorithms has been tested by applying the proposed methodology to a 12-bus radial distribution system. The produced results have shown that the proposed methodology is more effective and capable of providing better results than other analytical methods.

Following, Parizad et al. [6] tried to determine the optimum location and size of DG by reducing losses and stabilising voltage, using two different methods. The first approach aimed at real power losses through the development of an exact loss formula that determined the best location for DG installation. In the second approach, a voltage stability index was used to position DG in the optimum location. Power flow was computed by applying the forward-backward sweep method. Two distribution systems of 33-bus (radial) and 30-bus (loop) systems have been exploited in the study. The proposed techniques revealed significant improvement in terms of voltage profiles and power losses reduction.

In [7], fuzzy logic has been applied for locating the optimum placement of a single DG unit and a new analytical expression for DG sizing implemented in radial networks was proposed. The aim of this study was to improve voltage profile and minimize real and reactive power losses. Three different distribution systems (a 12-bus, a 33-bus and a 69-bus) were utilized in order to verify that the proposed methodologies could be applied in radial distribution systems of different sizes and arrangements. The results disclosed that an optimal size and location of a DG unit with significant reduction in real and reactive power losses was realisable. Furthermore, a noteworthy voltage profile improvement was attained. It must be declared that a forward-backward sweep

algorithm was applied for load flow analysis in contrast to the majority of other researchers that use the Newton-Rapson method.

Naik et al. [8] introduced a method that aimed to minimise power losses and improve voltage profiles of a distribution system with a DG unit coupled. They have chosen a 33-bus distribution system to apply their method on. Initially, a voltage sensitivity index was calculated for all the buses and then the bus with the lowest sensitivity index was chosen as the optimum place for the DG unit installation. Subsequently, several DG sizes were tested in order to identify the one that would result to the least possible power losses. In this study the forward-backward sweep algorithm was selected to perform the load flow analysis.

An analytical study for the calculation of the optimum size and the allocation of DG units at optimal positions was presented in [9]. The technique that aimed to reduce the power losses and to improve the voltage profiles of distribution systems has used a sensitivity index to identify the best location for the connection of the DG. The 13-bus IEEE radial distribution test system has been used for verification purposes and the main conclusion of this work was that minimum losses and a better voltage profile can be achieved with integrating a single DG unit of optimum size and in an optimum location rather the integration of several DG units.

A very interesting study has been introduced in [10]. The authors explored the results of the penetration of mixed distributed generation technologies to a medium voltage power distribution network. Power flow and short-circuit analyses were carried out to determine the changes caused by the DG penetration to the currents, losses, voltage profiles and short-circuit levels of the examined network. Their general conclusion was that arbitrary DG accommodation leads not only to network sterilisation, but also to the violation of technical constraints.

Balamurugan et al. conducted load flow and short circuit studies in an effort to investigate the impact of photovoltaics on the distribution systems [11]. They applied their analysis on the IEEE 34-bus system, with their main focus on total power losses, phase imbalances, fault levels and voltage profiles of the system. They have concluded that when the penetration level was increasing, there was an enhancement of the DG's

positive impact in terms of power losses and voltage profile. They have also observed that the same positive impact was sustained even when DG was installed in several different places within the distribution system.

3.3 The Impact of Distributed Generation in Voltage Profile and Power Losses

3.3.1 Voltage Profile

Distributed generation is supposed to support and improve the system's voltage but the question that is raised is up to what extent is this statement accurate, since it has been demonstrated that the penetration of DGs in the distribution system may cause overvoltages or undervoltages [12]. Furthermore, specific DG technologies vary their output power level over time, as in the case of photovoltaics and wind generators. As a consequence, voltage fluctuations occur that in turn deteriorate the power quality delivered to consumers.

Moreover, overvoltages and undervoltages in distribution networks with DG have been reported due to the incompatibility of DGs with the existing voltage regulation methods [12]. In general, the distribution networks are regulated with the help of voltage regulators, capacitors and the tap changing of transformers. These methods were designed for radial (unidirectional) power flow and have been proved to be very reliable and efficient in the past. However, nowadays, the installation of DGs in distribution networks had a substantial impact on the voltage regulation methods performance due to the meshed (bidirectional) power flow, introduced by DGs to the networks.

On the other hand, the implementation of DG had a positive impact on the distribution networks for the reason that they contribute to the reactive compensation for voltage control, to frequency regulation and they operate as spinning reserve in the case of main system's fault indices [12].

3.3.2 Power Losses

It has been proved that the distributed generation can minimize the power losses (both real and reactive) of distribution networks due to their installation near the load centers.

Several studies, most of which were presented earlier, demonstrated that the location and size of a DG unit play an important role in the power losses elimination. Consequently, the specific location of a DG in a distributed network and DG's specific capacity resulting in minimum power losses is in general identified as the optimum location. The DG allocation process is very similar to the capacitor allocation procedure aiming at the power losses reduction. The main difference between the two processes is that DG units exhibit impact upon both real and reactive power, while the capacitor banks influence only the reactive power flow. It has been proven, that in the case of networks with increased power losses, installing a relative small distributed generation unit strategically connected to the network, may result in substantial power losses reduction [12].

3.4 Voltage Profile and Power Losses Studies on Distribution Networks with Distributed Generation

3.4.1 Simulation Process

For the voltage profiles and power losses analysis of distribution networks with coupled distributed generation, NEPLAN software has been used. NEPLAN software is programmed to analyse, plan, improve and simulate electricity systems [13]. It consists of a very friendly graphical user interface and it allows the user to make modifications to the network's elements according to specific needs with the help of its extensive library.

Two different types of DGs (photovoltaic (PV) and wind generator) have been coupled with the examined distribution networks in order their impact on voltage profiles and power losses (real and reactive) to be investigated. Four different sizes of PVs and three different sizes of wind generators, of typical type and commonly used in the distribution networks, have been selected for the above studies. Table 3.1 presents the sizes of the seven DG units that have been exploited in the simulations [14].

The studies have been conducted on two different distribution networks. The first one is the IEEE 14-Bus Network System and the second one the IEEE 33-Bus Radial Distribution System. For both networks the following computation methodology has been followed:

Table 3.1: The sizes of the DG units used in the simulation studies [14].

| DG Name | Injected real power (MW) | Consumed reactive power (MVar) |
|----------------|---------------------------------|---------------------------------------|
| DG1-PV | 0.5 | - |
| DG2-PV | 1.0 | - |
| DG3-PV | 2.0 | - |
| DG4-PV | 4.0 | - |
| DG1-WG | 1.65 | 0.731 |
| DG2-WG | 2.0 | 0.582 |
| DG3-WG | 3.0 | 0.875 |

a) A load flow analysis is performed to the examined distribution network without connecting any DG to the network (base case load flow). For each bus the voltage profile and for each line the real and reactive power losses are calculated. It must be mentioned that for the load flow analysis, the extended Newton-Raphson method was used.

b) The buses with the highest priority are identified, as a result of comparing the calculated voltage profile of each bus with its nominal value.

c) Each one of the seven DG units is connected to the selected buses and load flow analyses are conducted calculating the network's voltage profiles, real and reactive power losses.

3.4.2 IEEE 14-Bus Network System

3.4.2.1 System Description

The IEEE14-Bus Network System is shown in Figure 3.1 and is consisting of fourteen buses and twenty lines (branches). The network presents voltage levels of 69 kV in five buses, 18 kV in one bus and 13.8 kV in eight buses. The maximum and minimum voltage limits for all buses are considered at $\pm 5\%$. The network is fed by three synchronous condensers and two generators, while it is loaded by total 259 MW and 81.4 MVar connected to twelve buses and of different power factors. Table 3.2 and Table 3.3 present the load data and line data of the examined system, respectively.

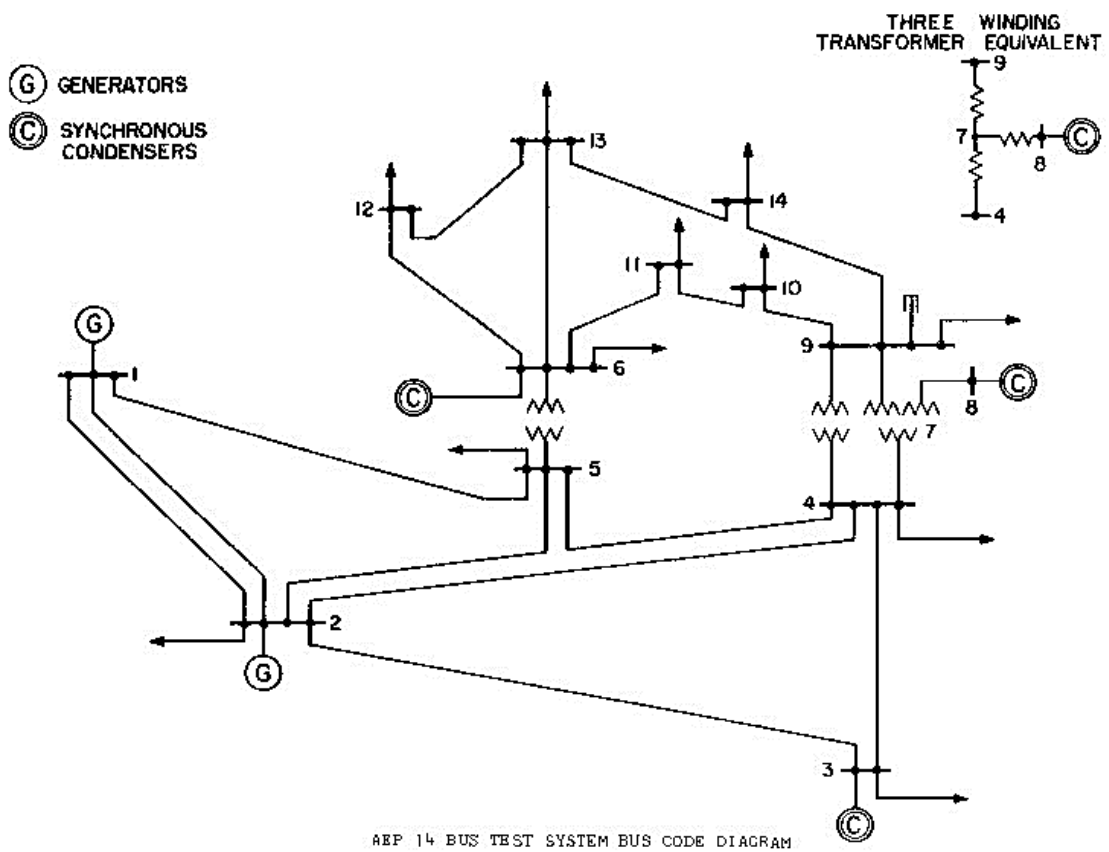


Figure 3.1: Single line diagram of the IEEE 14-Bus Network System [15].

Table 3.2: Load data of the IEEE 14-Bus Network System [15].

| Load | Location (bus bar) | Real load (MW) | Reactive load (MVar) |
|------------|--------------------|----------------|----------------------|
| LDBUS_2 | 2 | 21.7 | 12.7 |
| LDBUS_3 | 3 | 94.2 | 19.0 |
| LDBUS_4 | 4 | 47.8 | 4.0 |
| LDBUS_5 | 5 | 7.6 | 1.6 |
| LDBUS_6 | 6 | 11.2 | 7.5 |
| LDBUS_7 | 7 | 0.0 | 0.0 |
| LDBUS_9 | 9 | 29.5 | 16.6 |
| LDBUS_10 | 10 | 9.0 | 5.8 |
| LDBUS_11 | 11 | 3.5 | 1.8 |
| LDBUS_12 | 12 | 6.1 | 1.6 |
| LDBUS_13 | 13 | 13.5 | 5.8 |
| LDBUS_14 | 14 | 14.9 | 5.0 |
| Total load | | 259 | 81.4 |

Table 3.3: Line data of the IEEE 14-Bus Network System [15].

| Line Name | From bus | To bus | Length (km) | Line impedance | | |
|-----------|----------|--------|-------------|---------------------|--------------------|---------------------------|
| | | | | Resistance (Ohm/km) | Reactance (Ohm/km) | Capacitance (μ F/km) |
| BRANCH-1 | 1 | 2 | 1 | 0.922681 | 2.817083 | 3.53009 |
| BRANCH-2 | 1 | 5 | 1 | 2.572368 | 10.61893 | 3.289402 |
| BRANCH-3 | 2 | 3 | 1 | 2.237193 | 9.425351 | 2.928370 |
| BRANCH-4 | 2 | 4 | 1 | 2.766617 | 8.394595 | 2.500480 |
| BRANCH-5 | 2 | 5 | 1 | 2.711389 | 8.278426 | 2.273164 |
| BRANCH-6 | 3 | 4 | 1 | 3.190346 | 8.142738 | 2.313279 |
| BRANCH-7 | 5 | 4 | 1 | 0.635593 | 2.004857 | 0.855779 |
| BRANCH-11 | 6 | 11 | 1 | 0.180879 | 0.378785 | 0 |
| BRANCH-12 | 6 | 12 | 1 | 0.234069 | 0.487164 | 0 |
| BRANCH-13 | 6 | 13 | 1 | 0.125976 | 0.248086 | 0 |
| BRANCH-15 | 7 | 9 | 1 | 0 | 0.209503 | 0 |
| BRANCH-16 | 9 | 10 | 1 | 0.060578 | 0.160921 | 0 |
| BRANCH-17 | 9 | 14 | 1 | 0.242068 | 0.514911 | 0 |
| BRANCH-18 | 10 | 11 | 1 | 0.156256 | 0.365778 | 0 |
| BRANCH-19 | 12 | 13 | 1 | 0.420720 | 0.380651 | 0 |
| BRANCH-20 | 13 | 14 | 1 | 0.325519 | 0.662769 | 0 |

3.4.2.2 Simulation Results

The IEEE14-Bus Network System was modeled with the help of NEPLAN software.

The single line diagram of the network in NEPLAN is presented in Figure 3.2.

A load flow analysis has been performed without connecting any DG (base case load flow) in order to calculate the voltage profiles at each bus and both the real and reactive power losses at each line. The base case voltage profiles of the network, as well as the deviation of the obtained values from the nominal values are presented in Table 3.4, while the obtained base case real and reactive power losses are presented in Table 3.5.

As it can be observed all buses are over their nominal voltage, but there are only four buses that violate the upper limit of 105 %, i.e., bus 1, bus 6, bus 8 and bus 12. From these buses only bus 6 and bus 12 are considered for the placement of DG units in an effort to improve the voltage profiles and to reduce the power losses of the network, since bus 1 and bus 8 have no load connected and have a voltage level of 69 kV and 18 kV respectively, which are not suitable for DG connections.

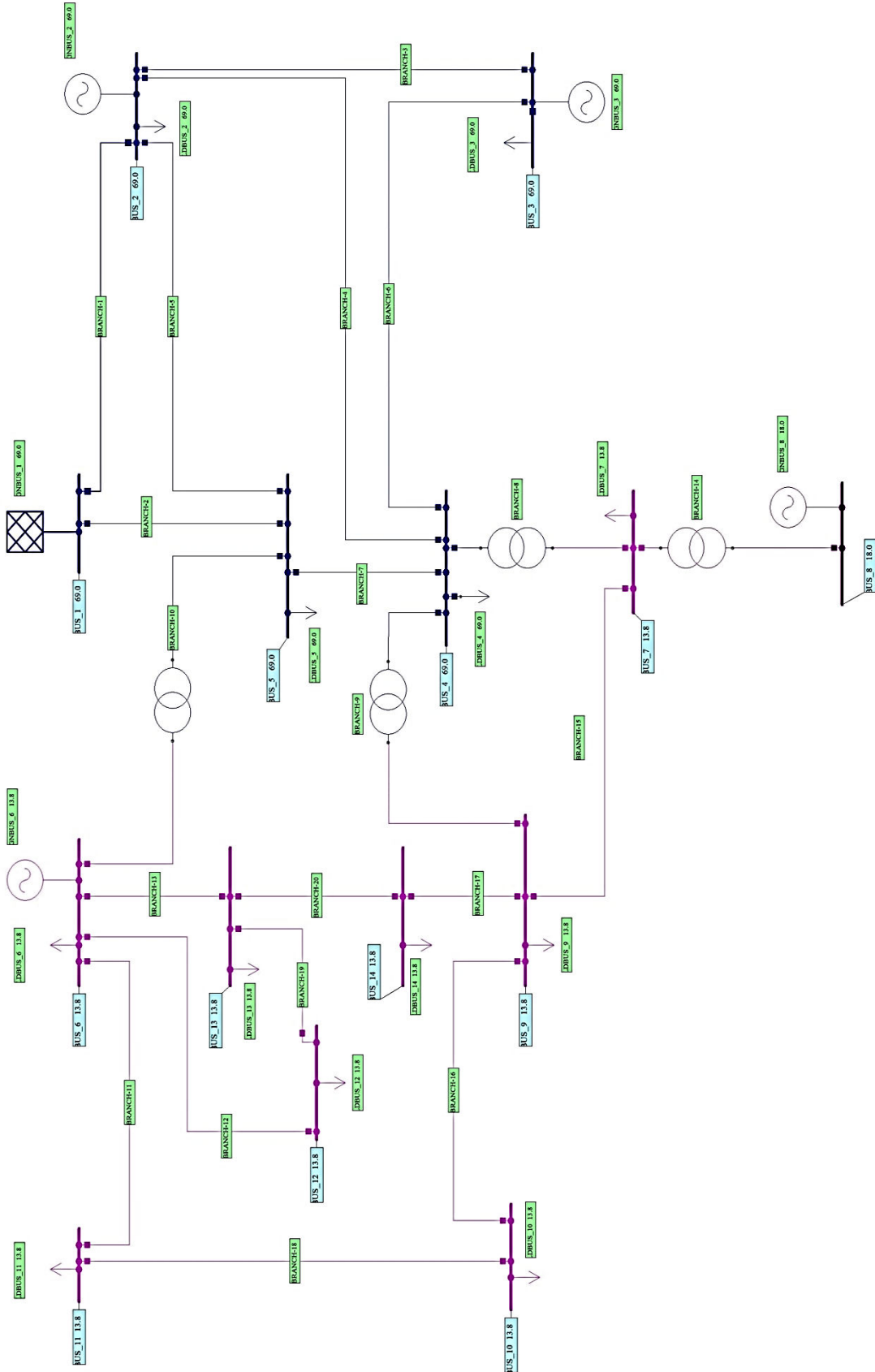


Figure 3.2: Single line diagram of the IEEE 14-Bus Network System in NEPLAN.

Table 3.4: Base case voltage profiles of IEEE 14-Bus Network System (with no DG).

| Bus No | U_n (kV) | U (kV) | u (%) |
|--------|------------|----------|---------|
| BUS_1 | 69.0 | 73.140 | 106.00 |
| BUS_2 | 69.0 | 72.105 | 104.50 |
| BUS_3 | 69.0 | 69.690 | 101.00 |
| BUS_4 | 69.0 | 69.803 | 101.16 |
| BUS_5 | 69.0 | 70.090 | 101.58 |
| BUS_6 | 13.8 | 14.766 | 107.00 |
| BUS_7 | 13.8 | 14.460 | 104.78 |
| BUS_8 | 18.0 | 19.561 | 108.67 |
| BUS_9 | 13.8 | 14.238 | 103.17 |
| BUS_10 | 13.8 | 14.226 | 103.09 |
| BUS_11 | 13.8 | 14.444 | 104.66 |
| BUS_12 | 13.8 | 14.536 | 105.33 |
| BUS_13 | 13.8 | 14.446 | 104.68 |
| BUS_14 | 13.8 | 14.076 | 102.00 |

Table 3.5: Base case power losses of IEEE 14-Bus Network System (with no DG).

| Line Name | P_{loss} (MW) | Q_{loss} (MVar) |
|-----------|------------------------|--------------------------|
| BRANCH-1 | 4.3119 | 7.3156 |
| BRANCH-2 | 2.7714 | 6.1383 |
| BRANCH-3 | 2.3382 | 5.2255 |
| BRANCH-4 | 1.6725 | 1.1189 |
| BRANCH-5 | 0.9218 | -0.7960 |
| BRANCH-6 | 0.3986 | -2.5180 |
| BRANCH-7 | 0.4763 | 0.1871 |
| BRANCH-8 | 0.0000 | 1.5094 |
| BRANCH-9 | 0.0000 | 1.2674 |
| BRANCH-10 | 0.0000 | 4.6951 |
| BRANCH-11 | 0.1183 | 0.2477 |
| BRANCH-12 | 0.0802 | 0.1669 |
| BRANCH-13 | 0.2496 | 0.4915 |
| BRANCH-14 | 0.0000 | 0.8592 |
| BRANCH-15 | 0.0000 | 0.9860 |
| BRANCH-16 | 0.0061 | 0.0161 |
| BRANCH-17 | 0.0904 | 0.1922 |
| BRANCH-18 | 0.0486 | 0.1138 |
| BRANCH-19 | 0.0107 | 0.0097 |
| BRANCH-20 | 0.1020 | 0.2077 |
| Total | 13.5966 | 27.4341 |

Each one of the seven DG units of Table 3.1 has been connected to bus 6 and bus 12 of the distribution network and a load flow analysis has been conducted. In total fourteen load flow analyses have been conducted and the results are presented in Figures 3.3 – 3.12. Figure 3.3 presents the voltage levels of all 13.8 kV buses of the system when PV DGs are connected at bus 6 while Figure 3.4 presents the voltage levels of all 13.8 kV buses of the system when PV DGs are connected at bus 12.

Voltage Profiles (PV at Bus 6)

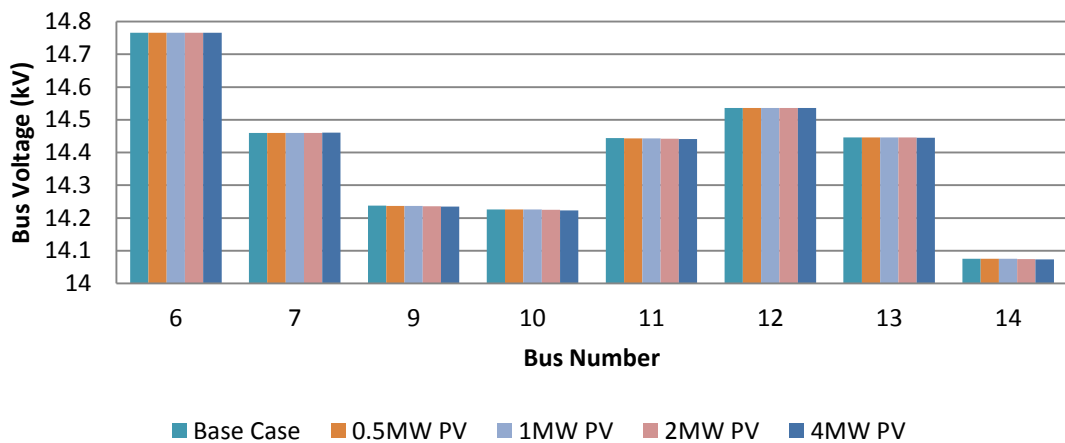


Figure 3.3: Voltage profiles of the 13.8 kV buses when a DG PV unit has been connected at bus 6.

Voltage Profiles (PV at Bus 12)

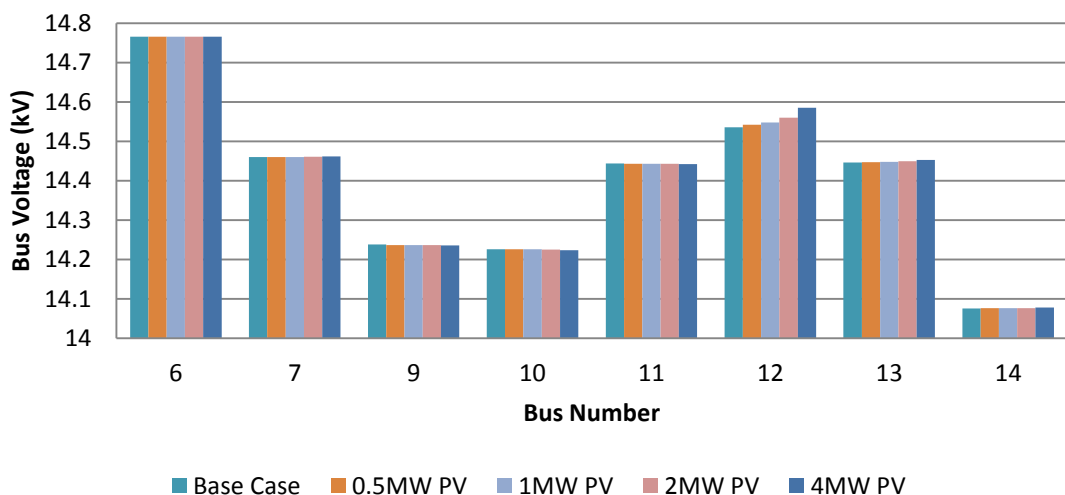


Figure 3.4: Voltage profiles of the 13.8 kV buses when a DG PV unit has been connected at bus 12.

Similarly Figure 3.5 presents the voltage levels of all 13.8 kV buses of the system when wind generator DGs are connected at bus 6 and Figure 3.6 presents the voltage levels of all 13.8 kV buses of the system when wind generator DGs are connected at bus 12.

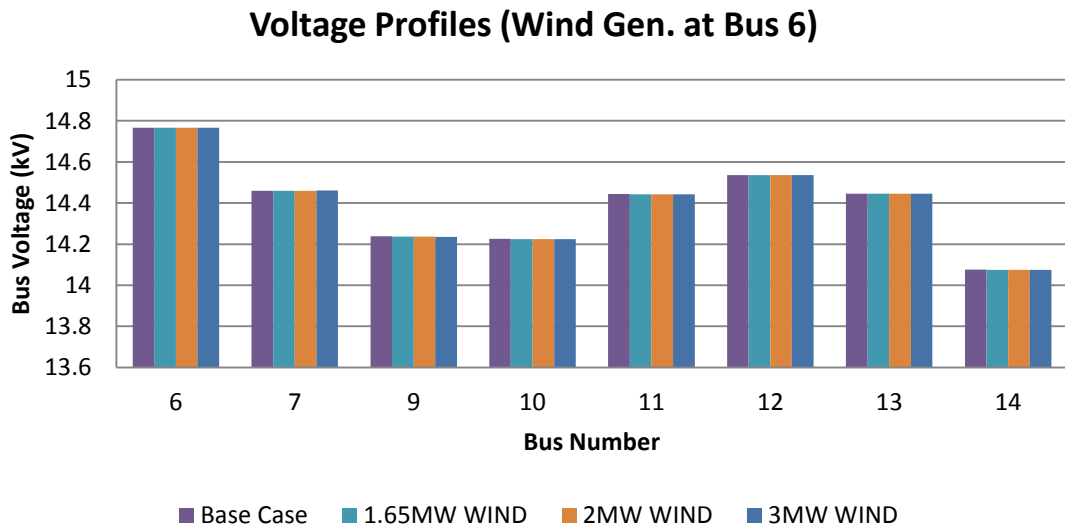


Figure 3.5: Voltage profiles of the 13.8 kV buses when a DG wind generator unit has been connected at bus 6.

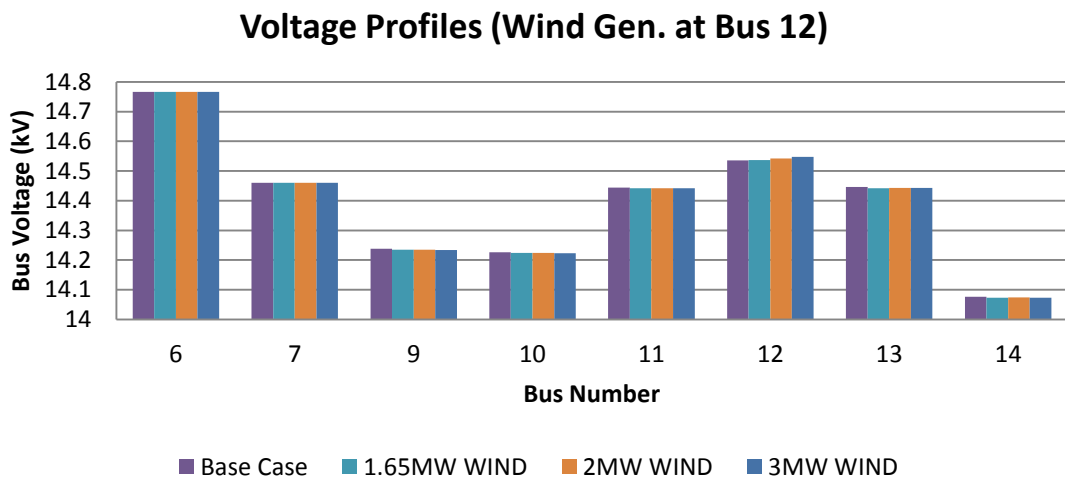


Figure 3.6: Voltage profiles of the 13.8 kV buses when a DG wind generator unit has been connected at bus 12.

The results show that both DG types (PV that injects real power to the network and wind generator that injects real power to the network but consumes reactive power) have a very small impact to the voltage profiles of the buses. In all cases the DG PV

units have slightly raised voltage levels, with this slight increase to be proportional to the DG PV unit's capacity. On the other hand the DG wind generator units have slightly improved the voltage profiles for six out of eight 13.8 kV buses with this improvement to be inverse proportional with the DG wind generator unit's capacity.

Figure 3.7 presents the total network real power losses, Figure 3.8 presents the total network reactive power losses and Figure 3.9 presents the total network apparent power losses of all o network's lines when PV DG units are connected at different buses.

Similarly, Figure 3.10 presents the total network real power losses, Figure 3.11 presents the total network reactive power losses and Figure 3.12 presents the total network apparent power losses of all lines of the network for the case that wind generator DG units are connected at various buses.

The results show that both PV DG type and wind generator DG type have reduced the distribution network's total real and reactive power losses. It is observed that the amount of reduction is almost the same, for the same type and size of DG, regardless of the bus that the DG was connected to. However it is proved that the size plays an important role in the total networks power losses since it has been observed that the larger the size of the DG the higher the total networks power losses reductions.

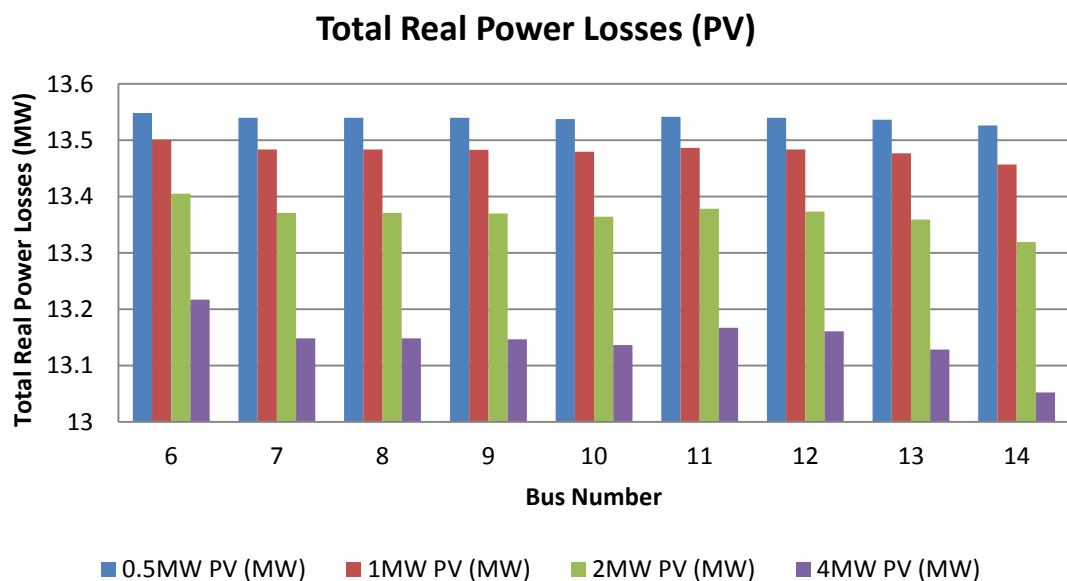


Figure 3.7: Total network real power losses when DG PV units have been connected at different buses.

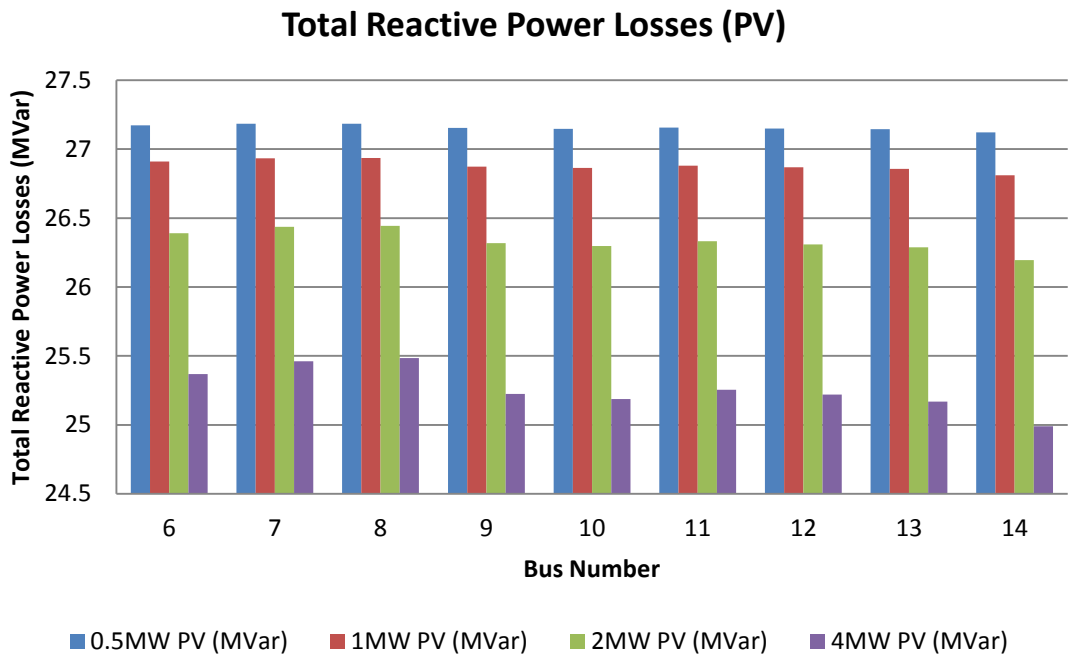


Figure 3.8: Total network reactive power losses when DG PV units have been connected at different buses.

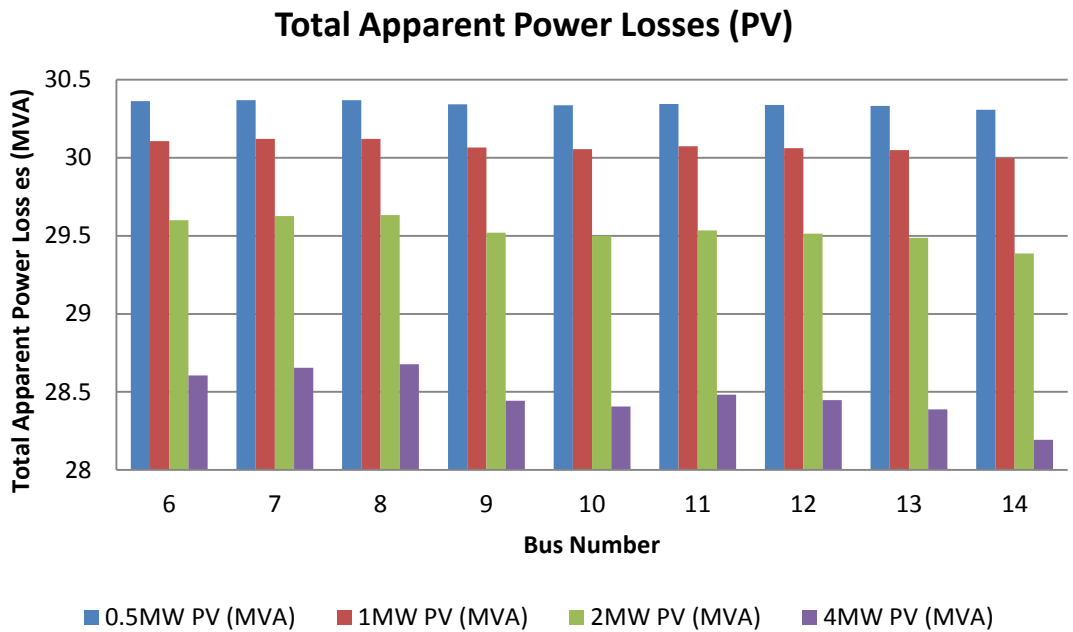


Figure 3.9: Total network apparent power losses when DG PV units have been connected at different buses.

Total Real Power Losses (Wind Gen.)

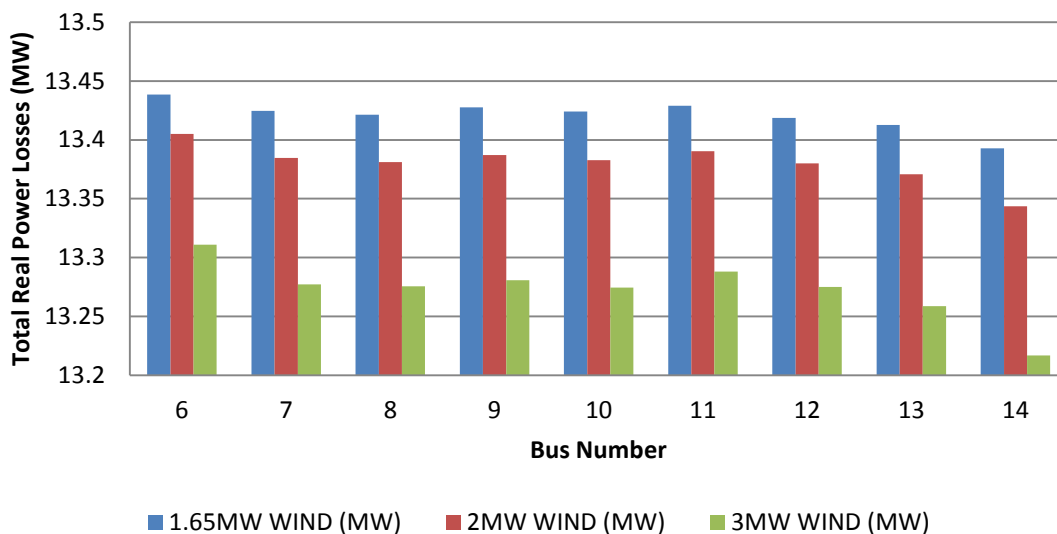


Figure 3.10: Total network real power losses when DG wind generator units have been connected at different buses.

Total Reactive Power Losses (Wind Gen.)

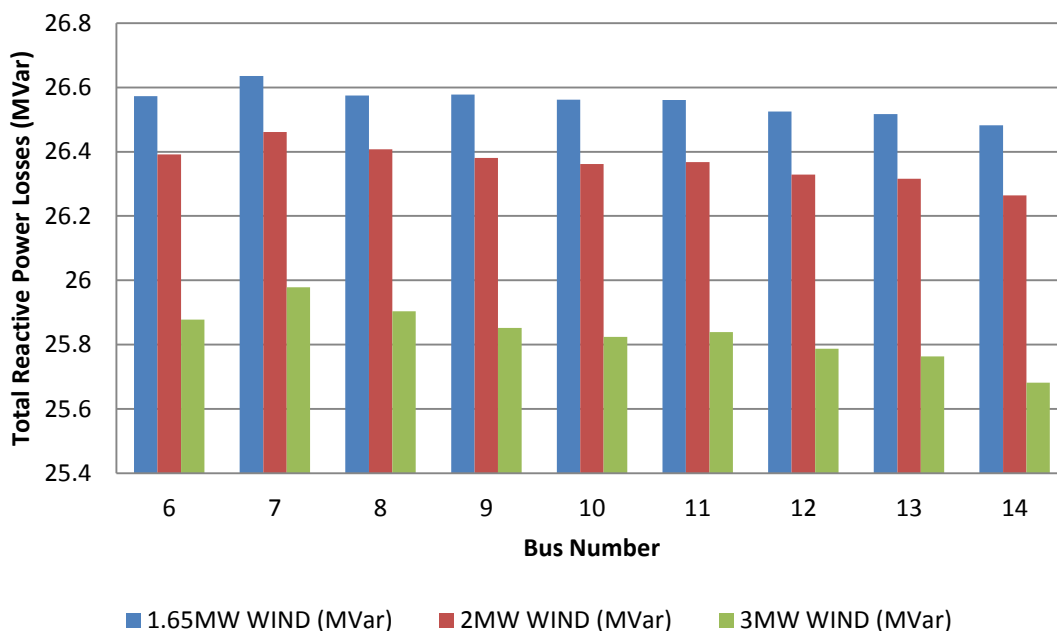


Figure 3.11: Total network reactive power losses when DG wind generator units have been connected at different buses.

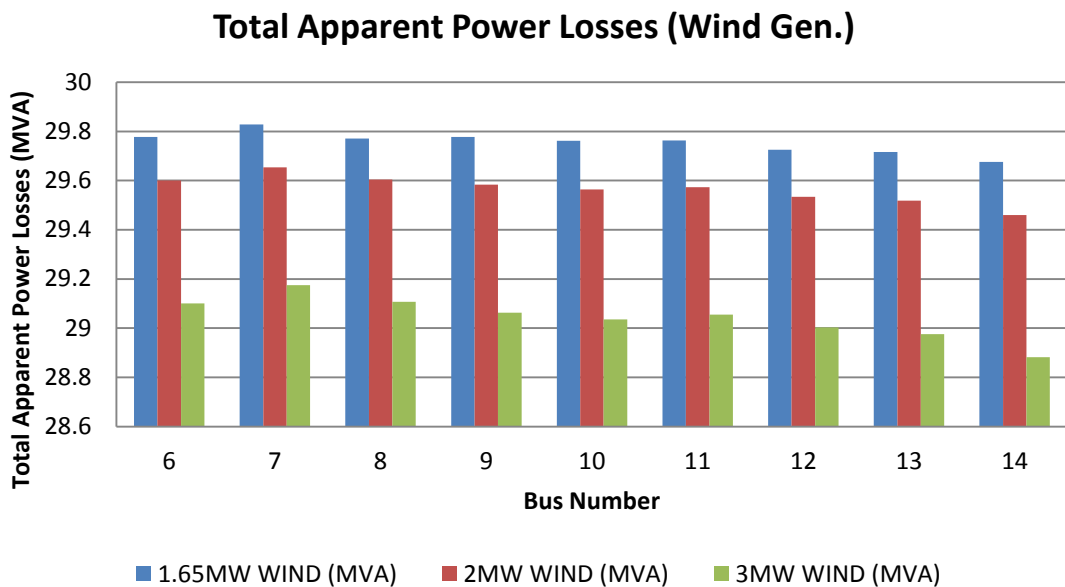


Figure 3.12: Total network apparent power losses when DG wind generator units have been connected at different buses.

3.4.3 IEEE 33-Bus Radial Distribution System

3.4.3.1 System Description

The IEEE 33-Bus Radial Distribution System is shown in Figure 3.13. It consists of thirty three buses and thirty two lines (branches). All buses have a voltage level of 12.66 kV. The maximum and minimum voltage limits for all buses are considered at $\pm 5\%$. The network is fed by a synchronous generator, while it is loaded from 3.715 MW and 2.3 MVar connected to thirty two buses of different power factors.

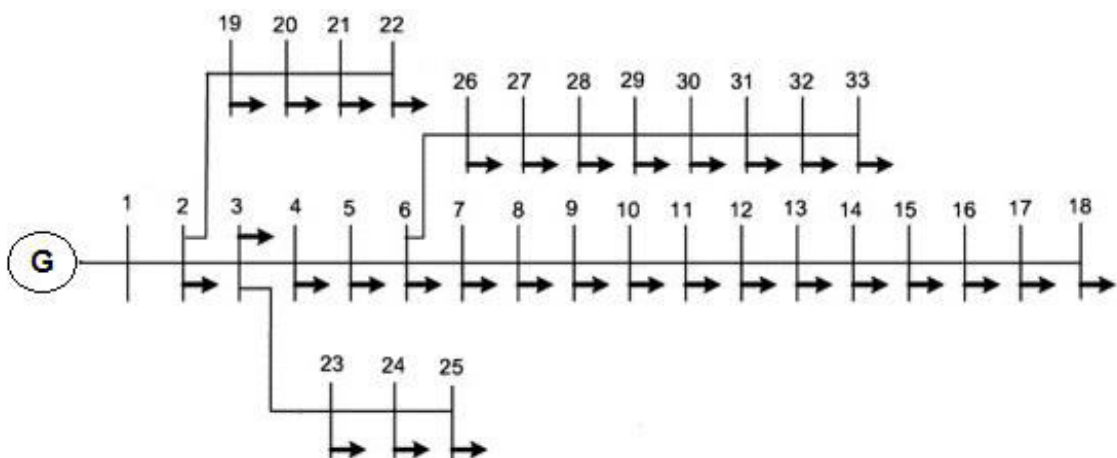


Figure 3.13: Single line diagram of the IEEE 33-bus radial distribution system [16].

Table 3.6 and Table 3.7 present the load data and line data of the examined system.

Table 3.6: Load data of the IEEE 33-Bus Radial Distribution System [16].

| Load | Location (bus bar) | Real load (kW) | Reactive load (kVar) |
|------------|-----------------------|-------------------|-------------------------|
| L2 | 2 | 100 | 60 |
| L3 | 3 | 90 | 40 |
| L4 | 4 | 120 | 80 |
| L5 | 5 | 60 | 30 |
| L6 | 6 | 60 | 20 |
| L7 | 7 | 200 | 100 |
| L8 | 8 | 200 | 100 |
| L9 | 9 | 60 | 20 |
| L10 | 10 | 60 | 20 |
| L11 | 11 | 45 | 30 |
| L12 | 12 | 60 | 35 |
| L13 | 13 | 60 | 35 |
| L14 | 14 | 120 | 80 |
| L15 | 15 | 60 | 10 |
| L16 | 16 | 60 | 20 |
| L17 | 17 | 60 | 20 |
| L18 | 18 | 90 | 40 |
| L19 | 19 | 90 | 40 |
| L20 | 20 | 90 | 40 |
| L21 | 21 | 90 | 40 |
| L22 | 22 | 90 | 40 |
| L23 | 23 | 90 | 50 |
| L24 | 24 | 420 | 200 |
| L25 | 25 | 420 | 200 |
| L26 | 26 | 60 | 25 |
| L27 | 27 | 60 | 25 |
| L28 | 28 | 60 | 20 |
| L29 | 29 | 120 | 70 |
| L30 | 30 | 200 | 600 |
| L31 | 31 | 150 | 70 |
| L32 | 32 | 210 | 100 |
| L33 | 33 | 60 | 40 |
| Total load | | 3715 | 2300 |

3.4.3.2 Simulation Results

The IEEE 33-Bus Radial Distribution System was modelled with the help of NEPLAN software. The network's single line diagram in NEPLAN is presented in Figure 3.14.

A load flow analysis has been performed without connecting any DG (base case load flow) in order to calculate voltage profiles at each bus and both real and reactive power losses at each line. The base case voltage profiles of the network and the deviation of the obtained values from the nominal values are presented in Table 3.8, while the obtained base case power losses are presented in Table 3.9.

Table 3.7: Line data of the IEEE 33-Bus Radial Distribution System [16].

| Line Name | From bus | To bus | Length (km) | Line impedance | |
|-----------|----------|--------|-------------|---------------------|--------------------|
| | | | | Resistance (Ohm/km) | Reactance (Ohm/km) |
| BRANCH-1 | 1 | 2 | 1 | 0.0922 | 0.0470 |
| BRANCH-2 | 2 | 3 | 1 | 0.4930 | 0.2511 |
| BRANCH-3 | 3 | 4 | 1 | 0.3660 | 0.1864 |
| BRANCH-4 | 4 | 5 | 1 | 0.3811 | 0.1941 |
| BRANCH-5 | 5 | 6 | 1 | 0.8190 | 0.7070 |
| BRANCH-6 | 6 | 7 | 1 | 0.1872 | 0.6188 |
| BRANCH-7 | 7 | 8 | 1 | 1.7114 | 1.2351 |
| BRANCH-8 | 8 | 9 | 1 | 1.0300 | 0.7400 |
| BRANCH-9 | 9 | 10 | 1 | 1.0440 | 0.7400 |
| BRANCH-10 | 10 | 11 | 1 | 0.1966 | 0.0650 |
| BRANCH-11 | 11 | 12 | 1 | 0.3744 | 0.1238 |
| BRANCH-12 | 12 | 13 | 1 | 1.4680 | 1.1550 |
| BRANCH-13 | 13 | 14 | 1 | 0.5416 | 0.7129 |
| BRANCH-14 | 14 | 15 | 1 | 0.5910 | 0.5260 |
| BRANCH-15 | 15 | 16 | 1 | 0.7463 | 0.5450 |
| BRANCH-16 | 16 | 17 | 1 | 1.2890 | 1.7210 |
| BRANCH-17 | 17 | 18 | 1 | 0.7320 | 0.5740 |
| BRANCH-18 | 2 | 19 | 1 | 0.1640 | 0.1565 |
| BRANCH-19 | 19 | 20 | 1 | 1.5042 | 1.3554 |
| BRANCH-20 | 20 | 21 | 1 | 0.4095 | 0.4784 |
| BRANCH-21 | 21 | 22 | 1 | 0.7089 | 0.9373 |
| BRANCH-22 | 3 | 23 | 1 | 0.4512 | 0.3083 |
| BRANCH-23 | 23 | 24 | 1 | 0.8980 | 0.7091 |
| BRANCH-24 | 24 | 25 | 1 | 0.8960 | 0.7011 |
| BRANCH-25 | 6 | 26 | 1 | 0.2030 | 0.1034 |
| BRANCH-26 | 26 | 27 | 1 | 0.2842 | 0.1447 |
| BRANCH-27 | 27 | 28 | 1 | 1.0590 | 0.9337 |
| BRANCH-28 | 28 | 29 | 1 | 0.8042 | 0.7006 |
| BRANCH-29 | 29 | 30 | 1 | 0.5075 | 0.2585 |
| BRANCH-30 | 30 | 31 | 1 | 0.9744 | 0.9630 |
| BRANCH-31 | 31 | 32 | 1 | 0.3105 | 0.3619 |
| BRANCH-32 | 32 | 33 | 1 | 0.3410 | 0.5302 |

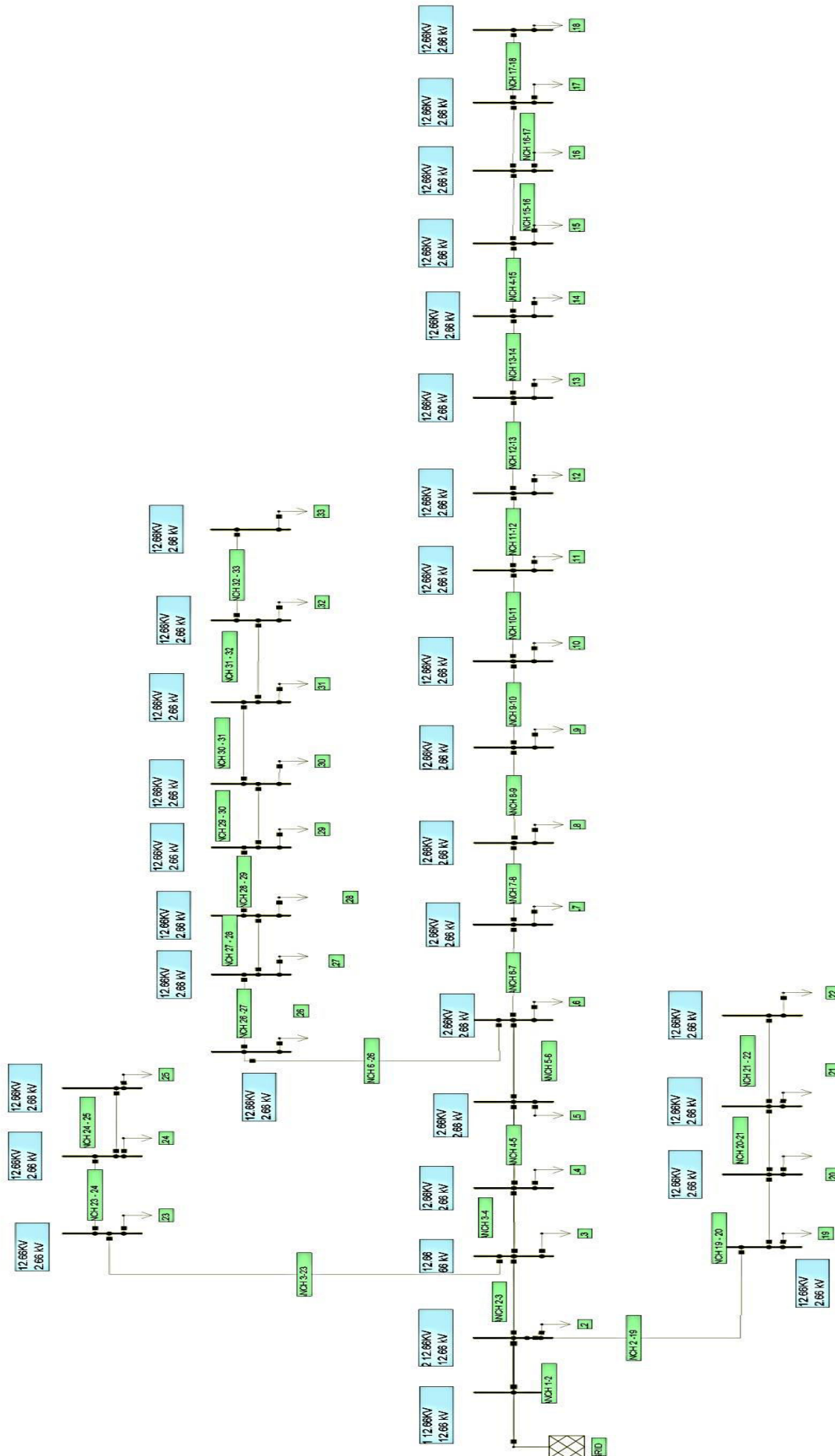


Figure 3.14: Single line diagram of IEEE 33-bus radial distribution system in NEPLAN.

Table 3.8: Base case voltage profiles of IEEE 33-Bus Radial Distribut. Sys. (no DG).

| Bus No | U_n (kV) | U (kV) | u (%) |
|--------|------------|--------|--------|
| BUS_1 | 12.66 | 12.660 | 100.00 |
| BUS_2 | 12.66 | 12.625 | 99.72 |
| BUS_3 | 12.66 | 12.505 | 98.77 |
| BUS_4 | 12.66 | 12.419 | 98.10 |
| BUS_5 | 12.66 | 12.334 | 97.43 |
| BUS_6 | 12.66 | 12.133 | 95.84 |
| BUS_7 | 12.66 | 12.089 | 95.49 |
| BUS_8 | 12.66 | 11.918 | 94.14 |
| BUS_9 | 12.66 | 11.839 | 93.51 |
| BUS_10 | 12.66 | 11.765 | 92.93 |
| BUS_11 | 12.66 | 11.754 | 92.84 |
| BUS_12 | 12.66 | 11.735 | 92.69 |
| BUS_13 | 12.66 | 11.658 | 92.08 |
| BUS_14 | 12.66 | 11.629 | 91.86 |
| BUS_15 | 12.66 | 11.611 | 91.72 |
| BUS_16 | 12.66 | 11.597 | 91.60 |
| BUS_17 | 12.66 | 11.571 | 91.40 |
| BUS_18 | 12.66 | 11.564 | 91.34 |
| BUS_19 | 12.66 | 12.618 | 99.67 |
| BUS_20 | 12.66 | 12.573 | 99.31 |
| BUS_21 | 12.66 | 12.564 | 99.24 |
| BUS_22 | 12.66 | 12.556 | 99.18 |
| BUS_23 | 12.66 | 12.580 | 99.37 |
| BUS_24 | 12.66 | 12.497 | 98.71 |
| BUS_25 | 12.66 | 12.455 | 98.38 |
| BUS_26 | 12.66 | 12.114 | 95.68 |
| BUS_27 | 12.66 | 12.088 | 95.48 |
| BUS_28 | 12.66 | 11.985 | 94.67 |
| BUS_29 | 12.66 | 11.912 | 94.09 |
| BUS_30 | 12.66 | 11.879 | 93.83 |
| BUS_31 | 12.66 | 11.827 | 93.42 |
| BUS_32 | 12.66 | 11.816 | 93.33 |
| BUS_33 | 12.66 | 11.812 | 93.30 |

As it can be observed almost all buses except from one retain voltage values lower than their nominal values, but seventeen buses violate the lower limit of 95 %. From these seventeen buses only bus 6, bus18 and bus 33 are candidates for the placement of DG units, in an effort to improve the voltage profiles and reduce the power losses of the

network. Bus 18 presents the lowest voltage profile within the network (91.34 %), bus 33 presents the lowest voltage profile in the second longest branch of the network and bus 6 presents a voltage profile within limits but has been selected for its “nodal”/strategically point within the network.

Table 3.9: Base case power losses of IEEE 33-Bus Radial Distribution Sys. (no DG).

| Line Name | P_{loss} (MW) | Q_{loss} (MVar) |
|------------------|------------------------------|--------------------------------|
| BRANCH-1 | 0.0107 | 0.0054 |
| BRANCH-2 | 0.0231 | 0.0118 |
| BRANCH-3 | 0.0159 | 0.0081 |
| BRANCH-4 | 0.0148 | 0.0075 |
| BRANCH-5 | 0.0301 | 0.0260 |
| BRANCH-6 | 0.0019 | 0.0062 |
| BRANCH-7 | 0.0116 | 0.0083 |
| BRANCH-8 | 0.0041 | 0.0030 |
| BRANCH-9 | 0.0035 | 0.0025 |
| BRANCH-10 | 0.0005 | 0.0002 |
| BRANCH-11 | 0.0009 | 0.0003 |
| BRANCH-12 | 0.0026 | 0.0021 |
| BRANCH-13 | 0.0007 | 0.0009 |
| BRANCH-14 | 0.0004 | 0.0003 |
| BRANCH-15 | 0.0002 | 0.0002 |
| BRANCH-16 | 0.0002 | 0.0003 |
| BRANCH-17 | 0.0001 | 0.0000 |
| BRANCH-18 | 0.0008 | 0.0007 |
| BRANCH-19 | 0.0107 | 0.0054 |
| BRANCH-20 | 0.0001 | 0.0001 |
| BRANCH-21 | 0.0000 | 0.0001 |
| BRANCH-22 | 0.0031 | 0.0021 |
| BRANCH-23 | 0.0050 | 0.0039 |
| BRANCH-24 | 0.0012 | 0.0010 |
| BRANCH-25 | 0.0015 | 0.0008 |
| BRANCH-26 | 0.0018 | 0.0009 |
| BRANCH-27 | 0.0060 | 0.0053 |
| BRANCH-28 | 0.0039 | 0.0034 |
| BRANCH-29 | 0.0017 | 0.0009 |
| BRANCH-30 | 0.0015 | 0.0015 |
| BRANCH-31 | 0.0002 | 0.0002 |
| BRANCH-32 | 0.0000 | 0.0000 |
| Total | 0.14830 | 0.10420 |

Each one of the seven DG units of Table 3.1 has been connected to bus 6, bus 18 and bus 33 of the distribution network and a load flow analysis has been conducted. In total twenty one load flow analyses have been conducted and the results are presented in Figures 3.15 – 3.20. Figure 3.15 presents the voltage levels of all buses of the system when PV DGs are connected at bus 6, Figure 3.16 presents the voltage levels of all buses of the system when PV DGs are connected at bus 18, while Figure 3.17 presents the voltage levels of all buses of the system when PV DGs are connected at bus 33.

Similarly, Figure 3.18 presents the voltage levels of all buses of the system when wind generator DGs are connected at bus 6, Figure 3.19 presents the voltage levels of all buses of the system when wind generator DGs are connected at bus 18 and Figure 3.20 presents the voltage levels of all buses of the system when wind generator DGs are connected at bus 33.

The results show that both DG types (PV that injects real power to the network and wind generator that injects real power to the network but consumes reactive power) have a significant impact to the voltage profiles of the buses. In all examined cases the DG PV units have increased the voltage levels, with this increase to be proportional to the DG PV unit capacity. On the other hand the DG wind generator units had presented a totally different impact on the voltage profiles of the distribution network. The improvement that has been achieved in the voltage profiles was not proportional to the DG wind generator unit capacity. The smallest sized wind generator DG unit (1.65 MW) has slightly improved the voltage profiles of all buses, while the largest sized wind generator DG unit (3 MW) presented a better improvement in voltage profiles from the 2 MW wind generator DG unit, only when was connected at bus 6 (middle point of the network). In the other two positions the improvement that was achieved from the 2 MW wind generator DG unit was much better than this of the 3 MW wind generator DG unit that has caused in several buses undervoltages much below from the acceptable lower limit. Finally something that concerns both types of DG units (PV and wind generator) and has been observed throughout the studies is that the connection position of DG unit is of paramount importance, not only to the bus that the DG is connected and to its neighboring buses, but also for the whole network since it can result to a totally different performance.

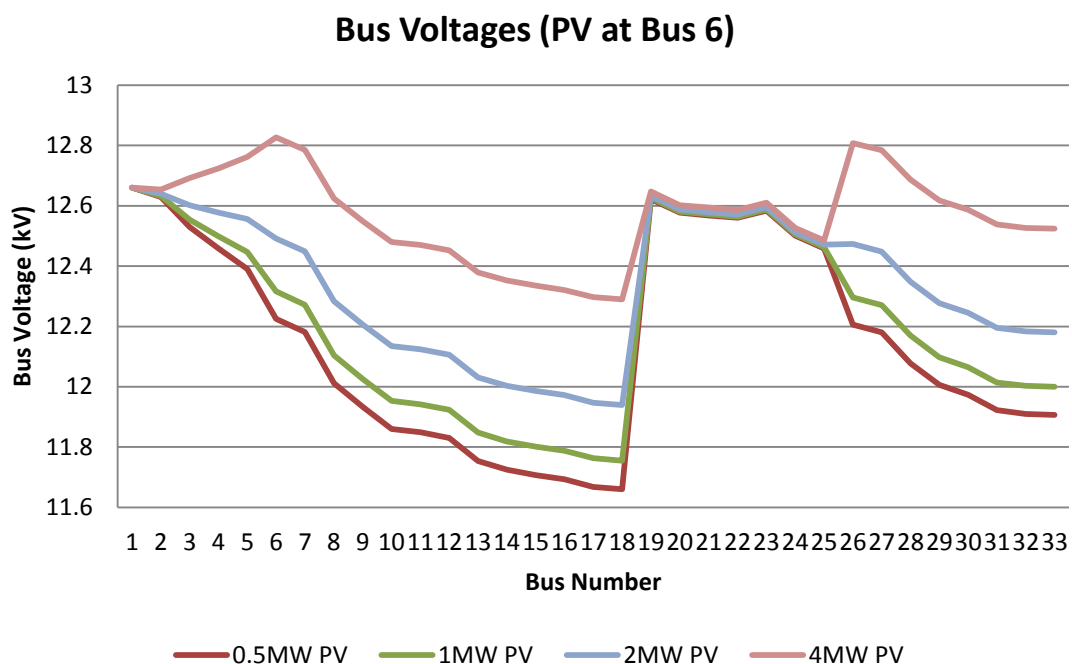


Figure 3.15: Voltage profiles of network buses when a DG PV unit has been connected at bus 6.

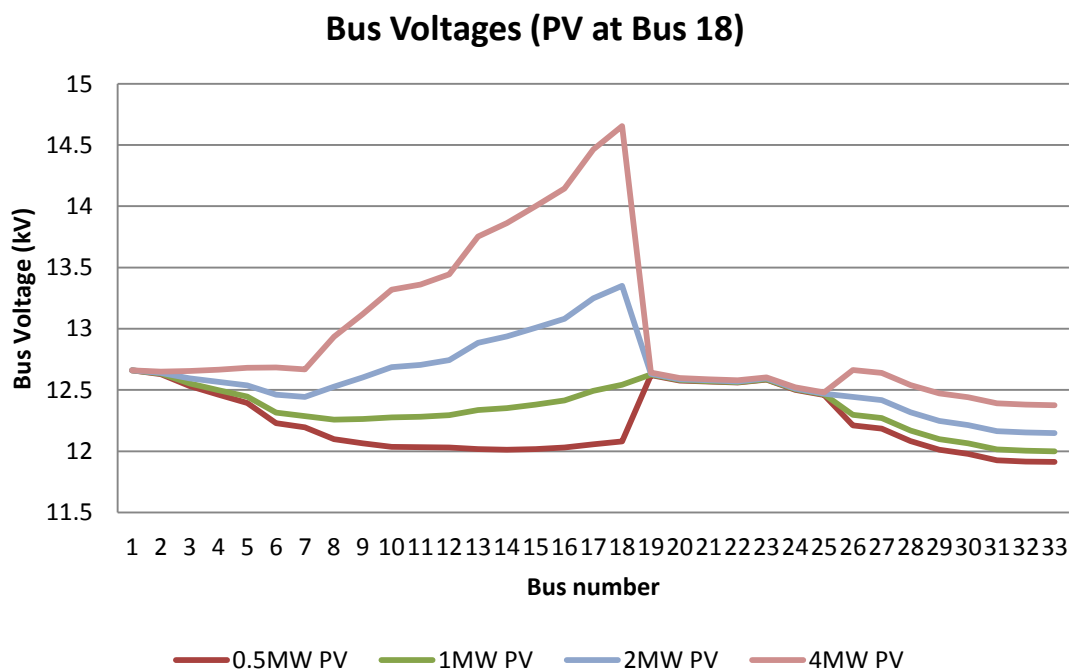


Figure 3.16: Voltage profiles of network buses when a DG PV unit has been connected at bus 18.

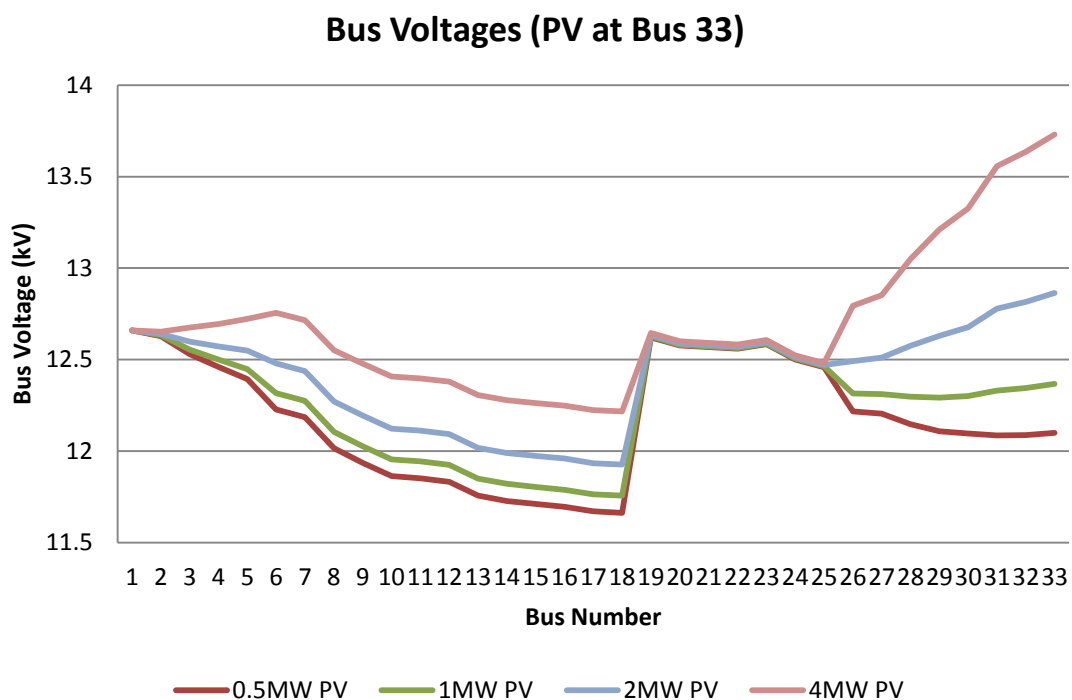


Figure 3.17: Voltage profiles of network buses when a DG PV unit has been connected at bus 33.

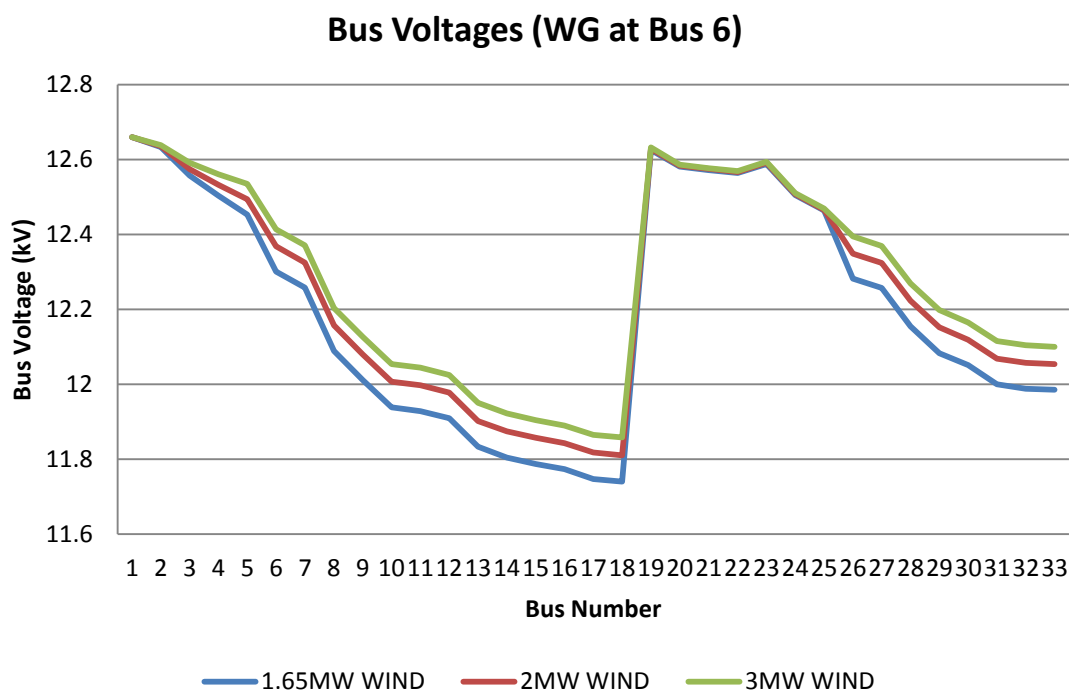


Figure 3.18: Voltage profiles of network buses when a DG wind generator unit has been connected at bus 6.

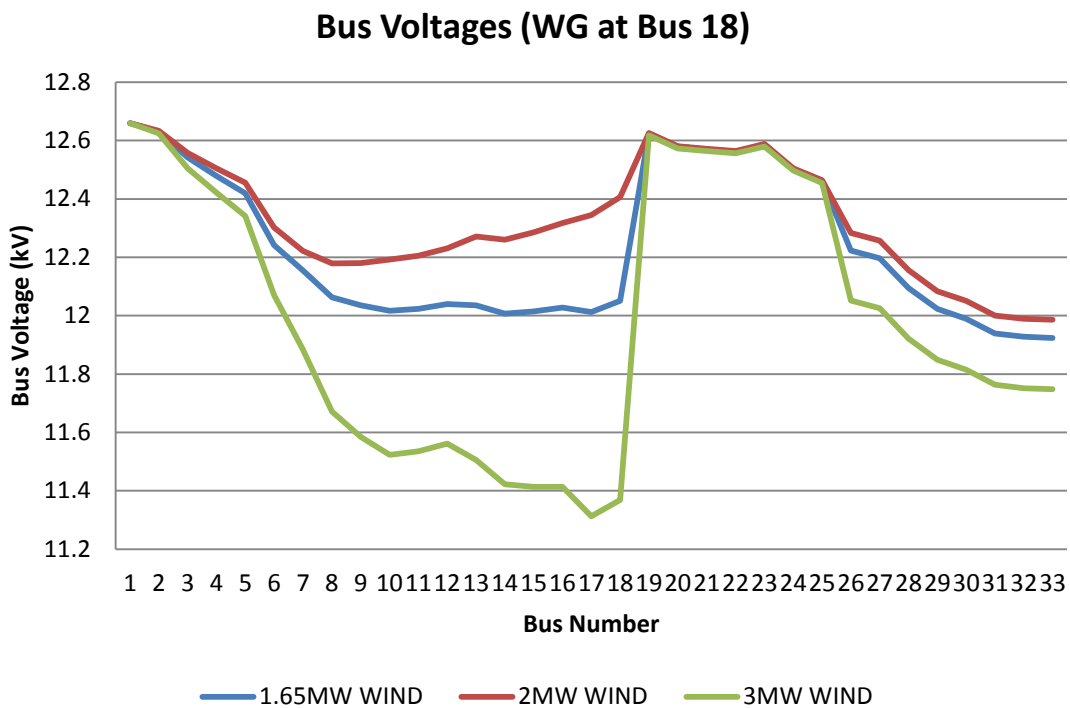


Figure 3.19: Voltage profiles of network buses when a DG wind generator unit has been connected at bus 18.

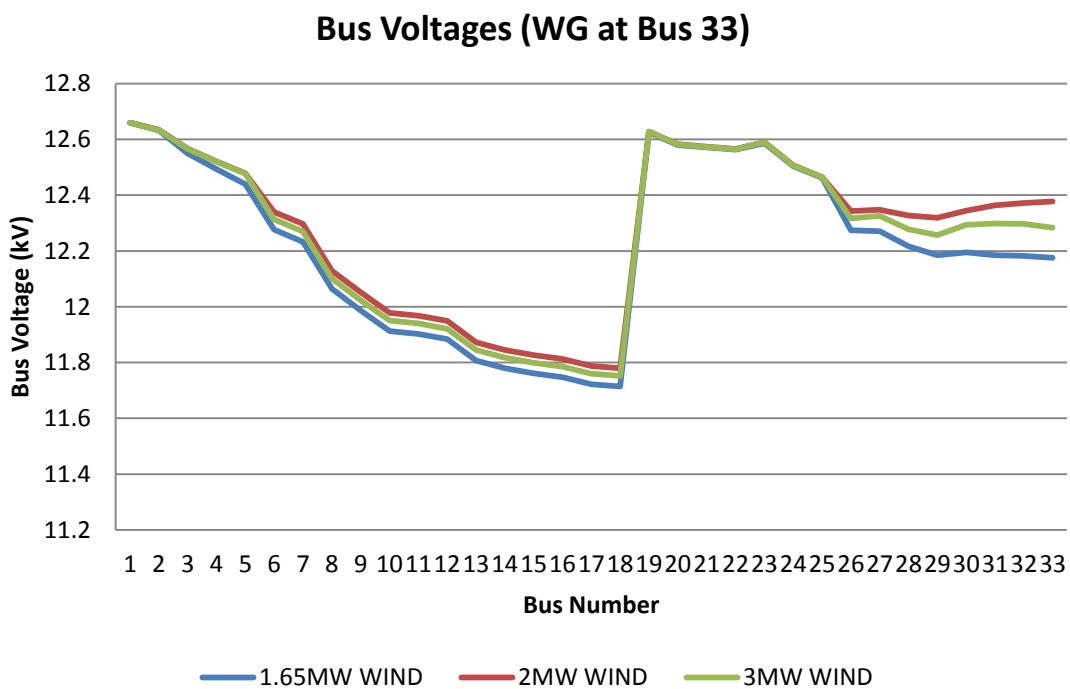


Figure 3.20: Voltage profiles of network buses when a DG wind generator unit has been connected at bus 33.

Figure 3.21 presents the total network real power losses, Figure 3.22 presents the total network reactive power losses and Figure 3.23 presents the total network apparent power losses of all lines of the network when PV DG units are connected at different buses.

Similarly, Figure 3.24 presents the total network real power losses, Figure 3.25 presents the total network reactive power losses and Figure 3.26 presents the total network apparent power losses of all lines of the network when wind generator DG units are connected at different buses.

The results have shown that the size of the connected DG, independently from the DG type, plays an important role in the total network power losses since it has been observed that the bigger the size of the DG the bigger the impact on the total network power losses of the system. Furthermore, the position that is installed the DG unit (of any type) is of paramount importance, since its influence on the total power losses of the network (both real and reactive) is totally different. Moreover it has been observed that the impact to the total power losses is proportional to the size of the DG unit.

More specifically the examined PV DG units have succeeded to reduce both real and reactive power losses only when they have been connected in bus 6 (middle point of the network). In the other positions all different PV DG unit sizes have resulted in the increase of both total real and reactive power losses of the system, except the 0.5 MW unit, that has resulted almost the same amount of system's total real and reactive power losses.

On the other hand none of the examined wind generator DG units have succeeded to reduce the total real and reactive power losses of the system, except of the case where the 1.65 MW DG unit has been connected in bus 6 (middle point of the network). The installation of the rest examined wind generator DG units, to the selected positions of the distribution network, have resulted in a huge increase of the total system real and reactive power losses.

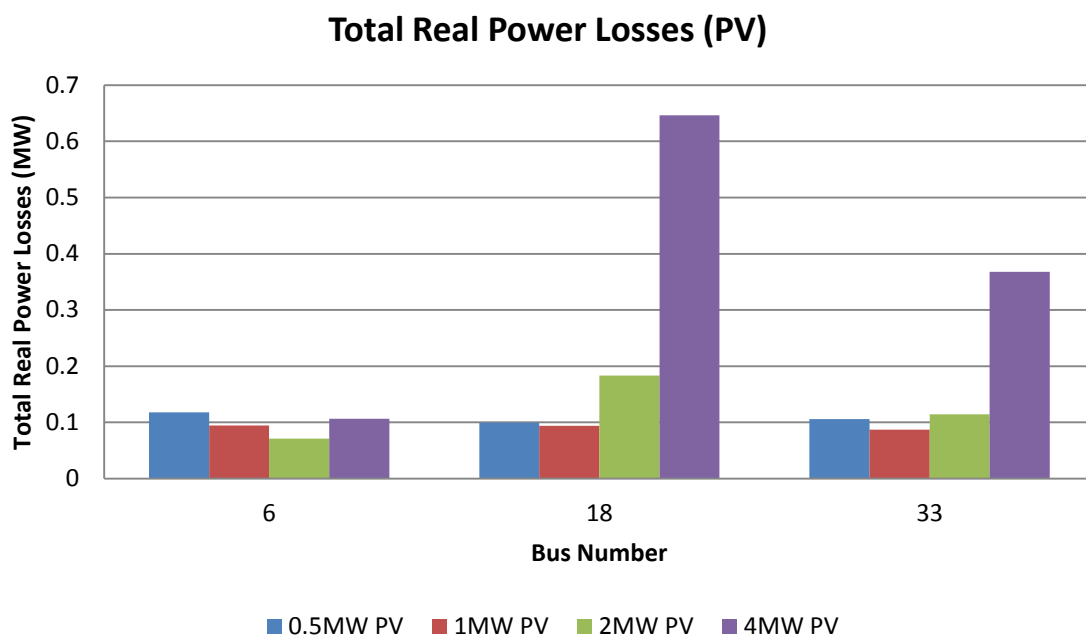


Figure 3.21: Total network real power losses when DG PV units have been connected at different buses.

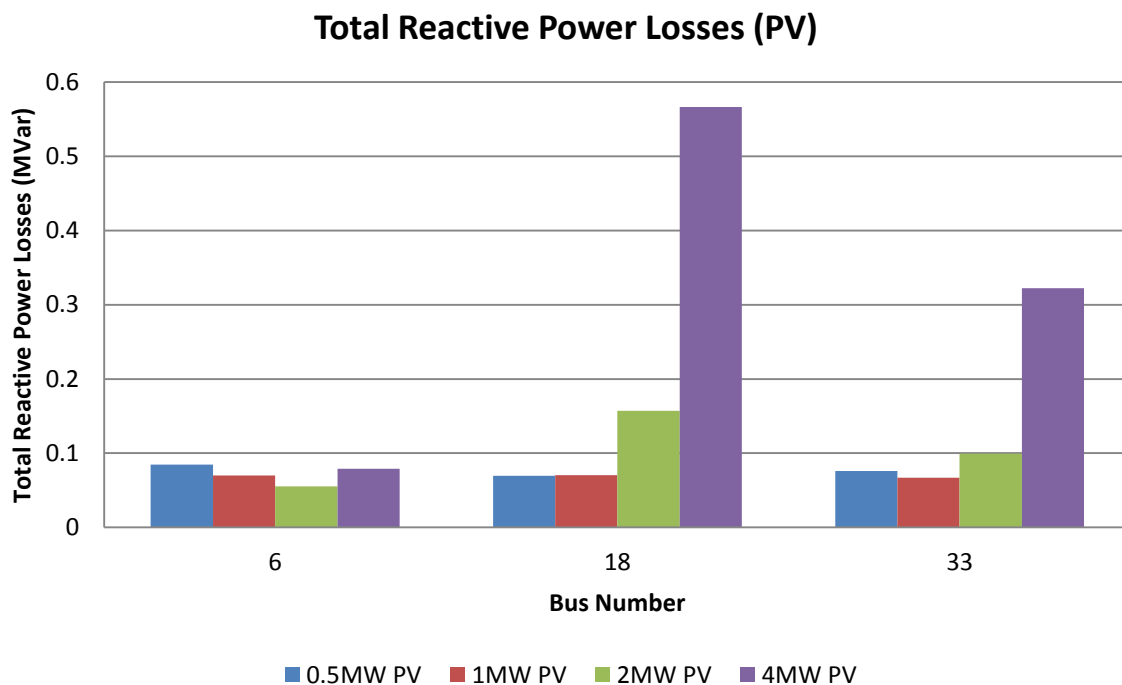


Figure 3.22: Total network reactive power losses when DG PV units have been connected at different buses.

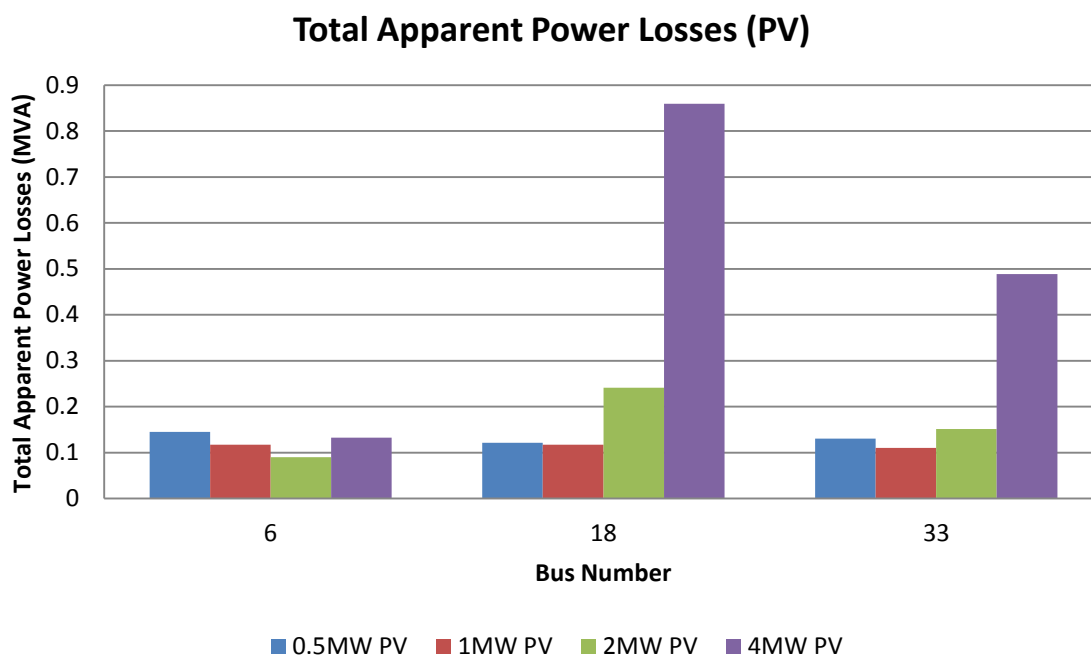


Figure 3.23: Total network apparent power losses when DG PV units have been connected at different buses.

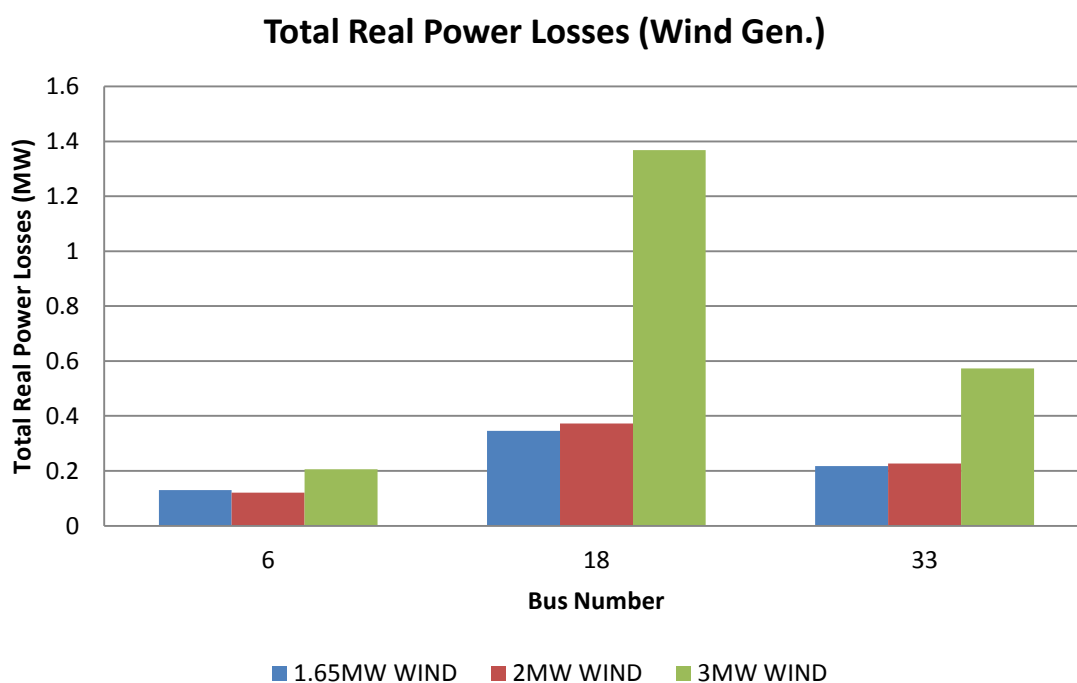


Figure 3.24: Total network real power losses when DG wind generator units have been connected at different buses.

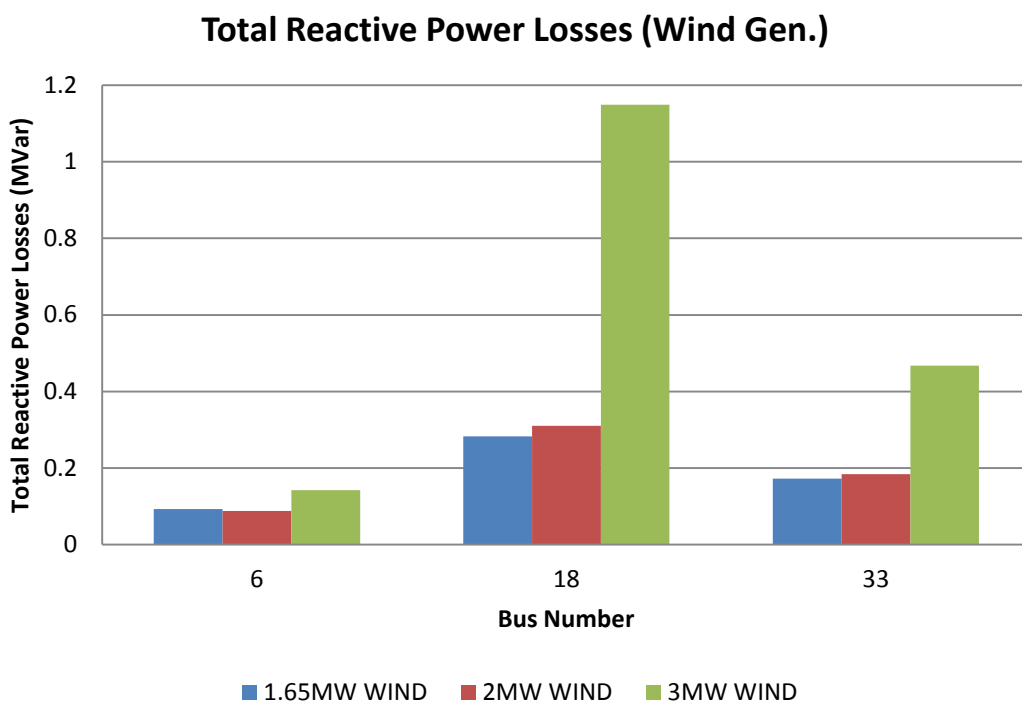


Figure 3.25: Total network reactive power losses when DG wind generator units have been connected at different buses.

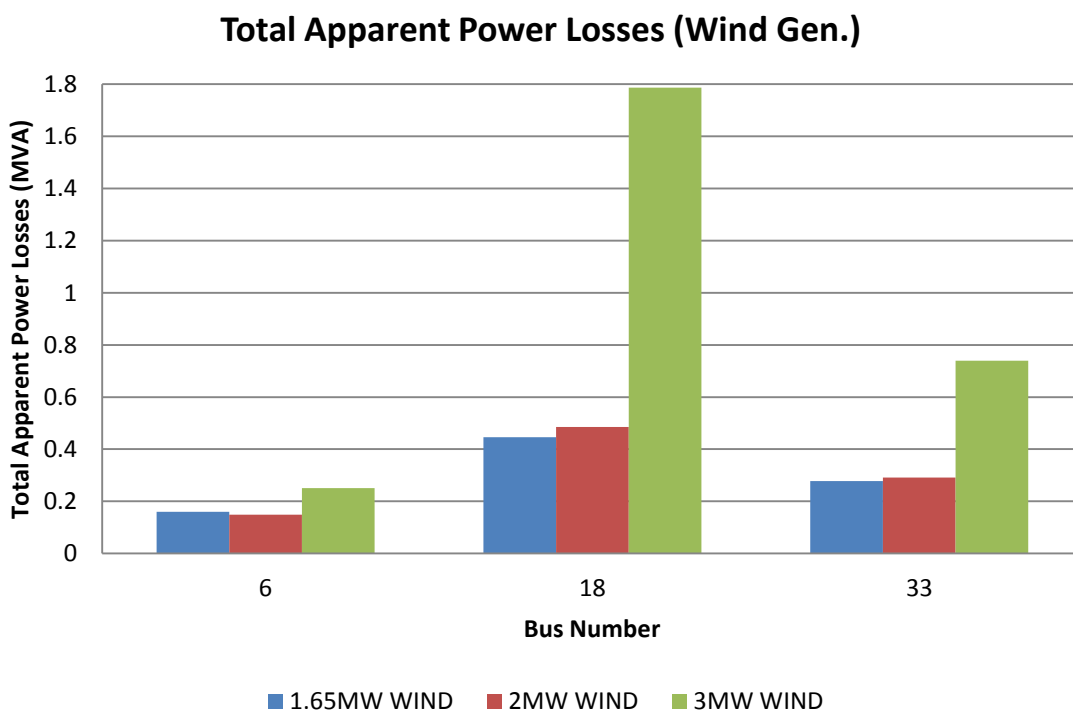


Figure 3.26: Total network apparent power losses when DG wind generator units have been connected at different buses.

3.5 Development of a Decision Making Algorithm for the Optimum Size and Placement of DG in Distribution Networks

A decision making algorithm for the optimum size and placement of a DG unit in distribution networks has been developed. The algorithm that is relative simple, flexible to changes and modifications can estimate the optimum DG size and can define the optimal location for a DG unit (of any type) to be installed, based on the improvement of voltage profiles and the reduction of the network's total real and reactive power losses. The algorithm has been implemented in MATLAB and the load flow analysis is performed with the use of NEPLAN, one of the most reliable power systems software.

The flow chart of the developed decision making algorithm is presented in Figure 3.27, and has the following structure:

Step 1: Define Network Model, Distributed Generation (DG) parameters, and number of test DGs.

Step 2: Perform Load Flow analysis to obtain steady-state base case parameters for Bus voltages and line losses.

Step 3: Sort Buses in ascending order of voltage deviation from nominal voltage for DG placement in the same order.

Step 4: For each test DG, connect DG at given Bus, Perform Load flow analysis and store results as a scenario.

Step 5: Repeat Step 4 for every Bus in ordered list.

Step 6: Sort all Load flow scenario results for all DGs placed at all buses according to lowest line losses or best voltage profile.

Step 7: Select scenario with lowest line losses or best voltage profile for optimum DG size and placement.

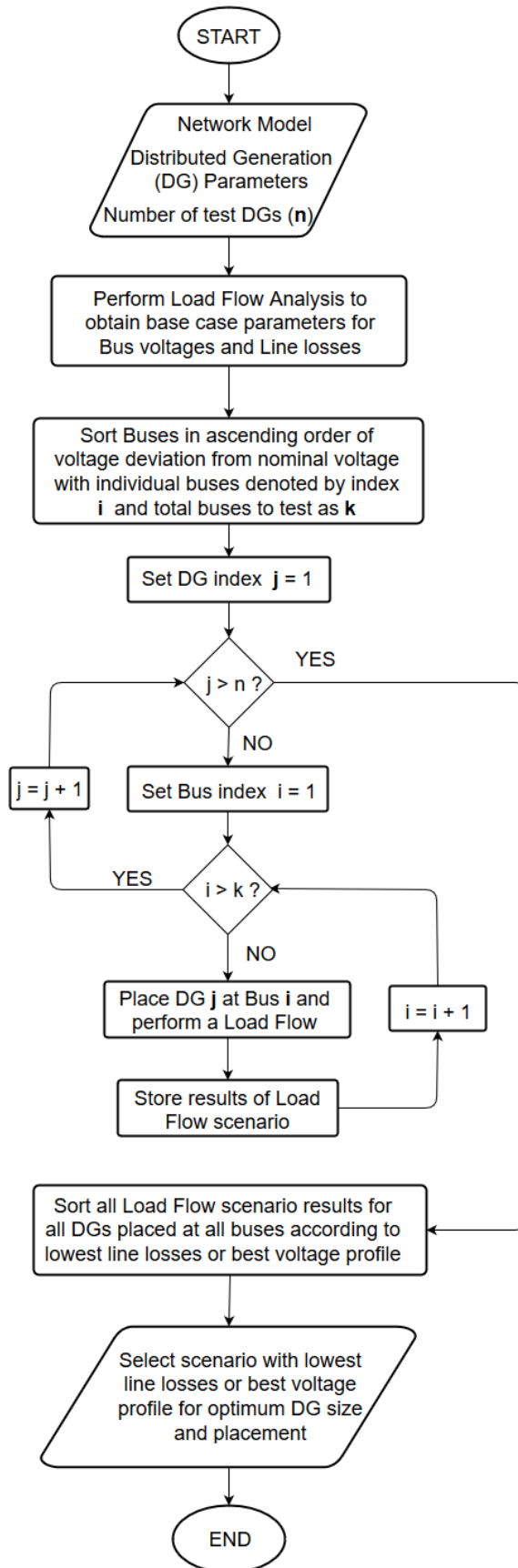


Figure 3.27: The flow chart of the proposed decision making algorithm.

3.6 Conclusions

This chapter analyses the studies that have been conducted on voltage profiles and total real and reactive power losses of two typical and widely implemented distribution systems, i.e., the IEEE 14-bus network system, and the IEEE 33-bus radial distribution system. A methodology has been applied to both networks where seven different DG units of different type and size have been installed at selected positions for both networks, targeting to observe improvements on the voltage profiles and reduction in the network's total power losses. The produced results have demonstrated that the size of a DG unit is strongly associated with the type of the examined network and with its installation location. Finally, a simplified decision making algorithm for the optimum size and placement of DGs in distribution networks has been developed and has been implemented.

3.7 References

- [1] Reddy SC, Prasad PVN, Laxmi AJ, Power quality and reliability improvement of distribution system by optimal number, location and size of DGs using Particle Swarm Optimization, 7th IEEE International Conference on Industrial and Information Systems (ICIIS), Chennai, India, 2012.
- [2] Jamian JJ, Mustafa MW, Mokhlis H, Abdullah MN, Comparative study on distributed generator sizing using three types of particle swarm optimisation, Proc. 2012 Third International Conference on Intelligent Systems Modelling and Simulation (ISMS), Kota Kinabalu, pp. 131-136, 2012.
- [3] Kotb MF, Shebl KM, El Khazendar M, El Husseiny A, Genetic algorithm for optimum siting and sizing of distributed generation, Proc. 14th Int. Middle East Power Systems Conference, Cairo University, Egypt, pp. 433-440, 2010.
- [4] Moradi M, Abedini M, A combination of genetic algorithm and particle swarm optimization for optimal DG location and sizing in distribution systems, Electrical Power and Energy Systems, vol. 34, pp. 66-74, 2011.
- [5] Yadav PS, Srivastava L, Optimal location of combined DG and capacitor for real power loss minimization in distribution networks, International Journal of Electrical and Electronics Engineers, vol. 7, no.1, pp.222-233, 2015.

- [6] Parizad A, Khazali A, Kalantar M, Optimal placement of distributed generation with sensitivity factors considering voltage stability and losses indices, Proc. 18th Iranian Conference on Electrical Engineering (ICEE), Isfahan, Iran, pp. 848-855, 2010.
- [7] Injeti SK, Kumar NP, Optimal planning of distributed generation for improved voltage stability and loss reduction, International Journal of Computer Applications, vol. 15, no.1, pp. 40-46, 2011.
- [8] Naik GS, Khatod DK, Sharma MP, Optimal allocation of distributed generation in distribution system for loss reduction, Proc. IACSIT Coimbatore Conference, Singapore, vol. 28, pp. 42-46, 2012.
- [9] Shaaban M, Petinrin JO, Sizing and sitting of distributed generation in distribution systems for voltage improvement and loss reduction, International Journal of Smart Grid and Clean Energy, vol. 2, no. 3, pp. 350-356, 2013.
- [10] Safigianni AS, Koutroumpezis GN, Poulivos VC, Mixed distributed generation technologies in a medium voltage network, Electrical Power Systems Research, vol. 96, pp. 75-80, 2013.
- [11] Balamurugan K, Srinivasana D, Reindlb T, Impact of distributed generation on power distribution systems, PV Asia Pacific Conference, Energy Procedia, vol. 25, pp. 93-100, 2012.
- [12] NEPLAN AG, <http://www.neplan.ch/>.
- [13] Viral R, Khatod DK, Optimal planning of distributed generation systems in distribution system: A review, Renewable and Sustainable Energy Reviews, vol. 16, pp. 5146-5165, 2012.
- [14] Vestas Wind Systems A/S, General specification, V82-165MW, V100-2MW, V90-3MW, www.vestas.com.
- [15] University of Washington, Power Systems Test Case Archive, <https://www.ee.washington.edu/research/pstca/>.
- [16] Kashem MA, Ganapathy V, Jasmon GB, Buhari MI, A novel method for loss minimization in distribution networks, International Conference on Electric Utility Deregulation and Restructuring and Power Technologies, London, United Kingdom, pp. 251-256, 2000.

Chapter 4

Syntactic Pattern Recognition of Power System Signals

4.1 Introduction

This chapter presents a hardware implementation for the real-time syntactic pattern recognition of power system waveforms that will be applied to the implementation of a protective relay that would efficiently prevent safety problems and economic losses caused by faults presented in power systems (distribution and transmission networks). The way that syntactic methods are applied to the recognition of power system signals and to the calculation of its parameters has thoroughly been examined and solution to the sub problems of selecting primitive patterns, defining a linguistic representation and formulating a pattern grammar is presented. The model used in order to formulate the pattern grammar is that of Attribute Grammars that are able to handle syntactic as well as semantic rules. Consequently, the proposed system is based on a proposed extension of Earley's parallel parsing algorithm. The proposed architecture was described in Hardware Description Language (HDL - Verilog), simulated in order to validate its functionality, synthesized on an XILINX FPGA board system and tested using waveforms and data provided by the Independent Power Transmission Operator (IPTO) in Greece.

4.2 Research Incentives

Power systems are large and complex systems where faults frequently occur that may cause safety problems to personnel, as well as to equipment, and lead to significant economic losses. An efficient protective relay would efficiently prevent these problems and losses. According to [1] microprocessor-based digital protective relays significantly improve protection relays since: i) the time needed to estimate the criteria

signals is shorter, ii) high accuracy may be achieved regarding the way input signals are filtered-out, iii) sophisticated corrections are applicable, iv) the protective relay can easily communicate and exchange data with systems connected to network responsible to protect and control, and v) the system may execute numerous self-monitoring tasks. Nevertheless, regarding safety, dependability and performance digital relays did not significantly improve system protection; as digital relays are based on the main principles using the criteria known for decades. In addition, safety, dependability and performance problems mainly are caused by balance between the safety demand, and performance and the dependability requirements. In case secure as possible regarding its algorithm, then it is proved to operate slowly. While, in case a relay is designed to react as fast as possible, it tends to operate incorrectly. There are basically two key factors that influence the limited recognition power of the classical relaying principles. First one is to improve the recognition process itself, while the second way is to increase the performance of the implementation. Previous approaches [1] in facing the problem of improving protective relays in power systems were mainly software implementations based on artificial neural networks.

In this chapter, with respect to the first key factor, the methodology of Syntactic Pattern Recognition (SPR) is followed and with respect to the second key factor, an efficient hardware implementation on FPGA (Field Programmable Gate Array) is proposed. Based on the up today publications in the technical literature, this is the first time that power system signals are recognized based on SPR techniques executed on a dedicated embedded system.

Attribute Grammar may be the underlying model of designing a system for the aforementioned application. In [1-7] the methodologies based on Artificial Intelligence (AI) applied to power system protection are reviewed and the application of artificial neural networks and fuzzy logic techniques is presented. A considerable number of applications and concepts have been presented including fuzzy logic approach to differential transformer protection and artificial neural networks application to the transformer protection, CT (current transformer) and CVT (capacitor voltage transformer) transients correction, and fault-type classification. However, the implementations presented are software approaches and do not succeed the maximum

possible performance. In [8] a real-time system implemented on an FPGA board is presented that tracks time varying waveforms distortions in power systems based mainly on a proposed amplitude tracking algorithm derived from amplitude demodulation. However, the frequency of the fundamental signal is assumed constant but in power systems, the fundamental frequency of the current and voltage is not always exactly the nominal value.

Although the SPR appears appropriate to the problem of protection relays and the calculation of power system signals' parameters, insufficiently progress has been made up to the present time [1]. The proposed methodology presents the application of the SPR method to recognition of power systems waveforms and to the measurement of power system parameters.

In the field of SPR, the recognition part is that of parsing an input string derived from the linguistic representation of the input signal using a predefined grammar, titled pattern grammar. The pattern grammar describes the patterns to be recognized in a formal way. One of the main sub tasks in any SPR application is the formulation of the pattern grammar. The proposed project methodology aims to give solutions to the sub problems of primitive pattern selection, linguistic representation, and pattern grammar formulation for the waveforms received by a protection relay. On top of that, a parallel hardware attribute evaluator, dedicated to power system signals is presented. In the case of power systems waveforms where additional morphologies may appear due to errors and numerous parameters' calculations should to be executed, grammars that may describe syntax and semantics as well are essential tools for the building of the pattern grammar. Hence, an efficient attribute grammar evaluator that parses the produced by the signal input strings is essential. The contribution of this chapter is summarized at the following:

- I. Define the linguistic representation of waveforms received by a protection relay.
- II. Define an attribute grammar capable of modeling the power system signals using the linguistic representation of point I.
- III. Design an efficient attribute grammar evaluator based on a proposed extension of Earley's [9] parallel parsing algorithm using the architecture presented in [10] for the application specific proposed grammar.

The proposed architecture was described in Verilog, simulated in order to validate its functionality, synthesized on an XILINX FPGA board system and tested using waveforms and data provided by the Independent Power Transmission Operator (IPTO) [12] in Greece.

4.3 Literature Review

In the following sub sections theoretical issues regarding grammars and parser implementations will be analyzed, in order to introduce the reader to necessary basic concepts useful in the following sections.

4.3.1 Languages and Grammars

Every formal language can be described using a grammar, which is a set of syntax rules for string construction. These rules describe how valid strings can be generated according to the language's syntax. All grammars have been classified by Noam Chomsky [13] in four major categories, known as the Chomsky hierarchy. One important category is that of Context Free Grammars (CFG), which can easily be extended with attributes or actions in order to handle probability evaluation.

4.3.1.1 Context Free Grammars

A CFG [14] G can be defined as a set $G=(N, T, P, S)$, where N is the set of non-terminal symbols, T is the set of terminal symbols, P is the set of grammar rules and S ($S \in N$) is the start symbol - the root of the grammar. $V = N \cup T$ is defined as the vocabulary of the grammar. Grammar rules are written in the form $B \rightarrow \gamma$, where $B \in N$ and $\gamma \in V^*$ (string consisting symbols from V). Typically, capital letters A, B, C, \dots denote non-terminal symbols, lowercase a, b, c, \dots terminal symbols, Greek lowercase $\alpha, \beta, \gamma, \dots$ strings of terminals and non-terminals. The notation $\alpha \beta$ means that β can be derived from α by applying rules of P . Every derivation begins with a sequence that consists only of the start symbol S ; otherwise it is called partial derivation. In each derivation step, either the leftmost or the rightmost non-terminal symbol of the string is replaced by the right hand side (RHS) of a production rule that has the specific non-terminal at its left hand side (LHS). The same procedure should be followed until there are no more non-terminal symbols left in the string but on the contrary it consists of

only terminal symbols. Parsing is the task of examining a string of symbols for syntactic accuracy. Recognizer is the algorithm that determines if an input string $\alpha = a_1a_2a_3 \dots a_n$ (string length equals to n) may be produced by a given grammar. In case recognizer produces a parse tree as well, then the algorithm is a parser. The parse tree is an ordered tree with root S , leaves the terminal symbols of input string, and nodes the syntactic rules that participate in the derivation process.

4.3.1.2 Augmenting Context Free Grammars

The expressive capabilities of CFGs may be augmented by associating attributes to each symbol of the grammar. The attribute signifies an explicit context-sensitive property of the corresponding symbol. This augmented CFG is called Attribute Grammar (AG) and is also defined as a set $AG = (G, A, SR, d)$, where G is a CFG, $A = \cup A(K)$ where $A(K)$ is a finite set of attributes. Symbolization $K.w$ represents an attribute w of symbol K . $A(K)$ is divided into two separate sets; $AS(K)$ is the set of synthesized attributes and $AI(K)$ is the set of inherited attributes. Attributes whose values are calculated using attributes at descendant nodes are called synthesized attributes. Attributes whose values are calculated using attributes at the parent and left nodes inherited attributes. No inherited attributes are assigned to the start symbol. Each of the syntactic rule of the CFG consists of semantic rules $SR(p)$ that define attributes according to other attributes of terminals and on terminals existing in the same syntactic rule. Function $d(\alpha)$ returns the domain of the attribute α . The method attributes will be calculated depends both on the tree traversal methodology and the attributes' dependencies to other attributes.

4.3.2 Parsing Algorithms and Implementations

Numerous parsing algorithms have been presented in the literature. A considerable number of parser implementations are mainly based on three widely known parsers presented by Cocke-Younger-Kasami (CYK) [15], Earley [9], and GLR [16] and their modifications [17-19] and improvements via parallelization [20, 21].

The CYK and Earley algorithms are “almost” identical [17] regarding complexity, since both use “dynamic programming” methods in which derivations matching longer portions of the input are built up by concatenating previously computed derivations

matching shorter portions. However the CYK algorithm necessitates the grammar to be represented using Chomsky Normal Form (CNF). This prerequisite is not limiting the general form of the CYK algorithm as all CFG can be represented in CNF. However, the transformation of a CFG G into an equivalent one in CNF G' may not be accomplished without a penalty. The size of the a grammar G' after the transformation in CNF can be at worst case of size $|G'| = |G|^2$ [22-24], where $|G|$ is the size of the CFG, defined as $\sum_{r \in P} |r|$, where $|r|$ is the length of rule r , i.e. the number of right hand side symbols (rhss) plus 1 (the left hand side symbol - lhss). However, the transformation time does not affect the performance of an algorithm as this transformation occurs only one time at the pre-computational level and the transformation time does not affect the execution time of the system and it is actually minor in relation to the other tasks of the same level. Yet, in case the produced grammar G' is greater than G , the execution time will radically increase, since it is grammar size ($|G'|$) depended. Furthermore, in case a grammar transformation is not necessary, along with the proposed automation of the design process, the pre-computational level consists only the task of hardware synthesis.

Both Earley and GLR algorithms can parse any CFG, examine the input string from left to right and do not need any backtracking during the parsing process. They are mainly used for the recognition of natural languages and can also be used for CFG that are ambiguous or need infinite look-ahead. They both have time complexity of $O(n^3)$ in general and have the time complexity of $O(n)$ for LR(k) grammar. In case the grammar is highly ambiguous and SCFG (Stochastic Context Free Grammar) is used, the time complexity of GLR is higher than Earley's algorithm. However, GLR is preferable for parsing applications such as software reverse engineering [19] and communication protocols [25]; to the best of the author knowledge there is no hardware implementation for the GLR parser.

Taking into consideration the above mentioned comparisons, the efficient hardware implementation of Earley's algorithm presented in [21] as well as the fact that main intention is to implement hardware parser for power system signals augmented with attributes, where this algorithm is more suitable, the proposed implementation is based on [9].

4.3.2.1 Earley's Parsing Algorithm

A top-down parser was presented in 1970 by Earley [9], using a symbol “.” called dot (implicitly known before Early) in all rules (called dotted rule). The value of the dot is to separate the rhss of the rule into two subparts. For the subpart on the left of the dot, it has been verified that it can generate the input string (or substring) examined so far. However, for the subpart on the right of the dot, it still remains to be checked whether or not it can generate the rest of the input string. When the dot is at the last position, the dotted rule is called *completed* [9]. Earley's algorithm makes use of three operations, known as predictor, completer and scanner. The algorithm examines the input string $\alpha = a_1 a_2 a_3 \dots a_n$ from left to right. While an input string symbol a_i is examined, a new set S_i of states is built that signifies the progress of the recognition process at this point of recognition. Earley's algorithm constructs $(n+1)$ sets (numbered from 0 to n). Every state is a triple $\{r, j, f\}$ where r is the rule enumeration, j represents the position of the dot in the rule and f shows the set that the state was first created. Each state may be represented using the formalism $i: {}_f X \rightarrow \zeta.Y\mu$, i.e. the syntax rule $X \rightarrow \zeta Y \mu$ with the dot in the j th position ($|\zeta|=j$) that was created in the f_{th} set belongs to set S_i . Earley's top-down parser is a dynamic programming procedure, which in each step computes all the sets of states that have recognized a part of the input and are possible states to recognize the whole input string. While the input symbols are read one after the other, new sets that consist of dotted rules are built. By applying the three operations to each set of states, the existence of the dotted rule $S \rightarrow \zeta.$, signifies that the input string is a sentence of the grammar.

The predictor operation checks if there is a state in the set that has a non-terminal symbol right after the dot and adds to this set all the rules that have this non-terminal at their left part adding first a dot at the beginning of the right part of the rule.

The completer operation checks if there is a state in the set that contains a completed dotted rule. The completer compares the non-terminal symbol at the left part of that rule (lhss) with the symbol at the right of the dot at each dotted rule that belong to the set indicated by f . If they match (successful completer), completer takes these dotted rules and adds them to the current set, after moving the dot one position to the right in these states.

The scanner operation checks if there is a state in the set that has a terminal symbol to the right of the dot, compares it to the next input symbol, and if they match, scanner adds this dotted rule to the next set but first it moves the dot over the non-terminal symbol.

Path is a series of states connected by predictor, scanner, or completer. A path is considered to be constrained by a string α if the terminals immediately to the left of the dot in all scanned states, in sequence, form the string α .

The operation \otimes that was initially presented by Chiang & Fu [20] may evaluate the order in which dotted rules are generated, during the recognition of the input string. This operation may have as inputs either two sets of dotted rules or a terminal symbol and a set of dotted rules and generates as result a set of dotted rules. Chiang & Fu's [20] version of Earley's [9] algorithm is a parallel parsing algorithm that given of a CFG G recognizes an input string of length n by creating a $(n+1) \times (n+1)$ parsing table PT . The elements $pt(i, j)$ of parsing table PT are sets of dotted rules

4.3.2.2 Hardware Implementations

In [21] an efficient architecture for the hardware implementation of the CFG parsers was presented. The efficiency of this architecture is based on an innovative combinatorial circuit responsible for the implementation of the fundamental operation \otimes . The time complexity of this circuit is $O(\log_2(|G|))$, ($|G|$ represents the size of the CFG). According to this architecture the cells of the parse table were computed in parallel using the presented combinatorial circuit C_{\otimes} . C_{\otimes} is constructed from the "characteristic" equations of the underlying CFG G , which are algorithmically derived. The usage of multiple C_{\otimes} circuits and the union of their outputs lead to the parallel evaluation of $pt(i, j)$. Consequently, there are two levels of parallelism i) a cell-level parallelism i.e. the parallel execution of the \otimes operations for each cell and ii) an architecture-level that corresponds to the tabular form of Earley's algorithm. The proposed system recognizes an input string of length n in $O(n \log_2(|G|))$ time. Due to the hardware nature of the implementation, the system presented in [21] attains a speed-up factor, compared to software approaches, that equals to two orders of

magnitude for small grammars and to six orders of magnitude for large real life grammars.

Based on the implementation of the combinatorial [21] circuit mentioned above for the syntax part of the attribute grammar, in [26] an efficient implementation of an attribute evaluator system was proposed. A special purpose hardware module was responsible for the semantic part of the Grammar. This module traverses the tree and evaluates the attributes using a stack that permits to achieve the attribute evaluation just by executing simple push and pop operations on particular stacks. Therefore, the presented system is designed using special purpose hardware, increasing the performance, as all sub-modules are synthesized into one FPGA board, reducing needless time for data transportation between sub-modules. In addition portability has been achieved. The hardware nature of the system allows the fast recognition of a considerable number of input strings that should be processed concurrently.

4.4 The Syntactic Approach in Power System Signals

4.4.1 Primitive Pattern Selection

In the literature, there are various segments have been presented as primitive such as lines and triangles. Lines are low level and triangles are difficult to extract. In regards to the linguistic representation of power system signals we have chosen the peak as primitive pattern. Peaks have also been used during recognition of a considerable number of signals such as ECG (ElectroCardioGram) [27]. This choice [28-29] seems to be a natural one because power system signal are mainly sinusoidal. Figure 4.1 shows the. Peak pattern may be defined by three specific points: the left peak boundary, the peak extremum, and the right peak boundary. The left arm of the peak is consisted of all points among the left peak boundary and the peak extremum. The right arm of the peak is consisted of all points among the peak extremum and the right peak boundary. Series of peaks will be represented as $\Pi_1\Pi_2\dots$ where Π_i of i_{st} peak. A peak can be other positive or negative and in what follows it will be symbolized as p or n respectively.

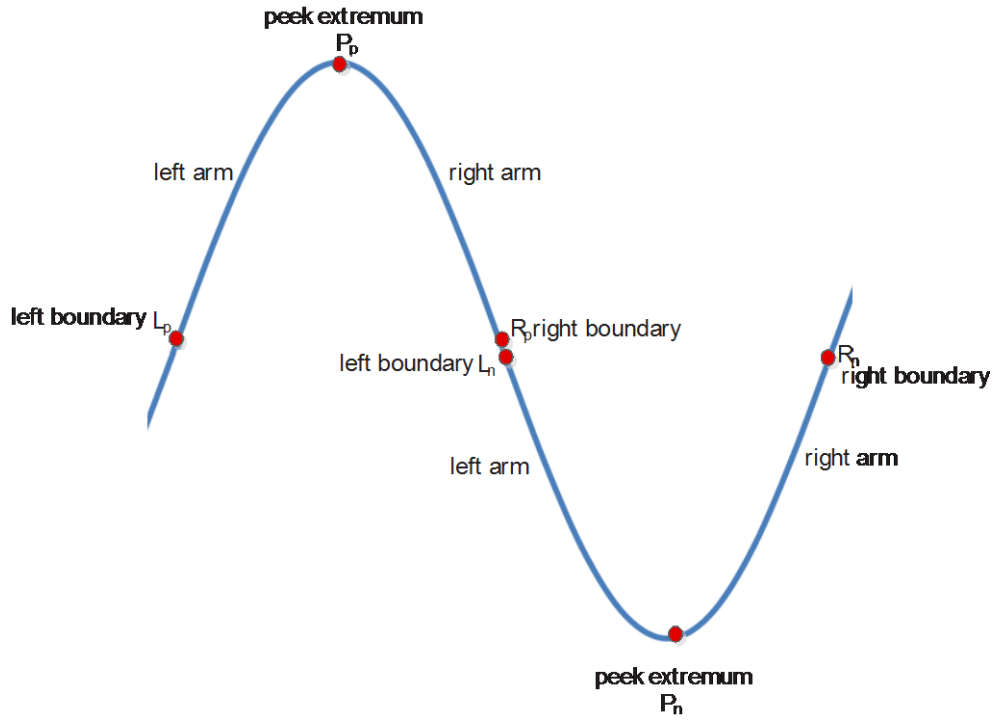


Figure 4.1: Positive and negative peak patterns.

Each sample point of a power system signal is presented as a couple (x_i, y_i) , where y_i is the amplitude in volts or amperes of the sample point i and x_i is the corresponding time. Attributes are assigned to all primitive patterns. Throughout the primitive extraction task the values of these attributes are evaluated in order to be used during the recognition task of the parser. These attributes are used during the recognition of the patterns as well as during the evaluation of their parameters. Consequently, they are used in a quantitative way for qualitative and quantitative purposes. Each peak Π_i has seven attributes. These attributes are symbolized as $\{x_{li}, y_{li}, x_{mi}, y_{mi}, x_{ri}, y_{ri}, e_i\}$, where:

- | | |
|------------------|--|
| x_{li}, y_{li} | coordinates of the left boundary of the peak Π_i . |
| x_{mi}, y_{mi} | coordinates of the peak extremum of the peak Π_i . |
| x_{ri}, y_{ri} | coordinates of the right boundary of the peak Π_i |
| e_i | energy of the peak Π_i defined as: |

$$e_i = \sum_{i=p}^q (y_i - y_{i-1})^2 \quad (4.1)$$

where: $p = x_{li} + 1$ and $q = x_{ri}$

For example, the normal e, i.e., e_{normal} for a sinusoidal, when frequency is equal to 50 Hz and amplitude is 230 V, is 64,428.36.

4.4.2 Linguistic Representation

The alphabet of terminal symbols $T = \{p, n\}$ has been selected for modelling the power system waveforms, where p represents a positive peak and n a negative peak. Thus, a string of symbols from the set T such as *pnnpnpn* or *npnpnp* denotes a power system waveform. Corresponding attributes are associated with each terminal symbol.

4.4.3 Pattern Grammar AG_{PSW}

In SPR, the recognition task is basically reduced to that of parsing a string that is the linguistic representation of the patterns to be recognized with a parser that utilizes a dedicated grammar, called pattern grammar. The pattern grammar defines the patterns in a formal way, and the design of the pattern grammar is always the crucial sub problem in any SPR application. The proposed methodology aims to give solutions to the sub problems of primitive pattern selection, linguistic representation, and pattern grammar formulation for the waveforms received by a protection relay.

In the case of power systems waveforms, where added morphologies exist due to errors, and where complicated measurements of the various parameters have to be achieved, grammars having strong expressive capabilities to describe syntax and semantics are needed as an underlying model for the construction of a pattern grammar. As a result of their capability in relating structural and statistical features and their power to handle syntactic and semantic information Attribute Grammars has been chosen as the tool of the proposed application. Attribute Grammar AG_{PSW} presented in Table 4.1 is proposed for the recognition of power systems waveforms (PSW).

AG_{PSW} is consisted of the non-terminal symbols belonging in set $N = \{S, PS, SP, SN\}$ where start symbol is the non-terminal symbol S, PS is the symbol indicating the start of the waveform to be recognized, SP is the symbol indicating the start of a subpart of the waveform starting from a positive peak and SN is the symbol indicating the start of a subpart of the waveform starting from a negative peak. The terminal symbols belonging in set $T = \{n, p\}$ where n denotes positive peak and n denotes negative peak; vocabulary of the grammar is equal to $V = N \cup T$. The syntactic rules of the grammar

are presented in the column entitled “Syntactic Rules” of Table 4.1, while the semantic rules in the next column of the same table.

Table 4.1: Syntactic and semantic Rules of AG_{PS}.

| No | Syntactic Rules | Semantic Rules |
|----|------------------------------|--|
| 1 | $S \rightarrow PS$ | $S.fr = (PS.c/2) * (1 / (PS.f - PS.s))$ $S. = (e_{normal} * PS.c) / (PS.e)$ |
| 2 | $PS \rightarrow SP$ | $PS.c = SP.c$ $PS.s = SP.s$ $PS.f = SP.f$ $PS.e = SP.e$ |
| 3 | $PS \rightarrow SN$ | $PS.c = SN.c$ $PS.s = SN.s$ $PS.f = SN.f$ $PS.e = SN.e$ |
| 4 | $SP \rightarrow SP_1 \ SP_2$ | $SP.c = SP_1.c + SP_2.c$ $SP.s = SP_1.s$ $SP.f = SP_2.f$ $SP.e = SP_1.e + SP_2.e$ |
| 5 | $SN \rightarrow SN_1 \ SN_2$ | $SN.c = SN_1.c + SN_2.c$ $SN.s = SN_1.s$ $SN.f = SN_2.f$ $SN.e = SN_1.e + SN_2.e$ |
| 6 | $SP \rightarrow p$ | $SP.c = 1;$ $SP.s = p.xl;$ $SP.f = p.xr;$ $SP.e = p.e;$ |
| 7 | $SP \rightarrow p \ n$ | $SP.c = 2;$ $P.s = p.xl;$ $P.f = n.xr;$ $SP.e = p.e + n.e;$ |
| 8 | $SN \rightarrow n$ | $SN.c = 1;$ $SN.s = n.xl;$ $SN.f = n.xr;$ $SN.e = n.e;$ |
| 9 | $SN \rightarrow n \ p$ | $SN.c = 2;$ $SN.s = n.xl;$ $SN.f = p.xr;$ $SN.e = n.e + p.e;$ |

Terminal symbols p , n have the attributes presented in section “Primitive Pattern Selection”, while the non-terminal symbols have the attributes c , s , f and e where c attribute is used as a counter in order to store the number of peaks (either positive or negative) recognized till that point; s attribute is used to store the start point of the recognized substring; f attribute is used to store the last point of the recognized substring; and e attribute is used to store the sum of the energy e of peaks recognized till that point according to equation 4.1. In addition, start symbol S has two additional attributes called fr and noise (error) so as to calculate the frequency of the recognized waveform and the ratio of the normal energy e (e_{normal}) the waveform should have over the actual energy e the waveform has. It should be noted that all attributes are synthesized.

4.5 System Description

In the case of power systems, large time-series of input data are created due to the high sampling frequency. For example, when the scanning frequency is set to 800 Hz, a new sample is created every 1.25 ms leading to 48,000 samples per second. Given that the frequency of power system signals is 50 Hz (or 60 Hz in some countries), a unique peak is represented every 8 samples and a full period every 16 samples (800/50). Consequently, 6,000 sets of 8 samples that each describes a unique peak are created every second. Since every peak is described by a terminal symbol n or p , a powerful parser is needed able to recognize input strings of length 6,000 per second.

The proposed system [30] is based upon the attribute evaluator presented in [26] that is capable to achieve such a performance. Having chosen this system, certain modifications had to be performed in order to convert it to a suitable parser for the specific application. The main modifications imposed on the parser were focused on the two following tasks: a) extending it in order to recognize the presented grammar AG_{PSW} and b) modifying the architecture so as to cope with such long input strings in real-time.

Regarding the first task, according to the methodology presented in [26], the basic modules and the data structure had to be tuned. Specifically, the structure of the

fundamental operator \otimes , the various bit vectors, the size of the parse table PT and the mask bit-vectors were adjusted to the needs of the grammar AG_{PSW} . Regarding the second task, more crucial improvements had to be made. The design of the original parser does not support the recognition of such long input strings. For that reason, it was decided to split the long input string to multiple substrings of smaller predefined length. Hence, the values of specific attributes of the start symbol of a parse tree recognizing a subpart of the input string should be inherited by the start symbol of the next substring. This task is twofold; the hardware parser had to be changed by adding a new hardware module as well the grammar itself.

The first rule of AG_{PSW} presented in Table 4.1 had to be augmented with further semantic rules, as shown in Table 4.2, where the three basic attributes $S.fr$, $S.noise$ and $S.c$, have three instances: the current, the previous and the next state.

Table 4.2: Extended start rule of AG_{PSW} .

| No | Syntactic Rules | Semantic Rules |
|----|--------------------|--|
| 0 | $S \rightarrow PS$ | $S.fr = (PS.c/2) * (1 / (PS.f - PS.s));$ $S.noise = 1 - (e_{normal} * PS.c) / (PS.e);$ $S.c = PS.c ;$ $S.next.fr = \frac{S.fr * S.c + S.previous.fr * S.previous.c}{S.c + S.previous.c} ;$ $S.next.noise = \frac{S.noise * S.c + S.previous.noise * S.previous.c}{S.c + S.previous.c} ;$ $S.next.c = S.c + S.previous.c$ |

Clearly, the current state refers to the values of the examined substring, the previous state refers to the accumulated values of the substrings recognized so far and the next state refers to the values that will be transferred to the next stage of recognition substring and stored as previous state. The control of this transfer is managed by a dedicated hardware module that is embedded in the extended system. It should be noted that all syntactic rules are accordingly augmented by actions using the methodology presented in [26], leading into the correct tree decoration. The sub tasks of the proposed implementation are shown in Figure 4.2.

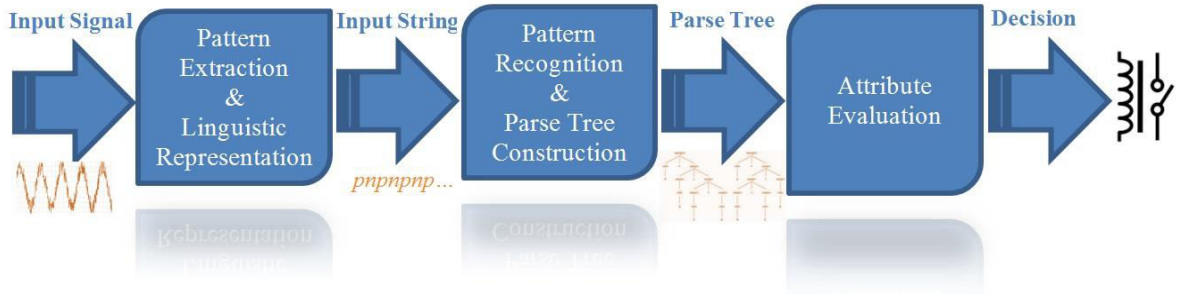


Figure 4.2: Sub tasks of the proposed implementation.

4.5.1 The Combinatorial Parser

The method in which set of dotted rules are constructed in parallel, during the recognition and parsing task of the given input string, may be efficiently performed by the operator \otimes . This operator was initially proposed by Chiang & Fu [20]. It is a binary operator that generates a new set of dotted rules takes when either two sets of dotted rules or a terminal symbol and a set of dotted rules are given as input. When the construction of all dotted rules sets is completed, this parallel parsing algorithm may determine if the given input string $\alpha = a_1 a_2 a_3 \dots a_n$ (n is the length of the input string) is a sentence that may be produced by a CFG G . The parsing task is completed when a $(n+1) \times (n+1)$ parsing table PT is constructed whose elements $pt(i, j)$ are sets of dotted rules.

Operation \otimes is defined [20] as follows:

Let's assume that $Z = Predict(N) = \cup_{A \in N} Predict(A)$ and

$Predict(A) = \{A \rightarrow \gamma.\delta \mid A \rightarrow \gamma\delta \in R \text{ and } \gamma \xrightarrow{*} \lambda\}$, λ is empty string

Given the sets of dotted rules Q and U and the terminal symbol b , operator \otimes is defined as follows.

$Q \otimes U = \{A \rightarrow \delta D \beta.\gamma \mid A \rightarrow \delta.D\beta\gamma \in Q, \beta \xrightarrow{*} \lambda, \text{ and } D \rightarrow \mu. \in U\}$,

and $\{B \rightarrow \phi C \xi.\eta \in Z \text{ and } \xi \xrightarrow{*} \lambda, C \xrightarrow{*} A\}$

$Q \otimes b = \{A \rightarrow \delta b \beta.\gamma \mid A \rightarrow \delta.b\beta\gamma \in Q, \beta \xrightarrow{*} \lambda$

and $\{B \rightarrow \phi C \xi.\eta \mid \gamma = \lambda, B \rightarrow \phi.C\xi\eta \in Z \text{ and } \xi \xrightarrow{*} \lambda, C \xrightarrow{*} A,$

Further details regarding the hardware implementation of operator \otimes may be found in reference [21]; therefore that implementation will not be analytically described since that it would be a repetition of what is presented in [21].

The proposed system includes three major sub modules: i) the Extended Parallel Parser, ii) the Tree Constructor and iii) the Attribute Evaluator. The recognition task is handled by parser that constructs the parse table as well, based on the examined input string. Once the parsing task has finished, a parse tree is created and then, while the parse tree is being traversed, all the attributes values are evaluated.

The following subsections, analyze the implementation details of all main sub-modules of the proposed architecture.

4.5.2 Extended Parallel Parser

Architecture for the efficient hardware implementation of CFG parsers was presented in [21]. The efficiency of this parser derives from the proposed combinatorial circuit that implements the operator \otimes proposed by Chiang & Fu [20]. Time complexity of this implementation for a grammar G of length $|G|$ is $O(\log_2(|G|))$. The PT (Parsing Table) may be filled using the architecture presented in Figure 4.3(a). The cells of PT may be constructed in parallel by the use of multiple \otimes operators, which are implemented by the combinational circuit C_{\otimes} . The PT cells of the main diagonal of the table are initialized to the set $Z=Predict(N)$, where N is the set of non-terminals symbols. Previously presented architectures parallelize the construction of the PT in regards n which is the input string length. The parallelization is accomplished by evaluating at each execution step all the cells $pt(i,j)$ that exist to the same diagonal line (diagonal line is a line parallel to the main diagonal.). The construction of cell $pt(i,j)$ is performed using the equation shown in Figure 4.3(b) that make use of all the cells $pt(i,k)$ and $pt(k,j)$ for which $(i+1) \leq k \leq (j-1)$ (see Figure 4.3(b, c)) should already have been computed. At m^{th} execution step t_{em} , processing element P_x computes $pt(x-m,x)$ and during the m^{th} communication step t_{cm} , P_x transmits $pt(x-m,x)$ together with $pt(x-m,x-1)$, $pt(x-m,x-2)$ via bit-vector u (see Figure 4.3(a)). In addition, all cells that have already been evaluated by processing P_x may be used, through bit-vector q , in

order to evaluate the cell that belongs to the same column. Consequently, all processing element P_x progressively evaluate the cells of the x^{th} column. By the use of multiple C_{\otimes} circuits the operators can be executed in parallel. The union of their outputs produces $pt(i,j)$ (see Figure 4.3(c)). Each processing element P_x takes as input the a_x input symbol.

Therefore, the proposed architecture has two levels of parallelism:

- i) A cell-level parallelism i.e. the parallel execution of the \otimes operations for each cell, and
- ii) An architecture-level parallelism that corresponds to the tabular form of Earley's algorithm.

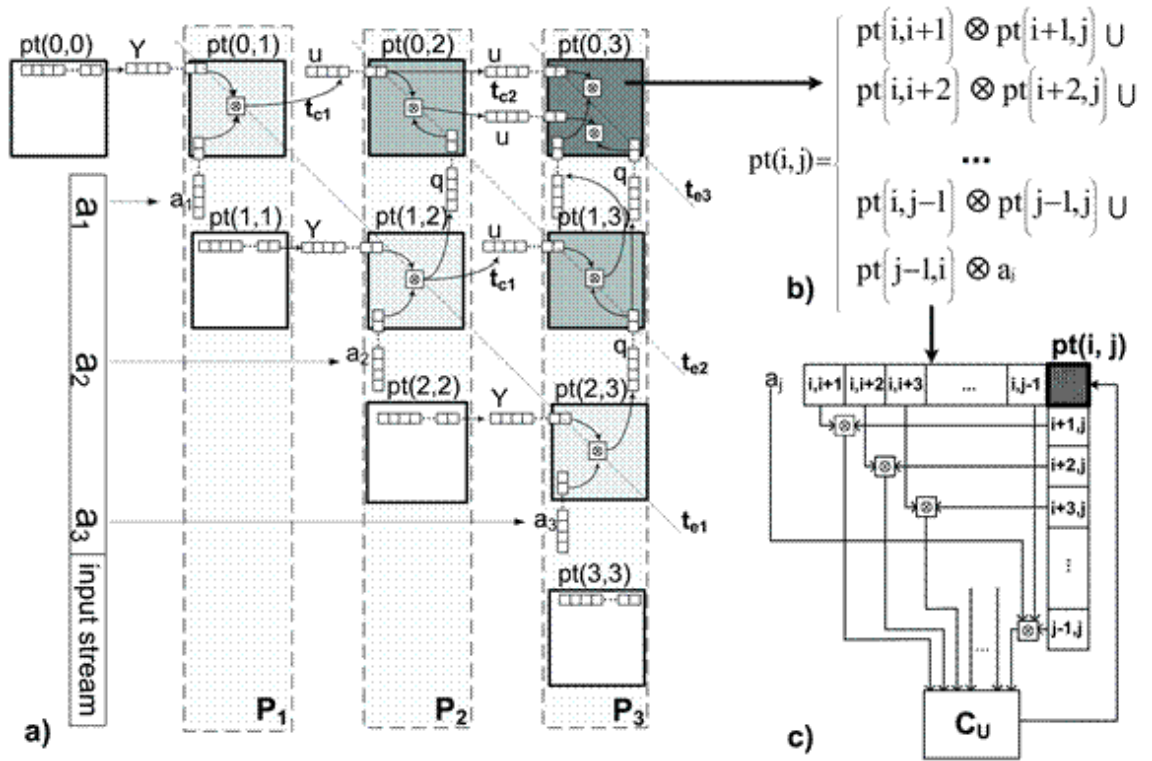


Figure 4.3: Parsing architecture presented in [21] for $n=3$.

The time complexity of the recognition task of the proposed implementation for an input string of length n in $O(n \log^2 |nG|)$. Considering the hardware implementation of the system proposed in [21], this system achieves a speed-up factor from two orders of magnitude for small grammars to six orders of magnitude for large real life grammars

compared to other software implementations. The characteristic equations of the examine grammar are used in order to construct C_{\otimes} . The design - architecture of the combinational circuit C_{\otimes} including its crucial sub circuits is shown in Figure 4.4.

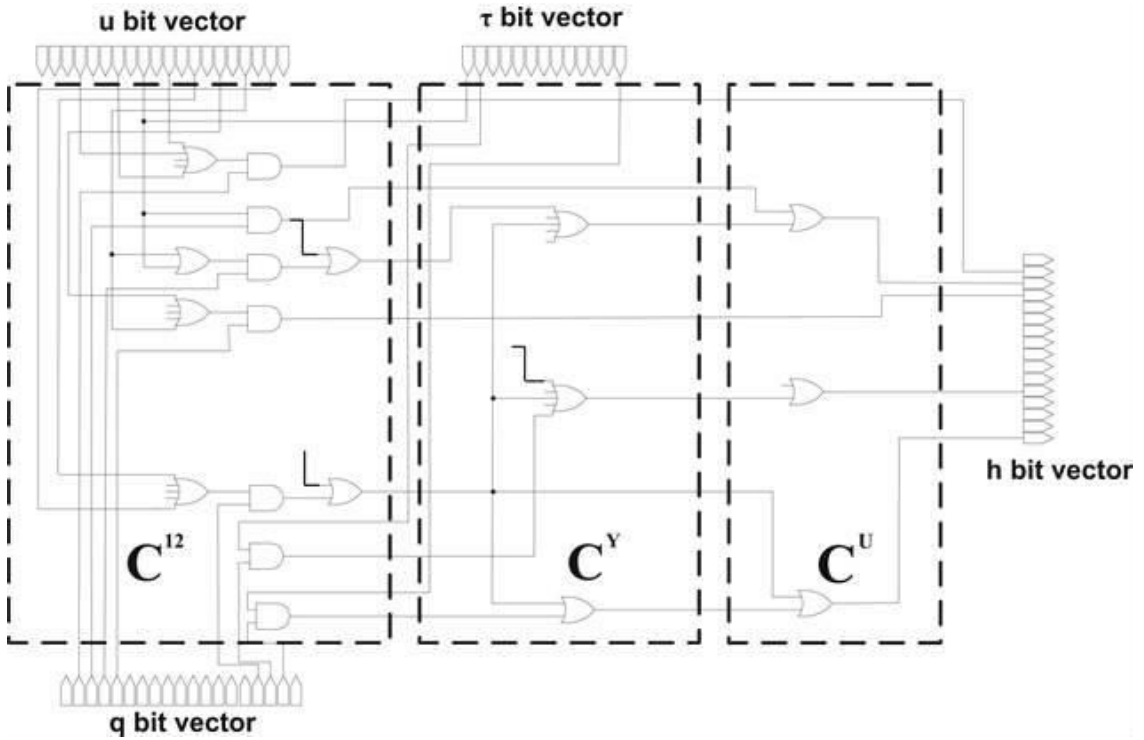


Figure 4.4: Architecture of the combinational circuit C_{\otimes} including its crucial sub circuits.

After selecting the parsing system proposed in [21], various modifications had to be performed in order to convert it to an appropriate parser for our application. Initially, this architecture should be extended so as to construct the parse tree which is a requirement for the attribute evaluation. The main parameter in this problem is that the parser should maintain its combinatorial nature that offers the abovementioned speed-up. Consequently, all modifications are made based on this requirement.

Storing the origin of the creation of each dotted rule is the most essential modification. According to \otimes operator definition, a dotted rule may be the output of an operation among two sets of dotted rules or among a set of dotted rule and one terminal symbol. Then the construction of cell $pt(i,j)$ is the union of the output of a multiple operations among two sets of dotted rules and the output of one operation among a set of dotted

rules and a terminal symbol (see Figure 4.3(c)). During the construction of a cell $pt(i,j)$, $n-1$ operations between two sets of dotted rules are required. Therefore, each dotted rule may have n potential origins is, where n is the length of the examined input string.

For example, in case $n = 2$:

$$pt(0, 2) = (pt(0,1) \otimes a_3) \cup (pt(0,1) \otimes pt(1,2))$$

Hence all dotted rules in cell $pt(0,2)$ may have derived from one of the three applications of operator \otimes . Consequently, a vector of bits of length n , called *source* bit vector, is essential so as to keep the origin of the dotted rule in the cell. For the abovementioned case, if bit $source[1] = 1$, then cell $pt(0,2)$ has been generated due to operation $pt(0,1) \otimes pt(1,2)$. In the event when more than one bits of bit-vector *source* are set due to operations among sets of dotted rules that specifies that the grammar is ambiguous.

During each execution step, the parser evaluates the dotted rules for the cells that exist in the same diagonal. When an execution step ends, a column of the PT is considered constructed and hence these data along with the *source* bit-vectors may be transferred to the next module that is the parse tree constructor, as shown in Figure 4.2. It should be noted that owing to the fact that the parser is executed in parallel, during an execution step, all generated dotted rules are generated and stored into the PT. Therefore in the PT is stored a considerable number of dotted rules. Most of these dotted rules will be proved to be useless in regards to the recognition of the examined input string. Moreover, only completed dotted rules should be utilized during the task of the construction of the parse tree, as a result only completed dotted rules are transferred from the PT to the tree constructor module. The selection of the completed dotted rules is really trivial and fast using to a bit-vector mask in which the bits that represent the positions of the completed dotted rules are set. The main architecture of the parser is shown in Figure 4.3(a) and the architecture of \otimes operator is shown in Figure 4.4.

As mentioned above, the first task is evaluation of the PT, given the input string using the proposed parser shown in Figure 4.3. In this figure, the main diagonal is not presented, as it has the initial pre-computed rules i.e. set Z . After the parsing task has

finished, i.e., all columns of the PT are evaluated and transformed to the next module; the task of parse tree construction is starting. This task starts from the top right cell of the PT, where a dotted having at the lhs the start symbol is required to be found. When this dotted rule is reached, it will be located as the root of the parse tree and the dotted rules that created that dotted rule will be fetched, using the *source* bit-vector and by applying the appropriate masks. The outcome is then for the moment stored in bit-vector called MASKED (Figure 4.5) which at the end should be kept as tree branch. Since there are two separate cases: a dotted rule derived from two dotted rules or a terminal symbol rule and a dotted, in the *source* bit-vector could have been stored one or two cell position. The same methodology is performed for all dotted rules found till it's found a dotted rule that belongs to the major diagonal of PT; this fact signifies the closure of the specific. Following the same procedure, the parse tree is generated branch by branch. In Figure 4.5 an analytic flowchart of the methodology to generate the parse tree given a PT is shown.

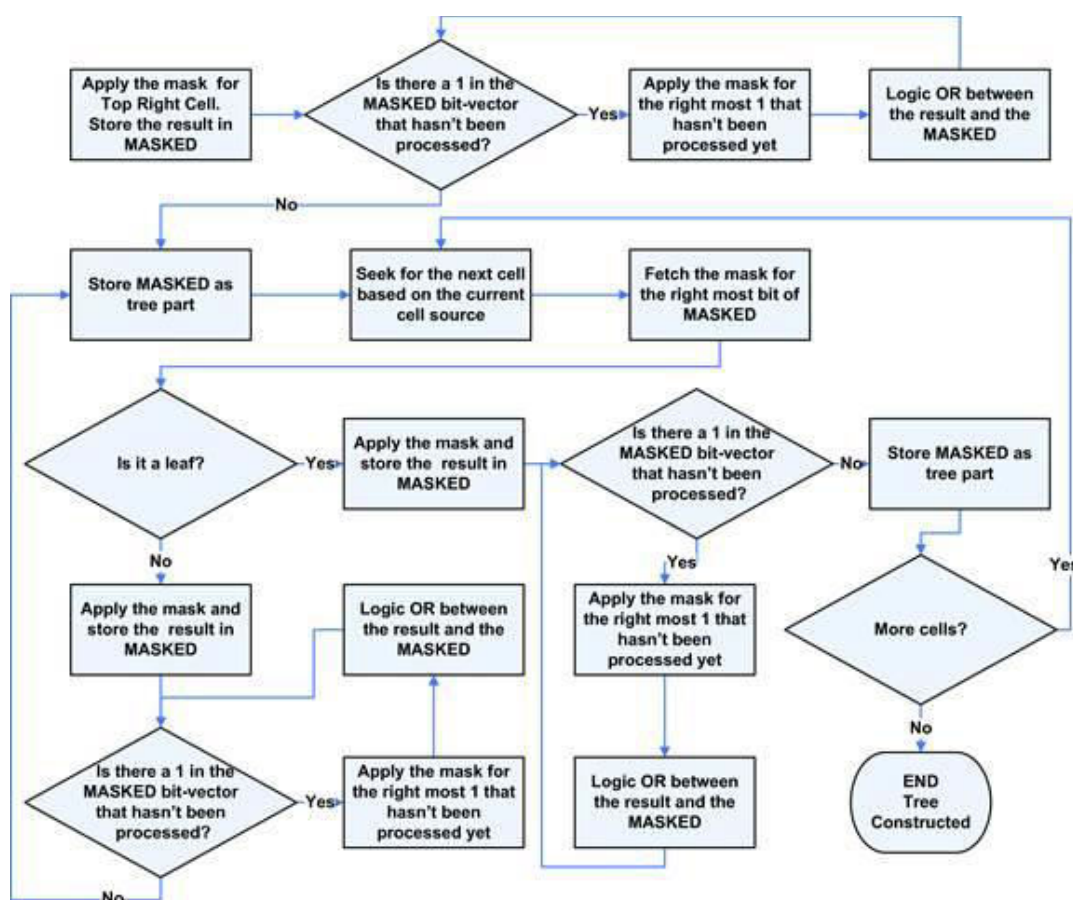


Figure 4.5: Flow chart of the methodology proposed to construct the parse tree.

It has to be clarified that completed rules belonging to the parse tree are distinguished from others dotted rules that coexist in a PT cell and therefore in the same bit-vector. This can be accomplished by the use of bit-vector masks for every single rule. The masks are constructed having in mind that a parent node in the parse tree has children nodes that have as left hand side symbol (lhss), of the corresponding rule, non-terminals that exist in the right hand side symbol (rhss) of the parent node.

An example will be given, in order to explain this procedure. Let's consider the rule $B \rightarrow CD$ that exist at the parent node. Then the rules at the children node may only have C or D as lhss. Hence, a mask for the examined dotted rule should be created that accepts just the rules having these non-terminals as lhss. As the masks have a bit vector format can easily be created using just AND gates. The creation of the masks takes place mechanically at the same time when the whole proposed system is. It should be clarified that by using masks parser complexity is not influenced, as only some additional AND gates are added to the final system and consequently the combinatorial nature and extreme performance of the parser is retained.

Using the flowchart of Figure 4.5 an FSM (Finite State Machine) has been created that actually is the Parse Tree Constructor. All parameters and constants of the FSM such as number of cells and bit-vector lengths are initially set by specific software that also designs the masks of the examined grammar.

The sub-modules Parser and Parse Tree Constructor generate the parse tree and initially its nodes are not decorated by attributes. Attribute Evaluation is the task/sub-module responsible for the decoration of the tree with attribute.

Regarding the attribute evaluation task a stack based approach has been adopted presented in [26]. A stack is created for each attribute synthesized or inherited exist in the grammar. The procedure of decorating the tree with attributes starts from the root. Primarily, all initial values of attributes are pushed into the corresponding inherited attribute stacks. The procedure followed for every node, including the root node, is to evaluate the attributes of the children nodes and then to evaluate the current node. The evaluation of the children nodes begins from the leftmost towards the rightmost. All the AG semantic rules are converted to push and pop actions, following a methodology

explained below. In every node, the push and pop actions dictated by the semantic rules are executed, beginning from the evaluation of inherited attributes and afterwards continuing with the synthesized. Because of the top-down and leftmost to rightmost nature of the algorithm, while pushing the inherited attributes into the stacks the tree is traversed towards its leftmost leaf. When reached, its synthesized attribute is evaluated and the parent (or the right sibling) node can start evaluating its synthesized attributes too. For functions between attributes stored into the same or different stacks, dedicated components are used that output the result which is then pushed into the appropriate stack. As expected, the end of the entire procedure is denoted by the evaluation of all the root node attributes. The path followed for the decoration of a simple parse tree is shown in Figure 4.6.

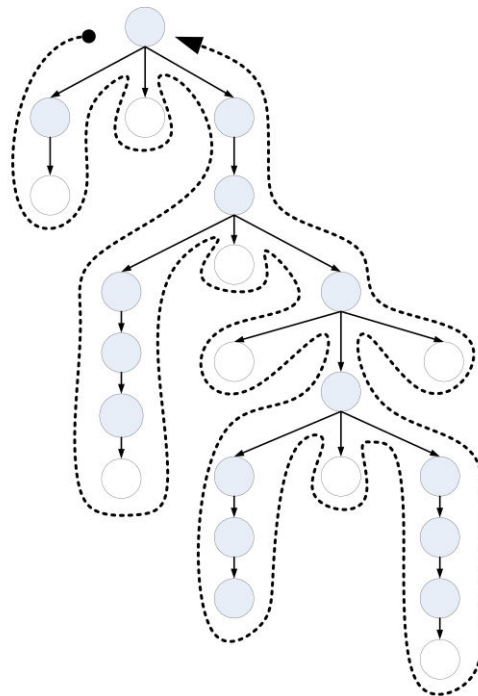


Figure 4.6: Parse tree traversal.

As already mentioned, the AG semantic rules are converted to push and pop actions. Regarding the synthesized attributes, every time the tree traversal reaches a leaf or a node whose descendant nodes attributes have already been evaluated, the synthesized attributes of the rhss are popped. These synthesized attributes are at the top of the corresponding stacks. Then, the synthesized attribute of the parent node is calculated according to the corresponding semantic rule and is pushed into the appropriate stack.

In this way, it is ensured that at the top of the synthesized attributes stacks, attributes of the children nodes (up to the current child) are placed in sequence.

Regarding the inherited attributes, a pop is done the first time the node is traversed and the inherited attribute I is needed. If in a rule an inherited attribute is used by more than one rhss, then the same number of pushes should be done into the corresponding stack. This is something reasonable, since every time a value from the stack is needed it has to be popped and therefore leaves the stack.

Finally, for the AG semantic rules that impose value transfer (for the same attribute), no action is required for either inherited or synthesized attributes because the equivalent actions would be a successive pop and push into the same stack.

The architecture for the semantic evaluation stage is shown in Figure 4.6. The parse tree should be traversed top-bottom and from left to right. Each branch is represented by a bit-vector of length p , where p is the number of syntactic rules. For example, the first branch (rules 0, 2 and 3) of that parse tree is represented by the bit-vector 00000000000000001101. When the attributes of a branch of the tree should be evaluated, the corresponding bit-vector is loaded to bit-vector *TreeBranch*. It is noted that the sequence of the syntactic rules in a branch of the tree it is not indicated in the representative bit-vector. For that reason when the platform reads the given input grammar sorts the syntactic rules appropriately so that the more significant bit that is set, should be evaluated first. Each module responsible for the attribute evaluation of a rule is enabled via signal En (Enable), which is driven by the result of the logical gate AND that takes as inputs the value of the corresponding bit of bit-vector *TreeBranch* and the signal EnN (Enable Next) that is set by the previous module. When a module finishes its execution (evaluation of attribute) sets signal EnN , in order to allow the next module to be executed. A module is going to be executed when $En=EnN=1$. In case the corresponding bit of bit-vector *TreeBranch* is 0, then $En=0$ and when the input EnN is going to be set the module will not be executed but it will just set its EnN in order to allow the next module to be executed. The input EnN of the most significant bit is always set as it has the greatest priority. Each module communicates via the control and data bus with the stacks it needs in order to evaluate the attributes. The whole process is

synchronized by a Control Unit which at each clock step enables one of the semantic submodules. Then the enabled submodule sends the corresponding control signals to the appropriate stacks, in order to execute the correct push or pop operations. Moreover, the Control Unit is responsible for advancing the semantic evaluation procedure.

The architecture presented in Figure 4.3 has been described in Verilog as a template. The platform using the parameters of the grammar modifies this template by defining all needed constants such as the length of the bit-vector *TreeBranch*. If complex functions are dictated by the semantics, special submodules are required. Therefore, these submodules cannot yet be produced automatically but have to be application specific functions provided by the user. In case semantic rules consist only of simple arithmetic expressions, they can be automatically generated (Figure 4.7).

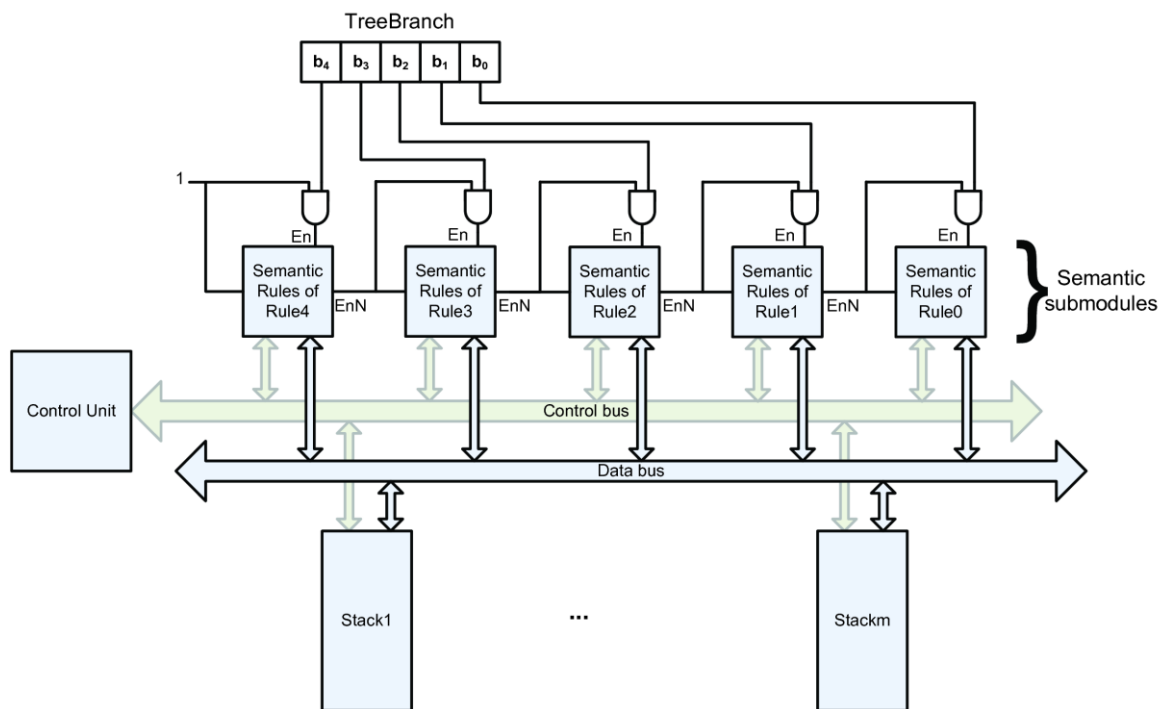


Figure 4.7: Semantic Evaluator architecture.

4.6 Results

The functionality of the proposed system has been tested using various waveforms and data provided by the Independent Power Transmission Operator (IPTO) [12] in Greece. Part of the data provided by IPTO is shown in Figure 4.8.

In this subsection, the time required for the parsing of 50 peaks by the proposed system will be presented. Nevertheless, a subset of the examined waveform consisting of the first 8 peaks will be used so as to explain all distinct tasks of the proposed system. The eight peaks are part of a voltage waveform VA measured by IPTO in November of 2008 and presented in Figure 4.9, where the first 0.08 sec are shown of a voltage waveform having 84 kV amplitude.

The sampling frequency is 800 Hz; hence, there is one sample every 0.00125 sec. In this toy scale example 64 samples are presented. For the waveform presented in Figure 4.9, the data gathered during the tokenize phase (first main task of the system: Pattern Extraction & Linguistic Representation) and their attribute values are presented in Table 4.3.

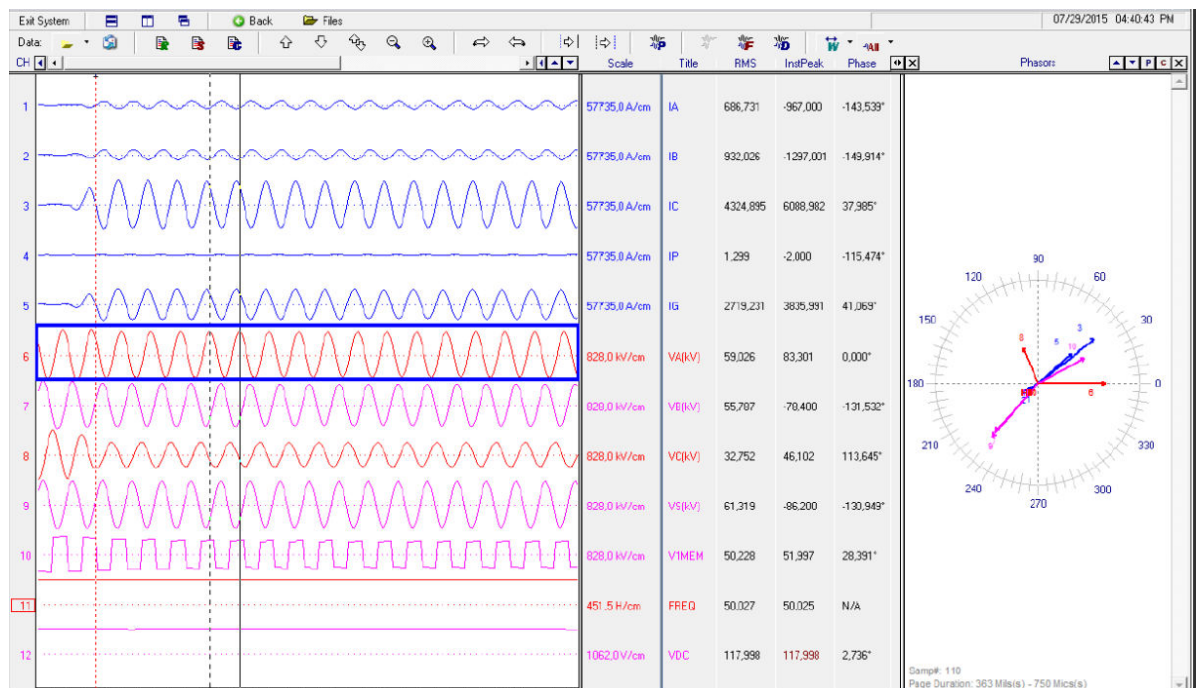


Figure 4.8: Subset of data provided by IPTO.

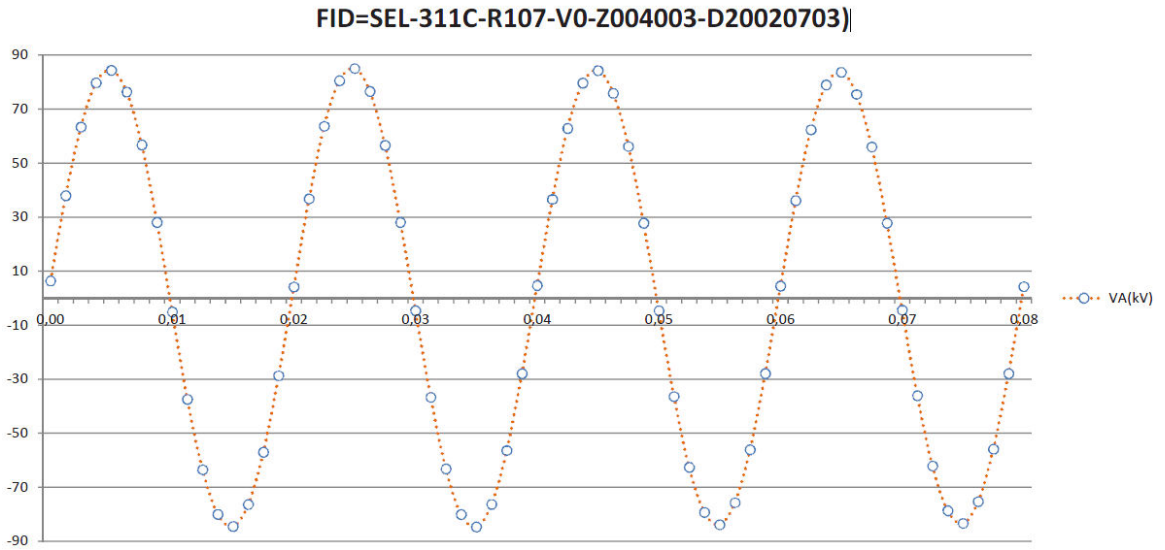


Figure 4.9: Examined waveform subset.

Table 4.3: Syntactic and semantic Rules of AG_{PSW} .

| Peak # | p/n | Attributes |
|--------|-----|---|
| 1 | p | $x_{l1} = 0, y_{l1} = 6.4; x_{m1} = 0.005, y_{m1} = 84.4;$ $x_{r1} = 0.01, y_{r1} = -5.1; e_1 = 4753.37$ |
| 2 | n | $x_{l2} = 0.01, y_{l2} = -5.1; x_{m2} = 0.015, y_{m2} = -84.5$ |
| | | $x_{r2} = 0.02, y_{r2} = 4.2; e_2 = 4,342.27$ |
| 3 | p | $x_{l3} = 0.02, y_{l3} = 4.2; x_{m3} = 0.025, y_{m3} = 85.1$ |
| | | $x_{r3} = 0.03, y_{r3} = -4.6; e_3 = 4,446.02$ |
| 4 | n | $x_{l4} = 0.03, y_{l4} = -4.6; x_{m4} = 0.035, y_{m4} = -84.7$ |
| | | $x_{r4} = 0.04, y_{r4} = -4.6; e_4 = 4,327.67$ |
| 5 | p | $x_{l5} = 0.04, y_{l5} = -4.6; x_{m5} = 0.045, y_{m5} = 84.3$ |
| | | $x_{r5} = 0.05, y_{r5} = -5.1; e_5 = 4,753.37$ |
| 6 | n | $x_{l6} = 0.05, y_{l6} = -4.6; x_{m6} = 0.055, y_{m6} = -83.9$ |
| | | $x_{r6} = 0.06, y_{r6} = 4.5; e_6 = 4,294.13$ |
| 7 | p | $x_{l7} = 0.06, y_{l7} = 4.5; x_{m7} = 0.065, y_{m7} = 83.7$ |
| | | $x_{r7} = 0.07, y_{r7} = -4.4; e_7 = 4,268.55$ |
| 8 | n | $x_{l8} = 0.07, y_{l8} = -4.4; x_{m8} = 0.075, y_{m8} = -83.4$ |
| | | $x_{r8} = 0.08, y_{r8} = 4.3; e_8 = 4,241.35$ |

Obviously, the produced input string is $pnpnpnpn$ and the parse tree generated (second main task of the system: Pattern Recognition & Parse Tree Construction) after the recognition task is that of Figure 4.10.

After creating the parse tree, our system evaluates the attributes of the symbols (third main task of the system: Attribute evaluation) traversing the tree using the methodology and the stack based technique presented in [26].

In case the input string symbol is greater than 10, our system splits the input string into subparts of length 10. Consequently, for the examined waveform of 50 peaks the input string has been divided into 5 substrings of length 10 and the overall noise (error) has been accumulated using the extended semantic rules of Table 4.2 and presented in Figure 4.11, where y axis depicts the existing percentage of noise (error) while input symbols are gradually recognized (x axis).

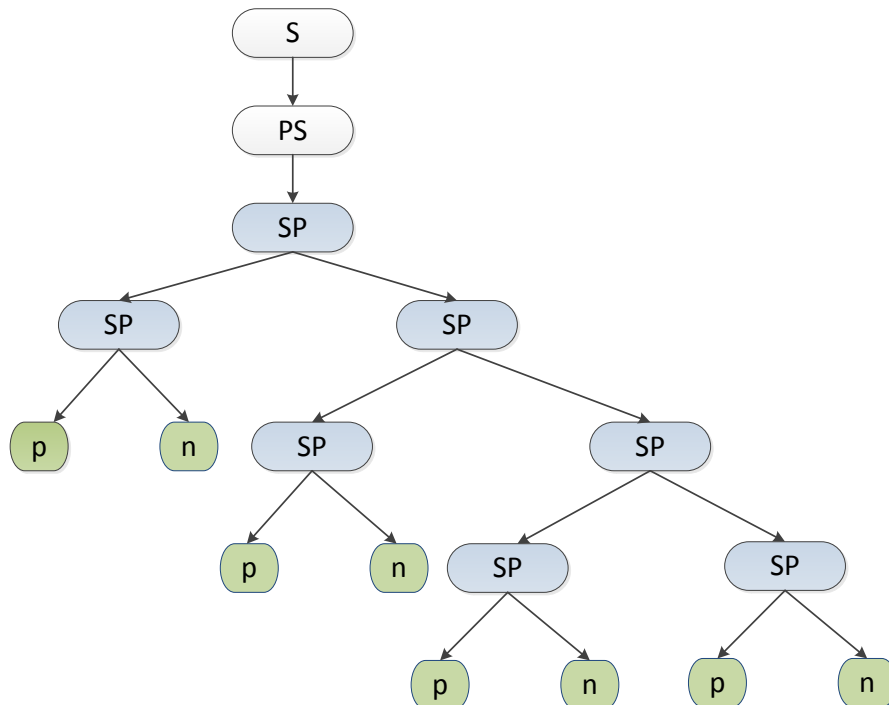


Figure 4.10: Parse tree for input string *pnpnpnpn*.

The time required by our system to recognize the input string of length 50 is about 250,000 nsec, while the partial time required per substrings of length 10 are presented in Figure 4.12 and is close to 50,000 nsec. All examples were implemented and executed on a Xilinx Virtex-5 ML506 FPGA board running at 100 Hz. Given that an input string of length 50 may be recognized in 250,000 nsec, then any input string of length 200,000 (50/250,000 nsec) may be recognized during a second. The

performance of the propose system fulfils the limitation set at the beginning of previous section, i.e., input string of length 6,000 per second.

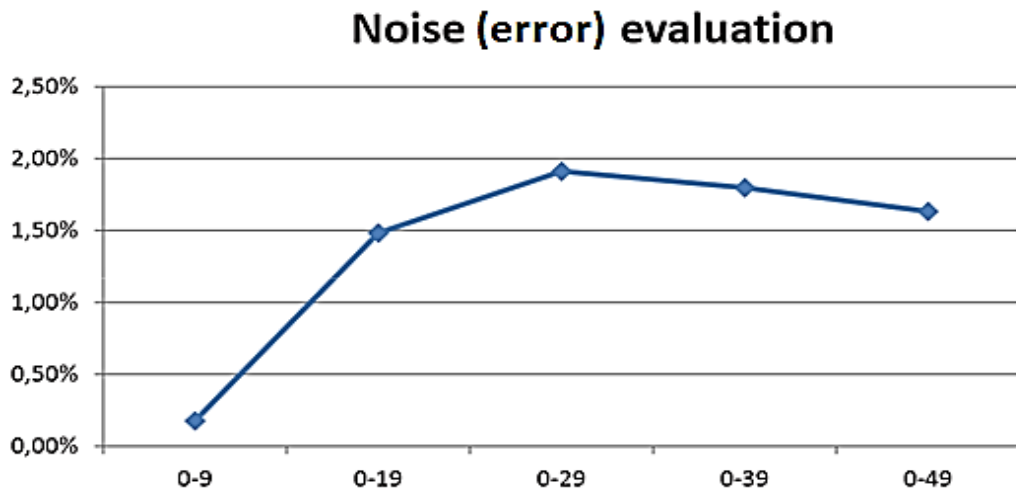


Figure 4.11: Noise (error) evaluation by gradually recognizing substrings.

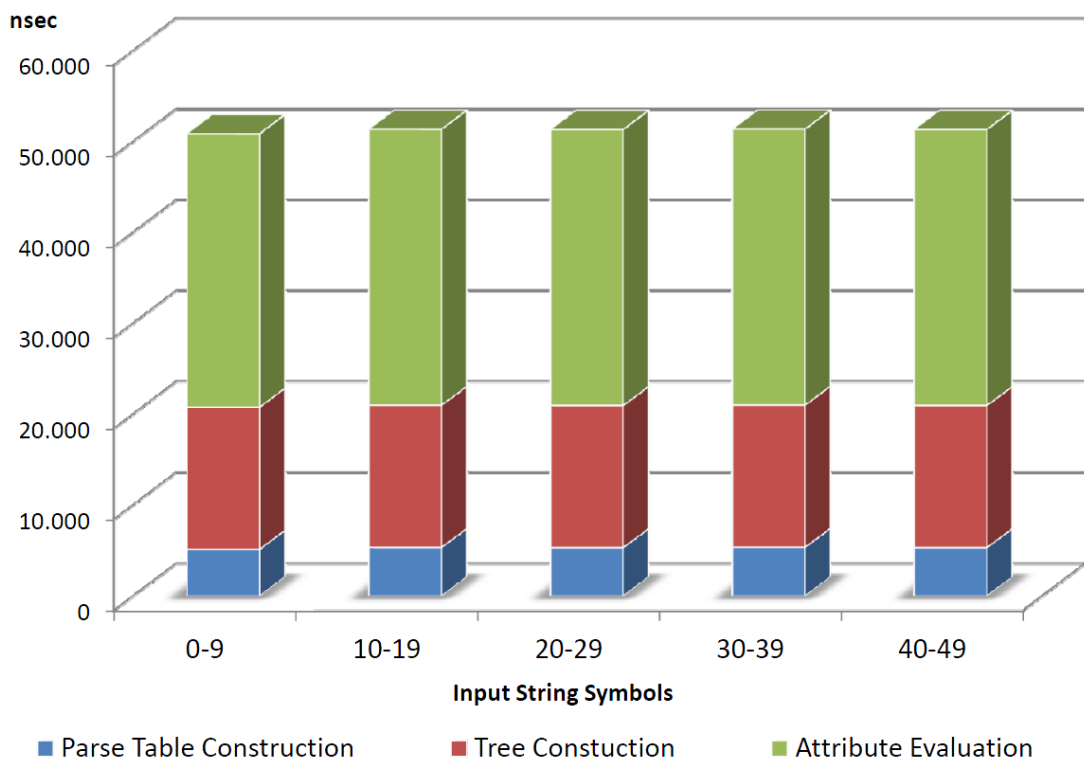


Figure 4.12: Performance evaluation of recognizing 50 peaks.

4.7 Conclusions

This chapter presents an application of the SPR theory to the recognition of power system signals and to the measurement of its parameters. A hardware implementation has been developed on a Xilinx Virtex-5 ML506 FPGA board running at 100 Hz in order the functionality of the proposed system to be tested using waveforms and data provided by the Independent Power Transmission Operator (IPTO) in Greece. The proposed methodology will be applied to the implementation of an efficient protective relay that would efficiently prevent safety problems and economic losses caused by faults presented in power systems.

4.8 References

- [1] Saha MM, Izykowski JJ, Rosolowski E, Fault location on power 430 networks, Springer Science & Business Media, 2009.
- [2] Aung MT, Milanovic JV, Stochastic prediction of voltage sags by considering the probability of the failure of the protection system, IEEE Transactions on Power Delivery, vol. 21, no. 1, pp. 322-329, 2006.
- [3] Qader MR, Bollen MH, Allan RN, Stochastic prediction of voltage sags in a large transmission system, IEEE Transactions on Industry Applications, vol. 35, no. 1, pp. 152-162, 1999.
- [4] Chicco G, Napoli R, Piglione F, Neural networks for fast voltage prediction in power systems, IEEE Power Tech Proceedings, vol. 2, Porto, Portugal, 2001.
- [5] Gupta S, Kazi F, Wagh S, Kambli R, Neural network based early warning system for an emerging blackout in smart grid power networks, Intelligent Distributed Computing, Springer, pp. 173-183, 2015.
- [6] Wong K, Ryan H, Tindle J, Power system fault prediction using artificial neural networks, International Conference on Neural Information Processing, Hong Kong, pp. 1181-1186, 1996.
- [7] Bourguet RE, Antsaklis PJ, Artificial neural networks in electric power industry, Technical Report of the ISIS, No. ISIS-94-007, University of Notre Dame, 1994.

- [8] Xu J, Meyer-Baese U, Huang K, FPGA-based solution for real-time tracking of time-varying harmonics and power disturbances, *International Journal of Power Electronics*, vol. 4, no. 2, pp. 134-159, 2012.
- [9] Earley J, An efficient context-free parsing algorithm, *Communications of the ACM*, vol. 13, no. 2, pp. 94-102, 1970.
- [10] Pavlatos C, Panagopoulos I, Papakonstantinou G, A programmable pipelined coprocessor for parsing applications, *Workshop on Application Specific Processors (WASP) CODES*, Stockholm, 2004.
- [11] Xilinx Inc., www.xilinx.com.
- [12] Independent power transmission operator (IPTO or ADMIE), <http://www.admie.gr/nc/en/home/>.
- [13] Chomsky N, Three models for the description of language, *IRE Transactions on Information Theory*, vol. 2, no. 3, 1956.
- [14] Aho AV, Lam MS, Sethi R, Ullman JD, *Compilers: Principles, Techniques, and Tools*, 2nd edition, Addison Wesley, 2006.
- [15] Younger DH, Recognition and parsing of context-free languages in time n^3 , *Information and Control*, vol. 10, no. 2, pp. 189-208, 1967.
- [16] Tomita M, Ng S-K, *The generalized LR parsing algorithm*, Kluwer Academic Publishers, 1991.
- [17] Graham SL, Harrison MA, Ruzzo WL, An improved context-free recognizer, *ACM Trans. Program. Lang. Syst.*, vol. 2, no. 3, pp. 415-462, 1980.
- [18] Ruzzo WL, *General context-free language recognition*, PhD Thesis, University of California, Berkeley, 1978.
- [19] Geng T, Xu F, Mei H, Meng W, Chen Z, Lai C, A practical GLR parser generator for software reverse engineering, *JNW*, pp. 769-776, 2014.
- [20] Chiang Y, Fu K, Parallel parsing algorithms and VLSI implementations for syntactic pattern recognition, *IEEE Transactions on Pattern Analysis and Machine Intelligence*, vol. 6, pp. 302-314, 1984.
- [21] Pavlatos C, Dimopoulos AC, Koulouris A, Andronikos T, Panagopoulos I, Papakonstantinou G, Efficient reconfigurable embedded parsers, *Computer Languages, Systems & Structures*, vol. 35, no. 2, pp. 196-215, 2009.

- [22] Harrison MA, Introduction to Formal Language Theory, Addison Wesley, Reading, Mass., 1978.
- [23] Kelemenova A, Complexity of normal form grammars, Theoretical Computer Science, vol. 28, no. 3, pp. 299-314, 1984.
- [24] Blum N, Koch R, Greibach normal form transformation revisited, Inf. Comput., vol. 150, no. 1, pp. 112-118, 1999.
- [25] Na J, Kim C-K, GLR: A novel geographic routing scheme for large wireless ad hoc networks, Computer Networks, vol 50, no. 17, pp. 3434-3448, 2006.
- [26] Dimopoulos AC, Pavlatos C, Papakonstantinou G, A platform for the automatic generation of attribute evaluation hardware systems, Computer Languages, Systems & Structures, vol. 36, no. 2, pp. 203-222, 2010.
- [27] Trahanias P, Skordalakis E., Syntactic pattern recognition of the ECG, IEEE Transactions on Pattern Analysis and Machine Intelligence (PAMI), vol. 12, no. 7, 1990.
- [28] Pavlatos C, Vita V, Ekonomou L, Syntactic pattern recognition of power system signals, 19th WSEAS International Conference on Systems (part of CSCC '15), Zakynthos Island, Greece, pp. 73-77, 2015.
- [29] Pavlatos C, Vita V, Linguistic representation of power system signals, Electricity Distribution, Energy Systems Series, Springer-Verlag Berlin Heidelberg, pp. 285-295, 2016, DOI 10.1007/978-3-662-49434-9_12.
- [30] Pavlatos C, Dimopoulos AC, Vita V, An efficient embedded system for the fault recognition of power system signals, IET Science, Measurement and Technology, (Under Review).

Chapter 5

Lightning Protection of Modern Distribution Networks

5.1 Introduction

Any distribution network (lines and electrical equipment) is exposed to many stresses on a daily basis, caused by atmospheric discharges and switching overvoltages, triggering interruptions to the electric networks' normal operation, equipment damage and failure, several safety issues, unsatisfied consumers and an increasing maintenance and operation cost for Distribution Systems Operators. Even though plenty of research has already been conducted during the past years in this research area and many efficient practices and methodologies have been presented in the technical literature for lightning protection of distribution networks aiming to the minimization of lightning faults, the evolution and modification of modern networks, with constant and cumulative integration of distributed generation (DG) units, has offered ground for further research, study and analysis.

This chapter demonstrates numerous sensitivity analyses that have been conducted on modern distribution networks (with DG) in an effort to contribute to a more efficient lightning protection. At first, a typical distribution network has been modeled, then a series of simulations have been conducted and subsequently the developed overvoltages triggered from lightning hits of different lightning current peak magnitudes and on different positions on the distribution line have been calculated. The impact of several grounding resistances in the developed overvoltages, as well as the protection of the lines through different surge arresters' models has been examined. As a final point, the presence or not of DG units, of different sizes, in the distribution network has been studied, leading to the extraction of very important conclusions, which will significantly support and assist electric utilities design engineers in the development of new protection schemes for modern distribution networks.

5.2 Literature Review

Lightning strikes and switching surges are the main sources of power supply interruptions, equipment damages and malfunctions. Shield wires, surge arresters and increased insulation levels (critical flashover voltage) are the most commonly used protective measures, in order to secure the system's reliability and reduce overvoltage faults of distribution networks [1].

Shield wires are commonly placed over the phase conductors, are grounded at every distribution lines' pole and their goal is to intercept lightning strikes that could otherwise terminate on the phases [1]. The objective of surge arresters, a device that presents high resistance for normal operating voltage and low resistance in case of overvoltages, is to lead the lightning or switching current to the ground. Surge arresters are installed on every pole and phase of a distribution line, according to the observed lightning level of the area and the calculated or observed lightning outage rate of the line. The increased insulation level (critical flashover voltage) forms the optimum lightning protection scheme for distribution lines from lightning induced voltages. The insulation level which is subject to the line's grounding resistance, plays also a major role in the distribution lines lightning protection. A more effective lightning protection scheme for distribution networks and the limitation or even elimination of faults caused by lightning, constitute the main objectives of all electric utilities on a global basis; therefore many motivating and break-through studies have been conducted and published in the technical literature.

Han, Seo and Kim analyzed the lightning overvoltages subject to the location of overhead shield wires [2]. They have modeled the Korean distribution system and they have performed numerous simulations considering only direct lightning. Their observations have proved the effectiveness of shield wires in lines lightning protection and have contributed in the validation of the Korean standards.

The evaluation of the effectiveness of shield wires in reducing the magnitudes of the surges induced by nearby strikes on distribution lines has been presented in [3]. The specific study is based on both computer simulations and test results obtained from scale model experiments, and took into consideration a combination of several

parameters such as the relative position of the shield wire with respect to the phase conductors, the grounding interval, the ground resistance, the strike current steepness, and the relative position of the strike channel with respect to the grounding points. Interesting results have been presented that could assist in the development of electric utilities' lightning protection schemes.

An external ground design applied on a distribution system for lightning performance improvement has been proposed in [4]. Simulations were conducted for the evaluation of lightning in terms of pole top voltage, critical current and backflashover rate. The study results revealed that the proposed external grounding system design can reduce significantly the effects of lightning and in turn improve the reliability, an extremely useful inference, especially for areas with high lightning outage rates.

Bhattarai et al. investigated the protection of wood pole distribution lines using surge arresters [5]. Different arrester configuration and spacing were tested, proving that lines can effectively be protected against lightning when adequate selection of surge arresters is done. They have presented very interesting results for both earthed and unearthed crossarm cases.

In [6] the lightning performance of overhead distribution lines was studied in terms of shield wires and surge arresters. Special attention was paid on induced voltages caused by lightning strikes on neighboring trees or adjacent objects and on the impact of grounding resistance and shield wire size in distribution lines' lightning performance, leading to beneficial results.

Similarly, the influence of grounding resistance and pole topology in the distribution networks' lightning performance was examined in [7]. Two different distribution networks types were studied, i.e., with and without shield wire, and both, direct lightning and backflashover were considered. It was observed that in the special case the networks were equipped with shield wire, the soil resistivity variation had a great impact on the backflashover, while the performance of unshielded networks was not influenced by the soil resistivity.

A methodology aiming to assist in the assessment of the optimum surge arrester for the lines lightning protection, has been presented in [8]. The methodology takes into consideration the arrester's risk of failure that is subject to several factors such as: the striking point, the lightning current waveform, the arrester itself and the system configuration. Therefore, for selecting the optimal arrester, all stresses must be estimated in the best possible way.

A statistical approach employing numerical integration and assessing the effect of several line parameters, soil resistivity, shielding of neighboring objects and lightning crest current distribution on the lightning performance of distribution lines was proposed in [9]. Direct lightning and induced voltages were simulated in this study. The proposed approach was implemented with the help of an application software and the given outcomes were in close consistency with filed data.

Another statistical method (Monte Carlo) for lightning performance studies of unshielded distribution lines was presented in [10]. In this study the effects of shielding from nearby objects, grounding resistance, critical flashover voltage and ground flash density were considered. Useful conclusions have been extracted while several mitigation steps for lightning performance enhancement were suggested.

In [11] an attempt to develop a practical procedure for determining the insulation level of overhead distribution lines was made. Laboratory test data were used and useful conclusions were obtained for both dry and wet conditions with positive and negative polarities of the impulses in an effort to contribute in the goal of a more effective lightning protection scheme for distribution lines.

Araujo et al. [12] studied the performance of a distribution lines' protection system (that was constituted by surge arresters), against lightning overvoltages, in the presence of distributed generation. Their study has provided interesting results and conclusions confirming the fact that distributed generation influences the effectiveness of lightning protection systems, thus its presence must be considerably taken into account and thoroughly studied in order to eliminate lightning faults.

5.3 Modern Distribution Network Configuration

5.3.1 Distribution Lines

The appropriate circuit representation of the lines is a critical issue, in order to guarantee the quality and the reliability of the lightning performance studies. In general, distribution lines cannot be modelled as lumped elements, since some of the line parameters depend on frequency. For electromagnetic transient studies the equations used for the estimation of the parameters of the line for steady state analysis are not appropriate, so the line parameters must be computed using auxiliary subroutines available in different electromagnetic transients programs. The majority of the simulation tools use basic types of line models, i.e., constant parameter models and frequency-dependent parameter models. The first category includes positive and zero sequence lumped parameter representation, PI-section representation and distributed parameter (Bergeron model) line representation. In the frequency-dependent model category, the most used models are frequency dependent line models for transposed and untransposed lines using constant modal, frequency dependent modal or no modal transformation matrix.

A typical line PI model is presented in Figure 5.1.

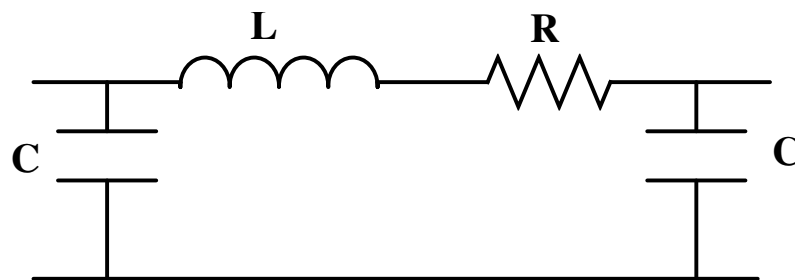


Figure 5.1: The PI model.

PI model is a simplified model for transient analysis studies, appropriate mainly for distribution lines or transmission lines of short length. In fact, PI model constitutes a discrete approximation of the constant distributed parameter model. PI model uses lumped parameters, which can result to false oscillation. The above disadvantage can be limited by connecting in parallel R-L elements.

Distributed and frequency dependent parameter models are best for transient studies. They use traveling wave solutions, which are valid over a much wider frequency range than PI-circuit models.

JMarti frequency-dependent model is more appropriate for the study of lightning performance of distribution lines, since it improves the reliability and the accuracy of the obtained results by approximating the characteristic admittance and the propagation constant by rational functions, in order to convert from mode domain to phase domain [13].

In the current work, the distribution line is represented by distributed parameters based on the Bergeron's traveling wave method [14]. The lossless distribution line is characterized by two values: the surge impedance and the wave propagation speed given by equations (5.1) and (5.2).

$$Z = \sqrt{\frac{L}{C}} \quad (5.1)$$

$$v = \sqrt{\frac{1}{LC}} \quad (5.2)$$

where:

L is the per-unit length inductance, and

C is the per-unit length capacitance.

The circuit representation of distribution lines is performed by using the Distributed Parameter Line Model of Simulink, based on the Bergeron's theory. The Distributed Parameter Line block uses an N-phase distributed parameter line model with lumped losses, based on the Bergeron's traveling wave method. The lossless distributed line is characterized by the surge impedance Z_C and the phase velocity v , according to the equations:

$$Z_C = \sqrt{l \cdot c} \quad (5.3)$$

$$v = \frac{1}{\sqrt{l \cdot c}} \quad (5.4)$$

where:

l is the per unit length inductance of the line, and
 c is the per unit length capacitance of the line.

The model considers that the voltage at the start of the line should arrive at the end of the line without changes, after a time given by the equation:

$$\tau = \frac{v}{d} \quad (5.5)$$

where:

τ is the transport delay of the voltage wave,
 v is the propagation velocity of the wave, and
 d is the length of the line

By lumping $R/4$ at both ends of the line and $R/2$ in the middle and using the current injection method the circuit of Figure 5.2 is extracted.

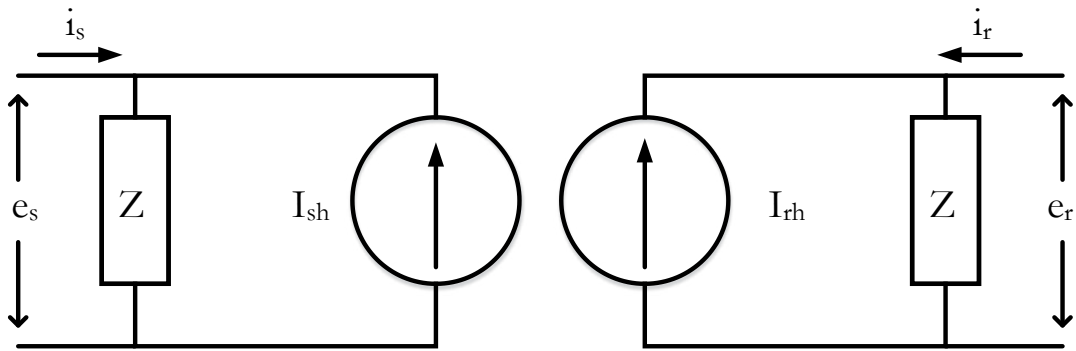


Figure 5.2: Two-port equivalent circuit model of a line.

The equivalent circuit of Figure 5.2 is governed by the equations:

$$I_{sh}(t) = \left(\frac{1+h}{2}\right) \cdot \left(\frac{1+h}{Z}\right) \cdot e_r(t-\tau) - h \cdot i_r(t-\tau) + \left(\frac{1-h}{2}\right) \cdot \left(\frac{1+h}{Z}\right) \cdot e_s(t-\tau) - h \cdot i_s(t-\tau) \quad (5.6)$$

$$I_{rh}(t) = \left(\frac{1+h}{2}\right) \cdot \left(\frac{1+h}{Z}\right) \cdot e_s(t-\tau) - h \cdot i_s(t-\tau) + \left(\frac{1-h}{2}\right) \cdot \left(\frac{1+h}{Z}\right) \cdot e_r(t-\tau) - h \cdot i_r(t-\tau) \quad (5.7)$$

$$Z = Z_C + \frac{r}{4} \quad (5.8)$$

$$h = \frac{Z_C - r/4}{Z_C + r/4} \quad (5.9)$$

where:

r is the per unit length resistance of the line.

The grounding resistance of the line is modeled as a lumped resistor, the wooden poles are modeled by a parallel combination of a resistor and a capacitor, while the insulators were modeled as voltage-dependent flashover switches [7].

5.3.2 Shield Wires

Overhead shield wires constitute the most common method, in order to improve the lightning performance and reduce the number of faults in distribution lines. Their role is to intercept lightning strikes, that otherwise would terminate on the phase conductors. Shield wires offer effective protection, when low values of ground resistance are achieved. When lightning strikes the pole structure or overhead shield wire, the lightning discharge current, flowing through the pole and pole ground resistance, produces potential differences across the line insulation. If the line insulation strength is exceeded, flashover occurs, i.e., a backflashover. Since the pole voltage is highly dependent on the pole resistance, consequently grounding resistance is an extremely important factor in determining lightning performance [1].

5.3.3 Metal Oxide Surge Arresters

The lightning performance of an electrical installation can be improved by installing surge arresters. The main scope of an arrester is to protect equipment from the effects of overvoltages. Metal oxide surge arresters present a highly non linear voltage-current characteristic, i.e., the arresters present high resistance for normal operating voltage and low resistance in case of overvoltage, in order to pass the lightning or switching current to the ground. The most significant technical characteristics of surge arresters according to the IEC 60099-4 are [15-17]:

- Continuous operating voltage (U_c). Designated rms value of power frequency voltage that may be applied continuously between the terminals of the arrester.
- Rated voltage. Maximum permissible rms value of power frequency voltage between arrester terminals at which is designed to operate correctly under temporary overvoltages.
- Discharge current. Impulse current which flows through the arrester.
- Residual voltage (U_{res}). Peak value of the voltage that appears between arrester terminals when a discharge current is injected.
- Rated discharge current. Peak value of lightning current impulse, which is used to classify an arrester.
- Lightning impulse protective level. Voltage that drops across the arrester when the rated discharge current flows through the arrester.
- Energy absorption capability. Maximum level of energy injected into the arrester at which it can still cool back to its normal operating temperature.

Figure 5.3 shows the cutaway of a typical metal oxide surge arrester, which consists of the electrodes, the varistor column, an internal fiber glass and the external insulation. Metal oxide surge arresters have dynamic behaviour, which is strongly depended on the frequency of the injected impulse current. Analytically:

- The residual voltage of the arrester increases as the current front time decreases [18, 19].
- The residual voltage reaches its maximum before the current maximum.

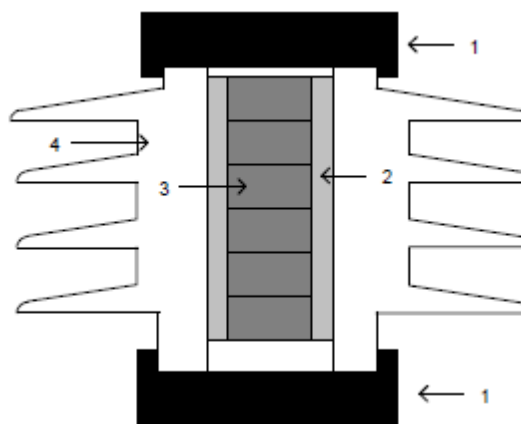


Figure 5.3: Metal oxide surge arrester cut (1: electrodes, 2: fiber glass, 3: varistor column, 4: external insulator) [20].

The most used frequency dependent metal oxide surge arresters models are the IEEE model [21], the Pinceti-Gianettoni model [22] and the Fernandez-Diaz model [23]. The last two models are simpler forms of the IEEE model.

The IEEE Working Group 3.4.11 [21] proposed the model of Figure 5.4, including the non-linear resistances A_0 and A_1 , separated by a R - L filter. For slow front surges the filter impedance is low and the non-linear resistances are in parallel. For fast front surges filter impedance becomes high, and the current flows through the non-linear resistance A_0 . L_0 is associated with magnetic fields in the vicinity of the arrester. R_0 stabilizes the numerical integration and C represents the terminal-to-terminal capacitance.

The equations for the above parameters are given as follows [21, 16, 17]:

$$L_1 = (15 d) / n \text{ } \mu\text{H} \quad (5.10)$$

$$R_1 = (65 d) / n \text{ } \Omega \quad (5.11)$$

$$L_0 = (0.2 d) / n \text{ } \mu\text{H} \quad (5.12)$$

$$R_0 = (100 d) / n \text{ } \Omega \quad (5.13)$$

$$C = (100 n) / d \text{ pF} \quad (5.14)$$

where:

d is the length of arrester column in meters, and

n is the number of parallel columns of metal-oxide disks.

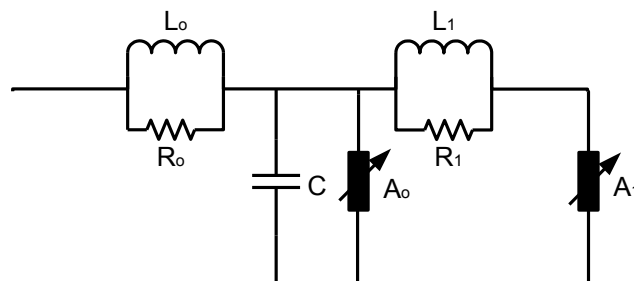


Figure 5.4: The IEEE model [21, 16, 17].

The Pinceti-Gianettoni model has no capacitance and the resistances R_0 and R_1 are replaced by one resistance (approximately 1 M Ω) at the input terminals, as shown in Figure 5.5 [22, 16, 17]. The non-linear resistors are based on the curves of [21]. The inductances L_0 and L_1 are calculated using the equations [22, 16, 17]:

$$L_0 = \frac{1}{4} \cdot \frac{V_{r(1/T_2)} - V_{r(8/20)}}{V_{r(8/20)}} \cdot V_n \quad \mu\text{H} \quad (5.15)$$

$$L_1 = \frac{1}{12} \cdot \frac{V_{r(1/T_2)} - V_{r(8/20)}}{V_{r(8/20)}} \cdot V_n \quad \mu\text{H} \quad (5.16)$$

where:

V_n is the arrester's rated voltage,

$V_{r(8/20)}$ is the residual voltage for a 8/20 10 kA lightning current, and

$V_{r(1/T_2)}$ is the residual voltage for a 1/ T_2 10 kA lightning current.

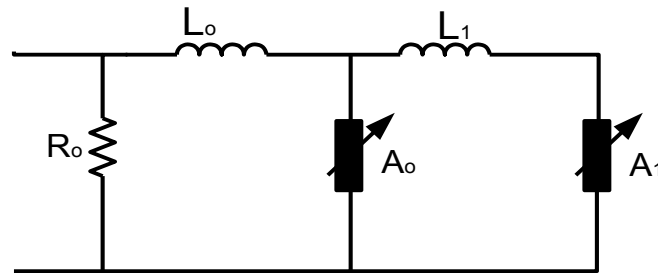


Figure 5.5: The Pinceti-Gianettoni model [22, 16, 17].

The advantage of this model in comparison to the IEEE model is that there is no need for arresters' physical characteristics, but there is only need for electrical data, given by the manufacturer.

The Fernandez – Diaz Model is also based on the IEEE model, A_0 and A_1 are separated by L_1 , while L_0 is neglected (Figure 5.6). C is added in arrester terminals and represents terminal-to-terminal capacitance of the arrester. This model does not require iterative calculations since the required data are obtained from the manufacturer's datasheet. The procedure for the computation of the parameters is given in [23, 16, 17]. The V-I

characteristics for A_0 and A_1 are calculated using manufacturers' data, considering the ratio I_0 to I_1 equal to 0.02. The inductance L_1 is given as:

$$L_1 = n L_1' \quad (5.17)$$

where:

n is a scale factor, and

L_1' is given in [23], computing the percentage increase of the residual voltage as:

$$\Delta V_{res} (\%) = \frac{V_{r(1/T_2)} - V_{r(8/20)}}{V_{r(8/20)}} \cdot 100 \quad (5.18)$$

where:

$V_{r(8/20)}$ is the residual voltage for a 8/20 lightning current, and

$V_{r(1/T_2)}$ is the residual voltage for a $1/T_2$ lightning current with the nominal amplitude.

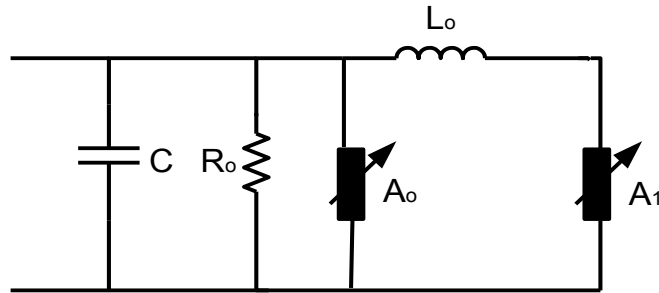


Figure 5.6: The Fernandez-Diaz model [23, 16, 17].

5.3.4 Distributed Generation Units

The implementation of distributed generation (DG) in the modern distribution networks is uninterrupted and is expected to increase in the coming years due to the many advantages that they present as it has extensively been analyzed in Chapter 2. Distributed generation that is mainly based on renewable energy sources, such as photovoltaics and wind generators, are mainly located near to consumer centres and provide a bidirectional flow. In this Thesis, and for the simulations that have been conducted, DG units were modeled as synchronous generators that inject into the network only real power (PV type).

5.4 Lightning Protection Studies for Modern Distribution Networks

5.4.1 System Configuration

The distribution network is consisting of unshielded wooden poles of 9.2 m height with average span length of 70 m. The wooden poles and the conductors' geometries are shown in Figure 5.7. Data from a real distribution line of nominal voltage of 20 kV (phase-phase, rms) has been used in these studies.

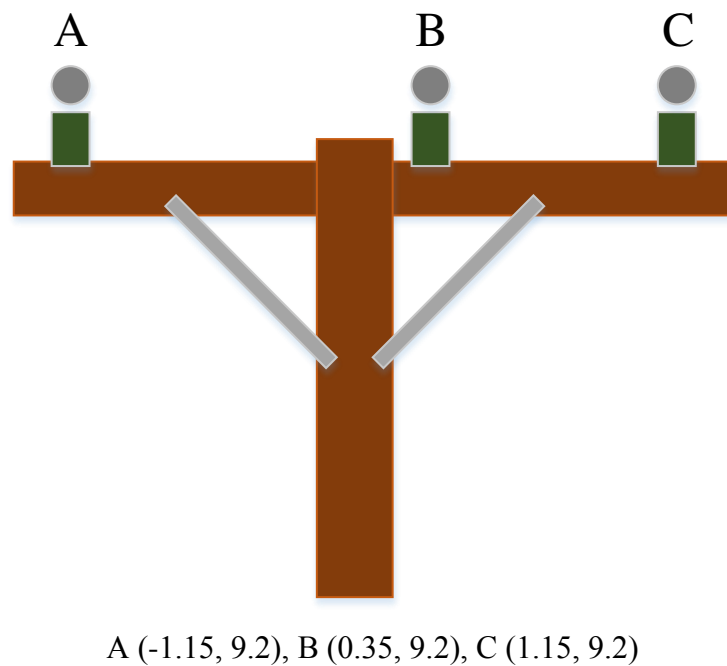


Figure 5.7: Unshielded wooden pole of a typical 20 kV distribution line.

The distribution line uses porcelain insulators of basic insulation level (BIL) of 125 kV. The characteristics of the three horizontally placed phase conductors are: A1, $3 \times 95 \text{ mm}^2$, $R_{\text{line}} = 0.215 \text{ Ohm/km}$ and $X_{\text{line}} = 0.334 \text{ Ohm/km}$. The distribution line that has a total length of 8 km is represented by distributed parameters based on the Bergeron's traveling wave method.

In Table 5.1 the characteristics of the 20 kV surge arrester are cited and will be used in the examined distribution line.

Table 5.1: Surge arrester characteristics.

| | |
|--|---------|
| Maximum Continuous Operating Voltage | 19.5 kV |
| Rated Voltage | 24 kV |
| Nominal Discharge Current | 10 kA |
| Maximum Residual Voltage (8/20 μ s, 10 kA) | 67 kV |
| Energy Capability | 60 kJ |

The grounding resistance of the line is modeled as a lumped resistor, the wooden poles are modeled by a parallel combination of a resistor and a capacitor, while the insulators were modeled as voltage-dependent flashover switches [7].

The under study distribution line is connected with three distributed generation (DG) units of PV type (inject real power to the line) and are considered as synchronous generators connected to the distribution network by transformers.

The injected to the distribution line lightning current is modeled as a double exponential waveform, with peak magnitude of 10 kA, rise time 1.2 μ s and time-to-half value of 50 μ s.

The simulation model of the under study distribution network is shown in Figure 5.8. The examined distribution line, which has been considered as unshielded, has been divided in four different segments with length of 2 km each, in order different positions to be defined (A, B, C, D, E) along the line's length. At these positions surge arresters were installed and the developed overvoltages for each position were calculated. Each one of the three DG units connected at points A, C and E were generated real power of 500 kW.

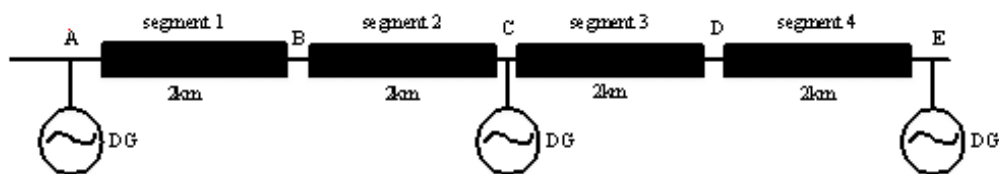


Figure 5.8: Simulation model of unshielded distribution network with DGs.

Four different sensitivity analyses, i.e., Sensitivity analysis for lightning strike hit position, Sensitivity analysis for lightning current peak magnitude, Sensitivity analysis for surge arresters models, and Sensitivity analysis for distributed generation sizes, were conducted to the distribution network for different scenarios in relation to the distribution line's grounding resistance that was varying from 1 to 60 Ohms.

MATLAB Simulink has been used in order the pre-described sensitivity studies to be performed.

5.4.2 Sensitivity Analysis for Lightning Strike Hit Position

A sensitivity analysis is conducted to the distribution network for each one of the six scenarios presented in Table 5.2.

Table 5.2: Simulation scenarios.

| No | Surge arrester position | | | | | DG unit position | | |
|----|-------------------------|---|---|---|---|------------------|---|---|
| | A | B | C | D | E | A | B | C |
| 1 | 0 | 0 | 0 | 0 | 0 | 0 | 0 | 0 |
| 2 | 1 | 0 | 1 | 0 | 1 | 0 | 0 | 0 |
| 3 | 1 | 1 | 1 | 1 | 1 | 0 | 0 | 0 |
| 4 | 0 | 0 | 0 | 0 | 0 | 1 | 1 | 1 |
| 5 | 1 | 0 | 1 | 0 | 1 | 1 | 1 | 1 |
| 6 | 1 | 1 | 1 | 1 | 1 | 1 | 1 | 1 |

(1 denotes the installation of equipment, 0 denotes the absence of equipment).

Lightning discharges with lightning current magnitude of 10 kA were applied at position A as shown in Figure 5.9. The obtained overvoltages at each one of the five different positions (A, B, C, D, E) are shown in Figures 5.10 – 5.14.

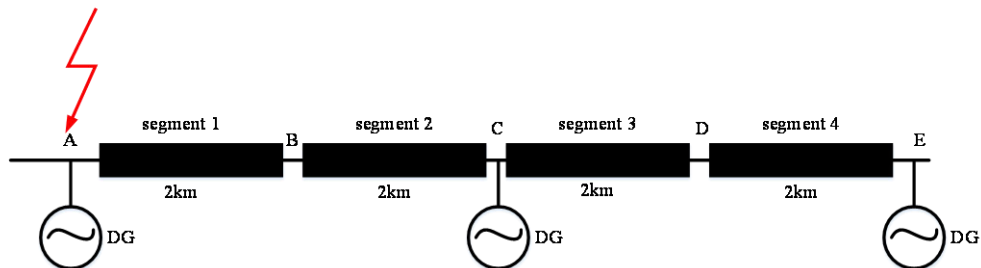


Figure 5.9: Simulation model of distribution line with DG that is hit in position A.

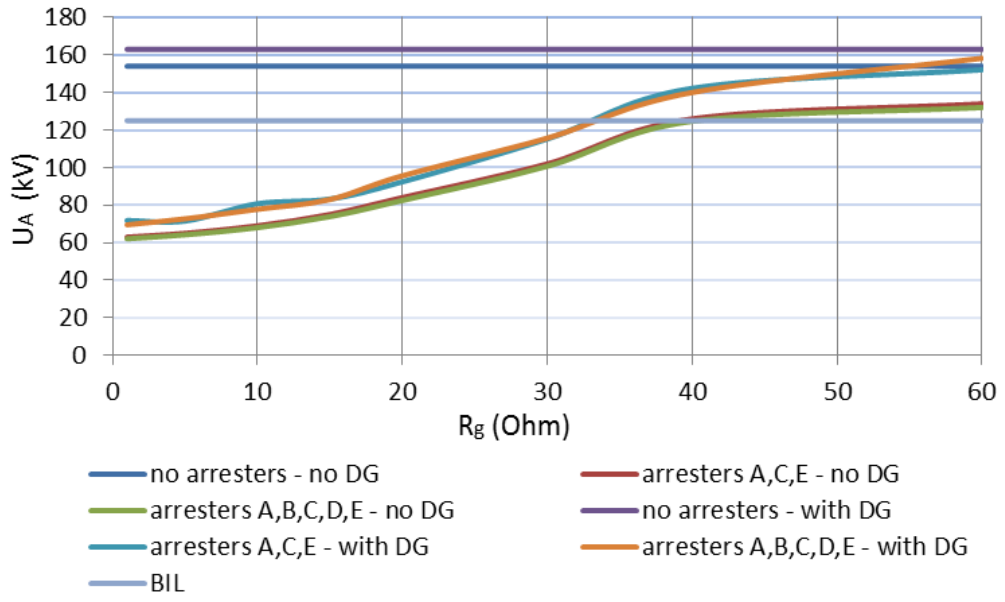


Figure 5.10: Developed overvoltage at position A, for lightning hit at position A, in relation to grounding resistance.

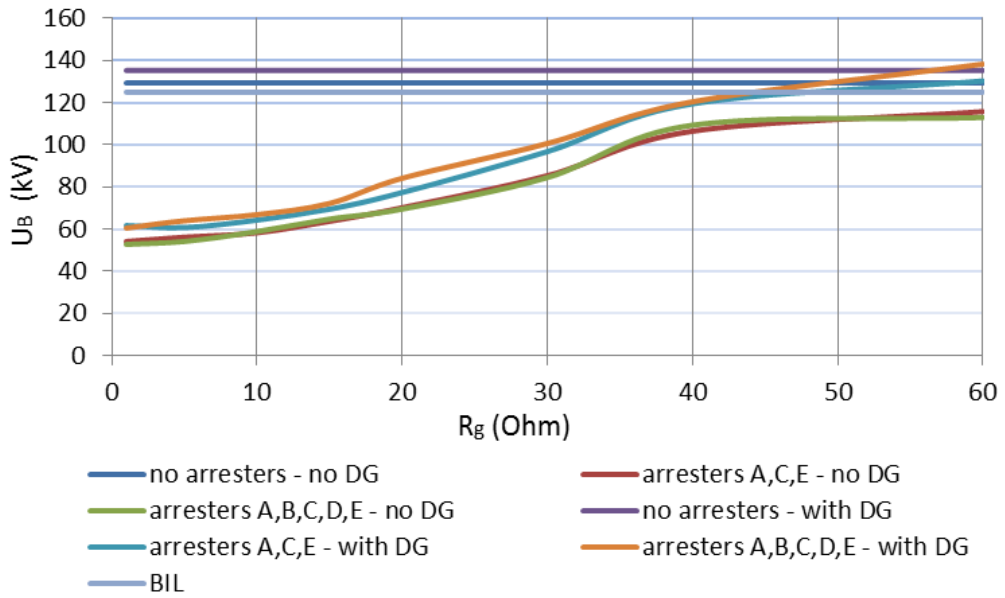


Figure 5.11: Developed overvoltage at position B, for lightning hit at position A, in relation to grounding resistance.

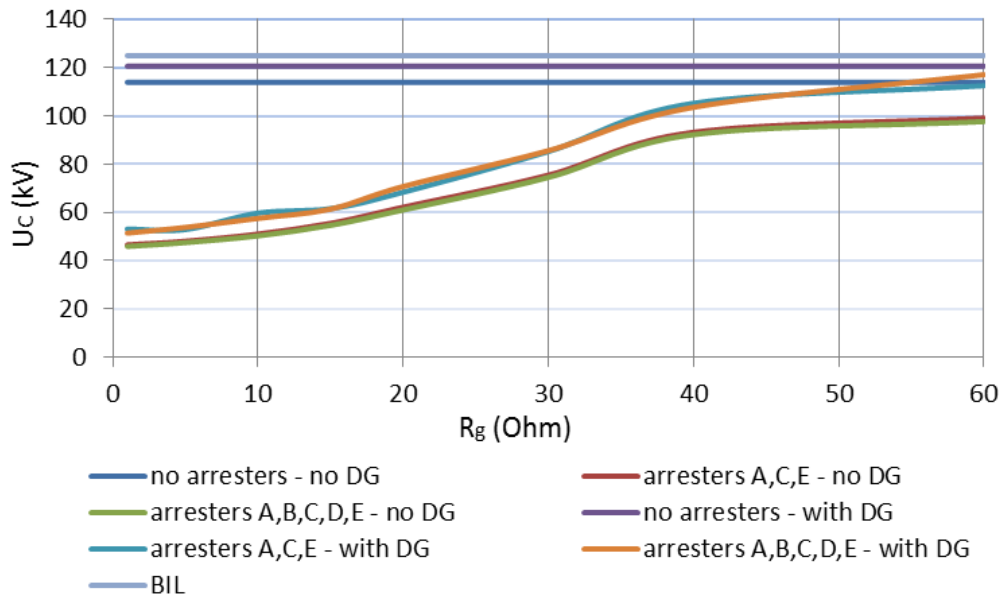


Figure 5.12: Developed overvoltage at position C, for lightning hit at position A in relation to grounding resistance.

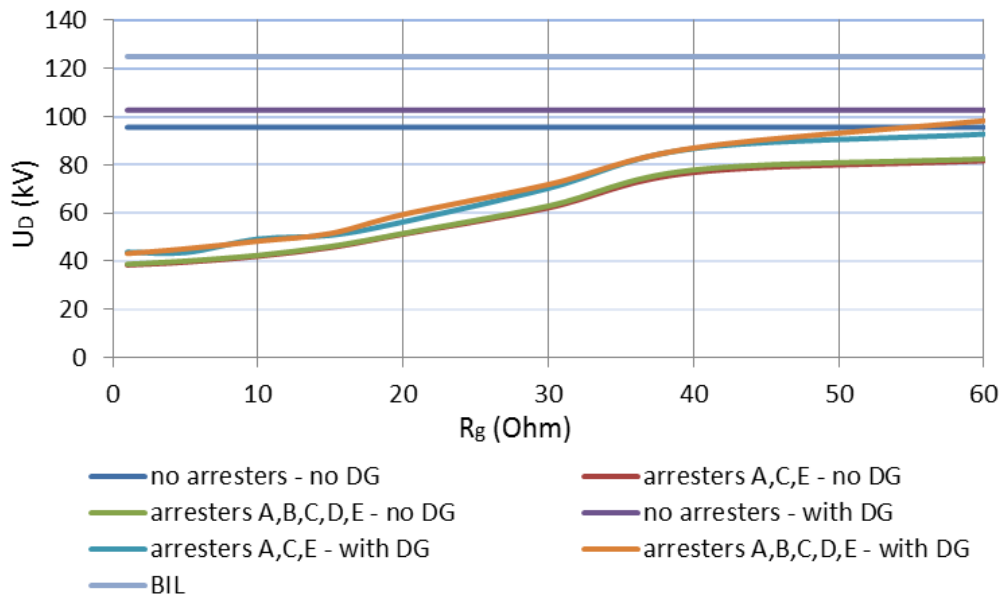


Figure 5.13: Developed overvoltage at position D, for lightning hit at position A, in relation to grounding resistance.

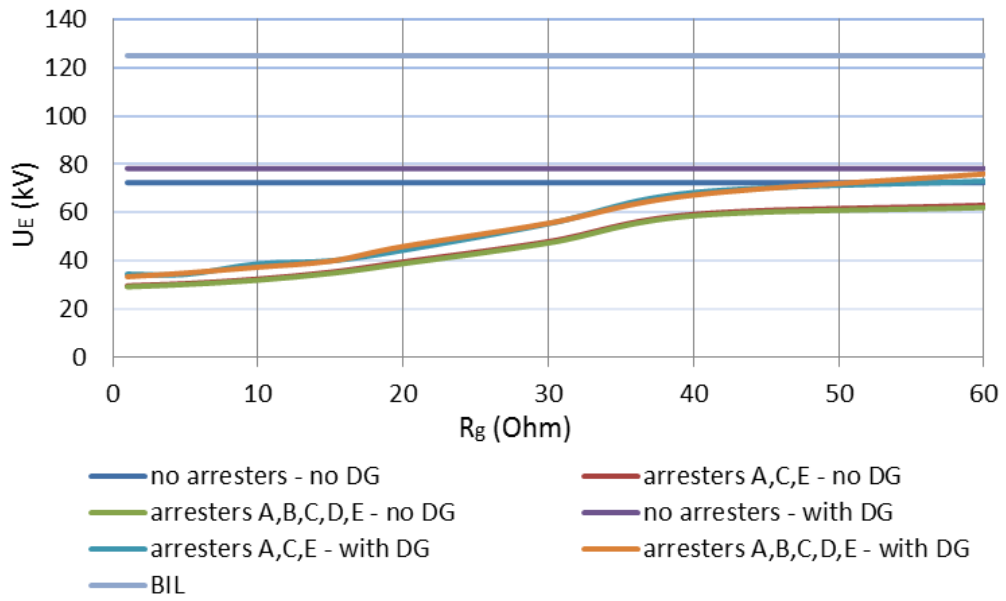


Figure 5.14: Developed overvoltage at position E, for lightning hit at position A, in relation to grounding resistance.

Lightning discharges with lightning current magnitude of 10 kA were applied at position C as shown in Figure 5.15. The obtained overvoltages at each one of the five different positions (A, B, C, D, E) are shown in Figures 5.16 – 5.20.

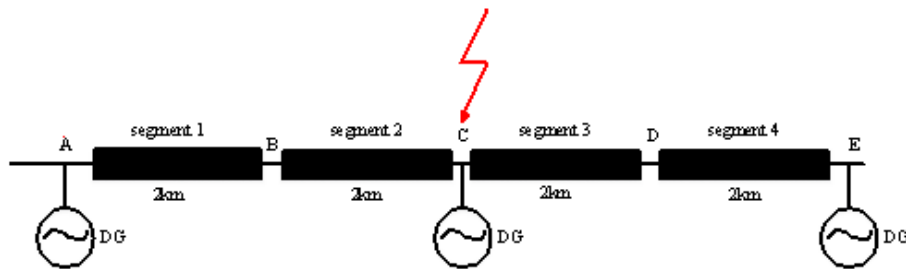


Figure 5.15: Simulation model of distribution line with DG that is hit in position C.

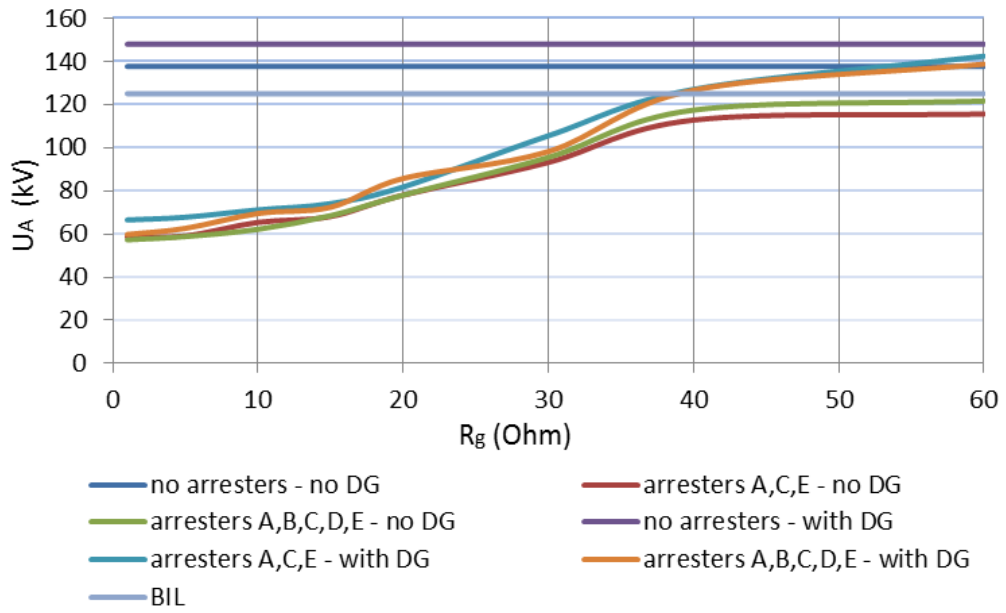


Figure 5.16: Developed overvoltage at position A, for lightning hit at position C, in relation to grounding resistance.

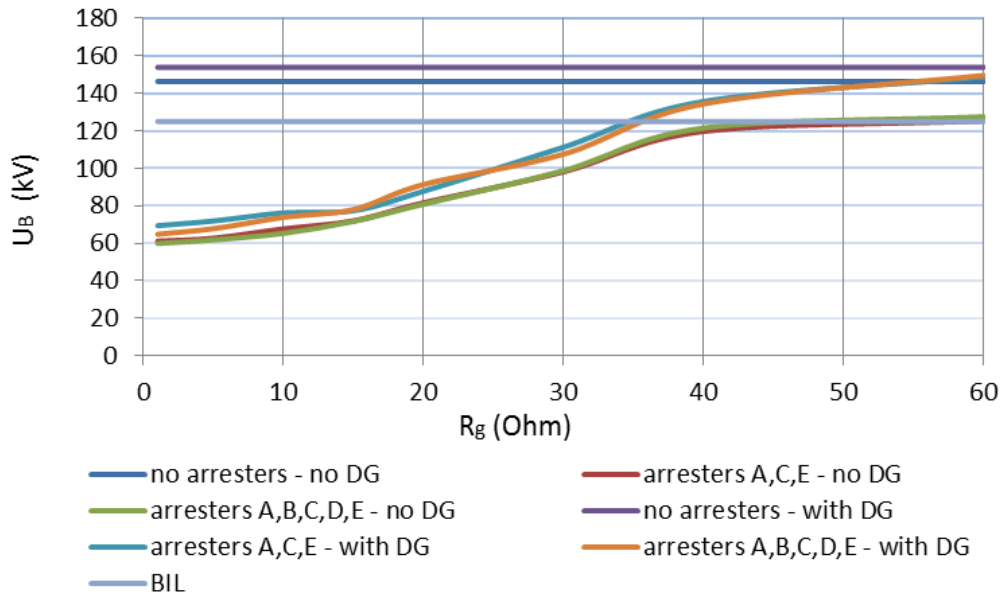


Figure 5.17: Developed overvoltage at position B, for lightning hit at position C, in relation to grounding resistance.

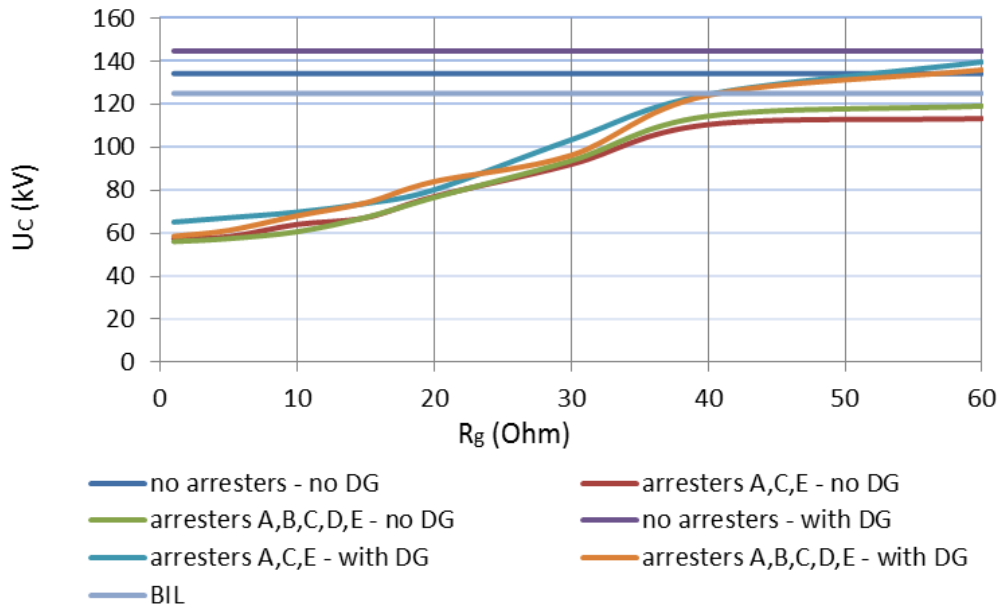


Figure 5.18 Developed overvoltage at position C, for lightning hit at position C in relation to grounding resistance.

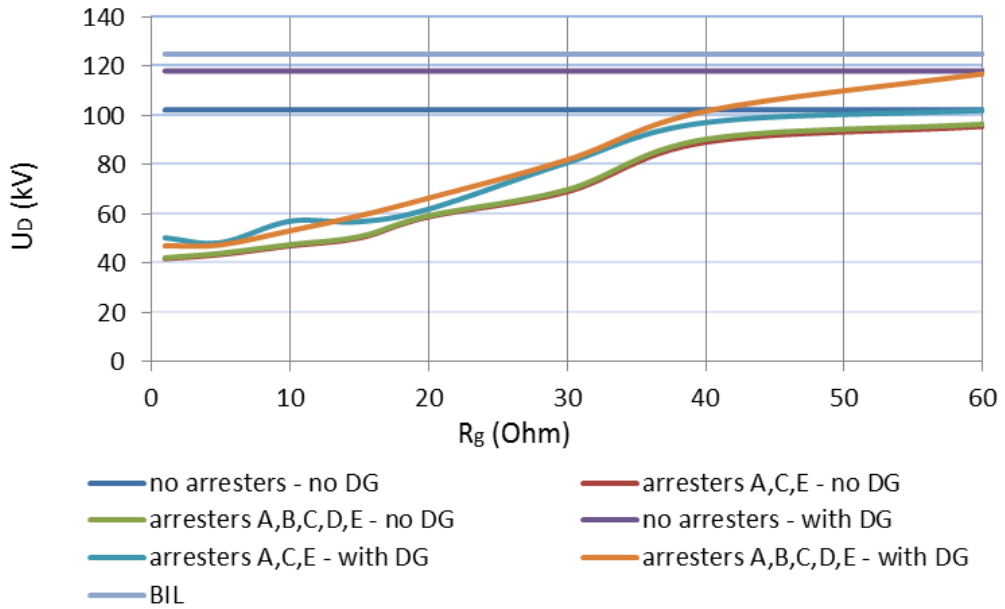


Figure 5.19: Developed overvoltage at position D, for lightning hit at position C, in relation to grounding resistance.

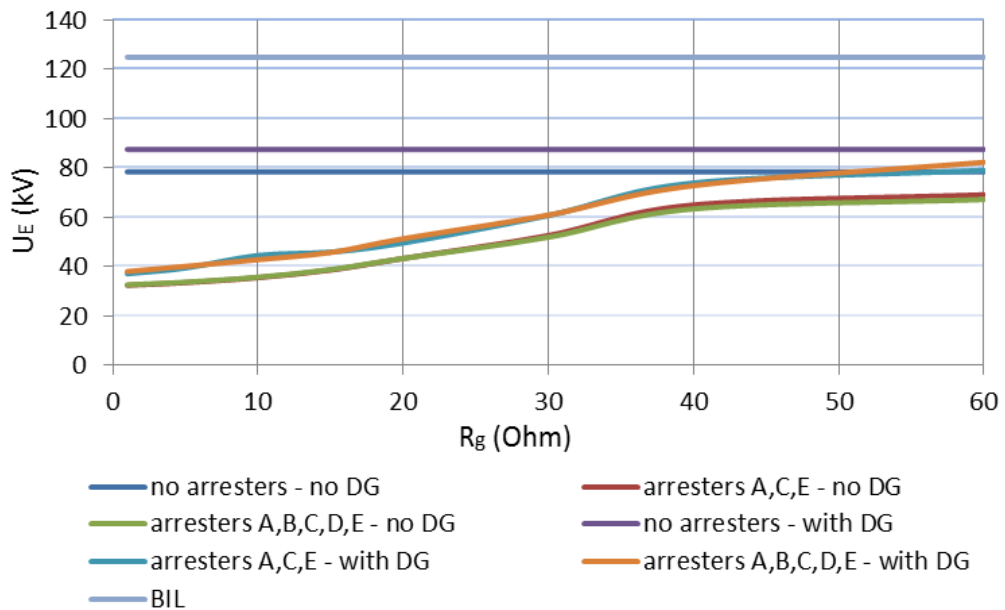


Figure 5.20: Developed overvoltage at position E, for lightning hit at position C, in relation to grounding resistance.

Based on the obtained results it can be observed that in cases where no arresters were installed on the distribution line, the variation of the grounding resistance had no effect in the developed overvoltages. This was something that was expected since the poles were made of wood, there were no active (under voltage) parts of the line connected to earth and the line was unshielded. However the overvoltages were attenuated as the distance from the lightning hit point was increased.

The installation of surge arresters in all available positions, in contrast to the installation of surge arresters to three (A, C, E) out of five positions, has shown that the developed overvoltages were reduced, although not significantly. Nevertheless the use of surge arresters in the examined distribution line is necessary for grounding resistance values greater than 40 Ohms since in these cases the overvoltages have exceeded the value of the basic insulation level of the line.

Finally based on the obtained results has been proven that the presence of distributed generation power plants affects significantly the magnitude of the developed overvoltages. In all examined cases the presence of DGs resulted in increased

overvoltages, something that must be taken seriously into account from electric utilities design engineers for the lightning protection of the modern distribution lines.

5.4.3 Sensitivity Analysis for Lightning Current Peak Magnitude

A sensitivity analysis has been conducted to the distribution network for four different lightning current peak magnitudes, i.e., 10 kA, 20 kA, 30 kA and 40 kA. The lightning discharges were applied at position A as shown in Figure 5.9.

Two case studies were considered. In the first one, arresters were installed at positions A, B, C, D, E and none DG unit was connected to the network. In the second one, arresters were installed at positions A, B, C, D, E and all three DG units were connected to the network. The obtained overvoltages at each one of the five different positions (A, B, C, D, E) for the first case study (no DG) are shown in Figures 5.21 – 5.25, while the obtained overvoltages at each one of the five different positions (A, B, C, D, E) for the second case study (with DG) are shown in Figures 5.26 – 5.30.

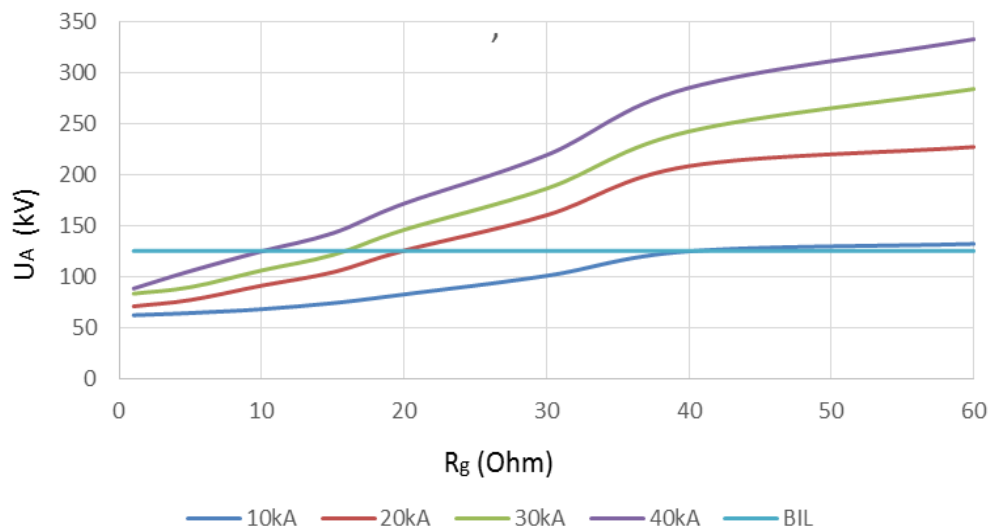


Figure 5.21: Developed overvoltages at position A for different peak lightning current magnitudes in relation to grounding resistance (no DG).

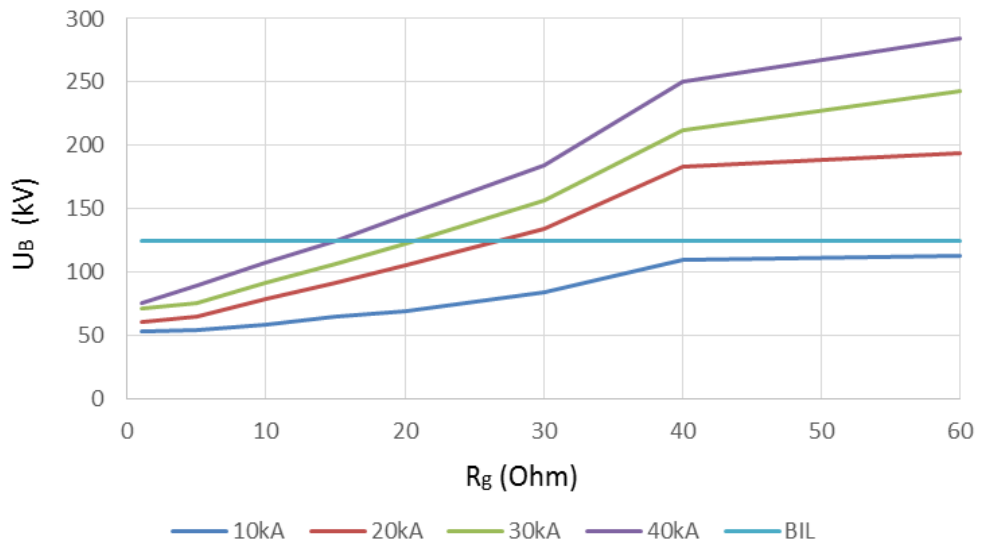


Figure 5.22 Developed overvoltages at position B for different peak lightning current magnitudes in relation to grounding resistance (no DG).

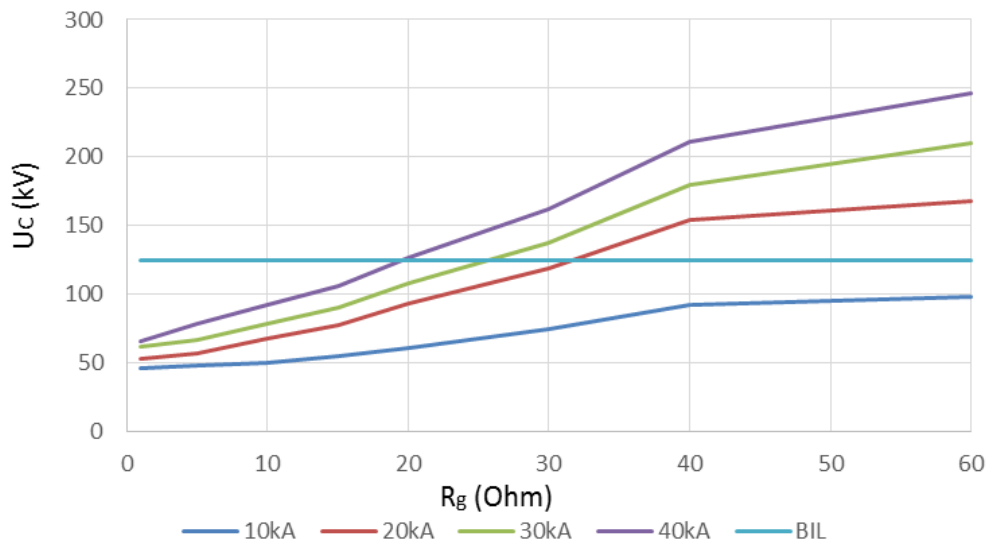


Figure 5.23: Developed overvoltages at position C for different peak lightning current magnitudes in relation to grounding resistance (no DG).

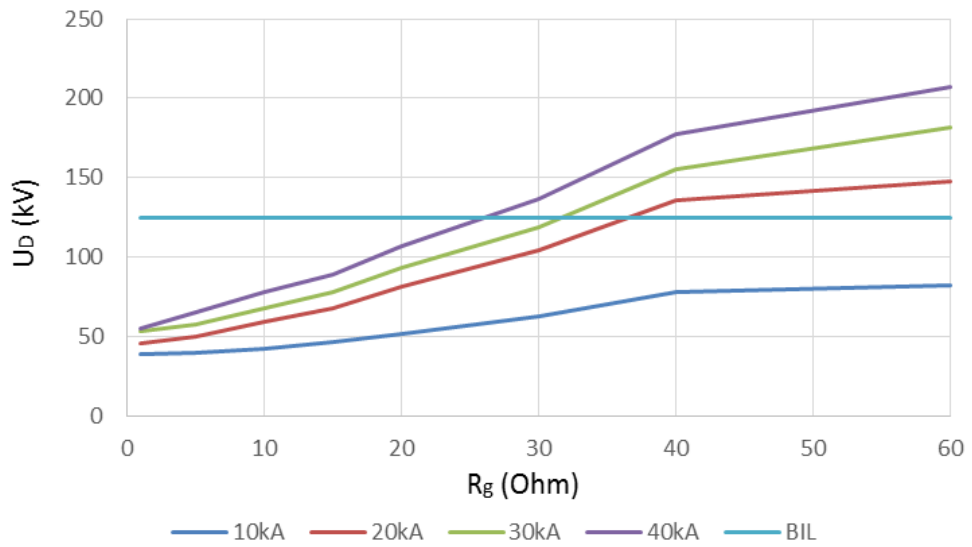


Figure 5.24: Developed overvoltages at position D for different peak lightning current magnitudes in relation to grounding resistance (no DG).

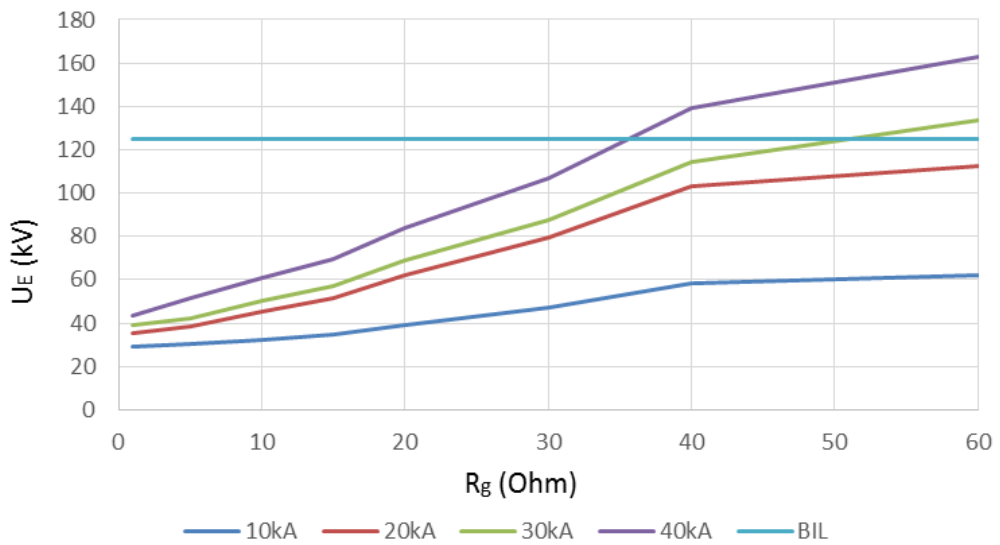


Figure 5.25: Developed overvoltages at position E for different peak lightning current magnitudes in relation to grounding resistance (no DG).

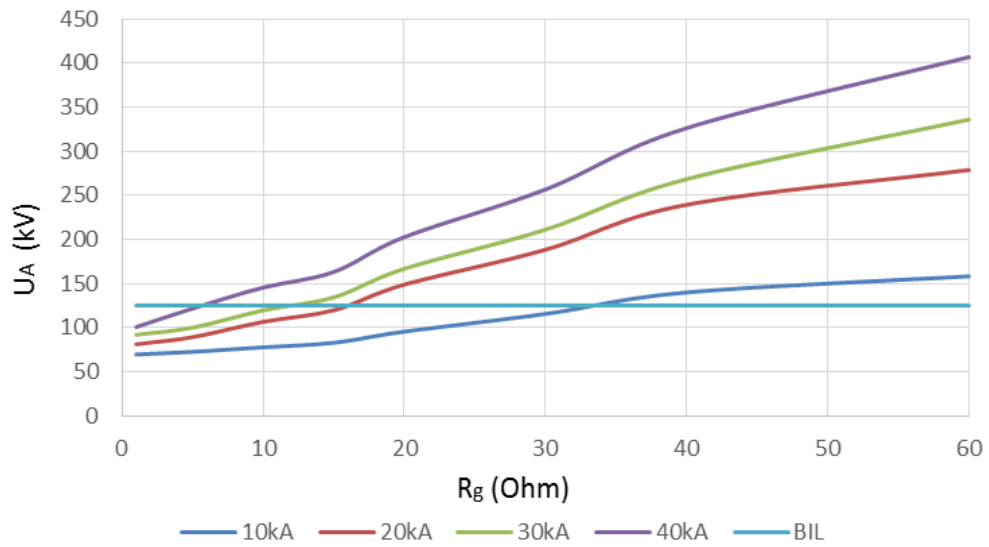


Figure 5.26: Developed overvoltages at position A for different peak lightning current magnitudes in relation to grounding resistance (with DG).

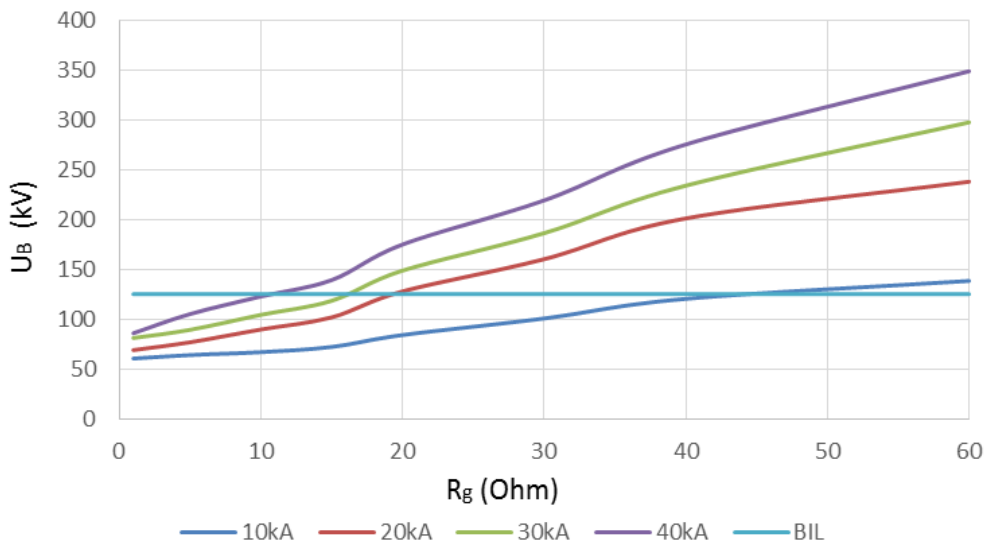


Figure 5.27: Developed overvoltages at position B for different peak lightning current magnitudes in relation to grounding resistance (with DG).

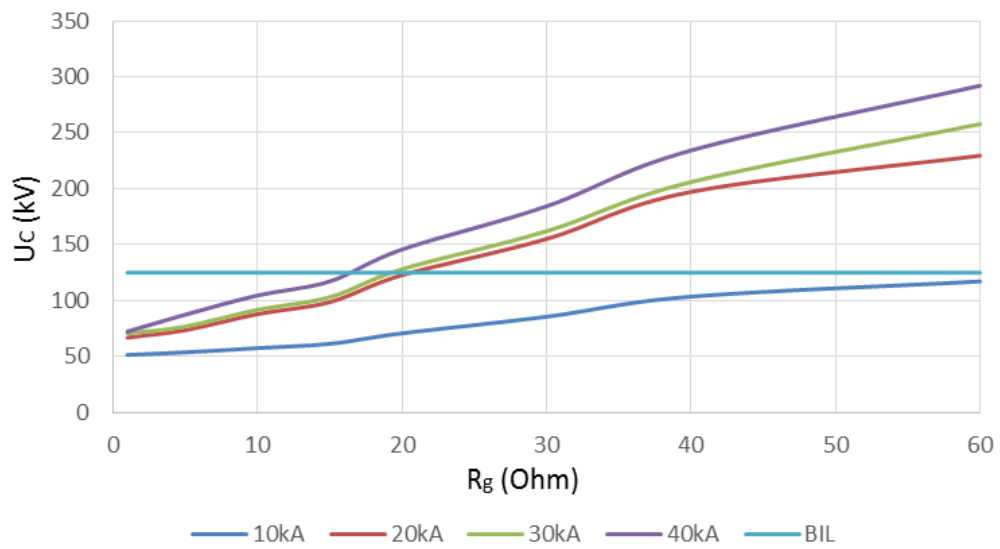


Figure 5.28: Developed overvoltages at position C for different peak lightning current magnitudes in relation to grounding resistance (with DG).

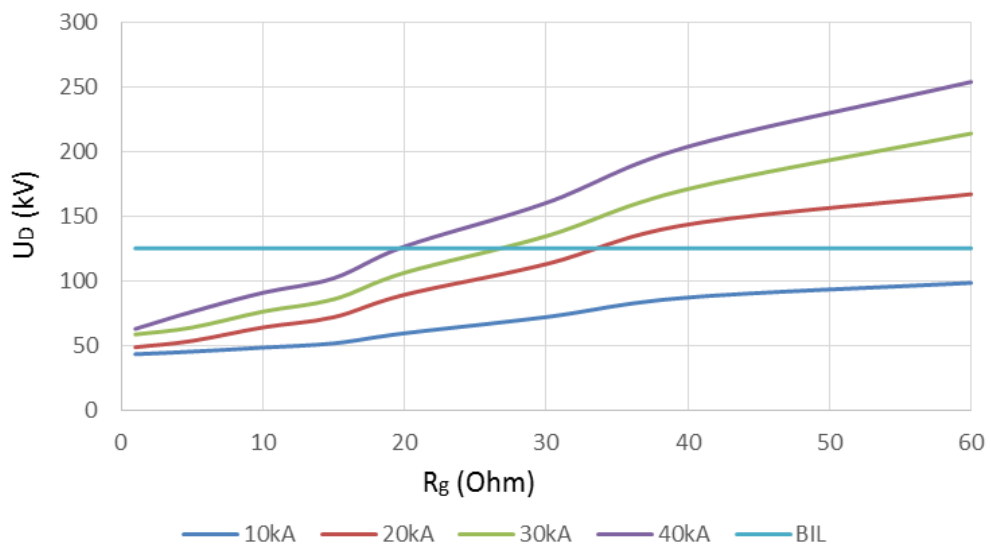


Figure 5.29: Developed overvoltages at position D for different peak lightning current magnitudes in relation to grounding resistance (with DG).

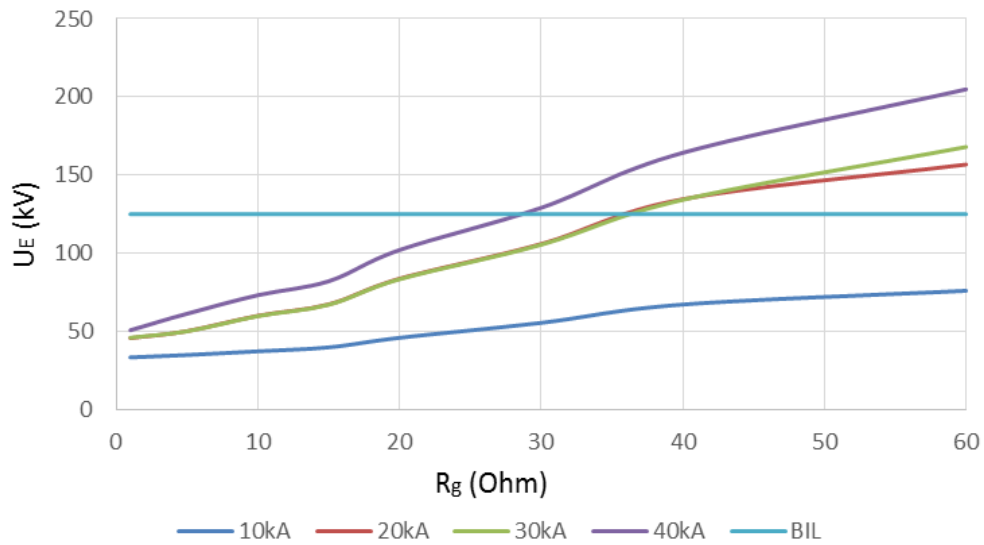


Figure 5.30: Developed overvoltages at position E for different peak lightning current magnitudes in relation to grounding resistance (with DG).

Based on the obtained results it can be observed that the variation of the grounding resistance had a proportional effect in the developed overvoltages. As it was expected, the overvoltages were attenuated as the distance from the lightning hit point was increased. The installation of the DG units to the network has shown that the developed overvoltages were significantly increased. In cases where the lightning hit point is close to the position that overvoltages are obtained (e.g., position A and B) it has been shown that the presence of DGs could result in a lightning fault for grounding resistance values of even a few Ohms, i.e., 10-20 Ohms. The overvoltages are much lower as the distance from the lightning hit point is increased but still they can result in lightning faults, since the obtained values are greater than the basic insulation level.

5.4.4 Sensitivity Analysis for Surge Arresters Models

A sensitivity analysis has been conducted to the distribution network for the three different surge arresters models, i.e., the IEEE, the Pincety, and the Fernandez model. The lightning discharges with lightning current magnitude of 10 kA were applied at position C as shown in Figure 5.15.

Two case studies were considered. In the first case study, arresters were installed at positions A, C, E and none DG unit was connected to the network. In the second case study, arresters were installed at positions A, C, E and all three DG units were connected to the network. The obtained overvoltages at each one of the three different positions (A, B, C) for the first case study (no DG) are shown in Figures 5.31 – 5.33, while the obtained overvoltages at each one of the three different positions (A, B, C,) for the second case study (with DG) are shown in Figures 5.34 – 5.36. It must be mentioned that although the overvoltages at positions D and E have been calculated, these are not presented in this Thesis, since they are symmetrical and identical with these in positions A and B.

The obtained results have shown that all three surge arresters models have similar performance and the calculated overvoltages values are very close to each other. As the distance from the hit point increases the overvoltages are reduced. The presence of DGs results in higher overvoltages. Finally it has been shown that the effectiveness of each surge arrester model is different depending on the presence, or not, of DGs to the network, therefore a careful selection of surge arrester model to be used in the lightning studies of electric utilities design engineers must be done, in an effort to obtain accurate results.

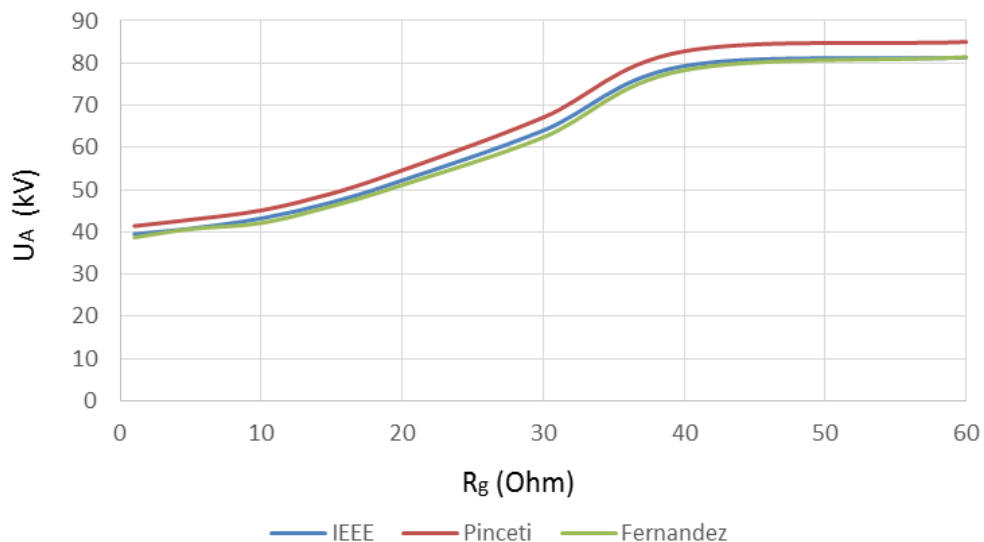


Figure 5.31: Developed overvoltages at position A for different surge arresters models in relation to grounding resistance (no DG).

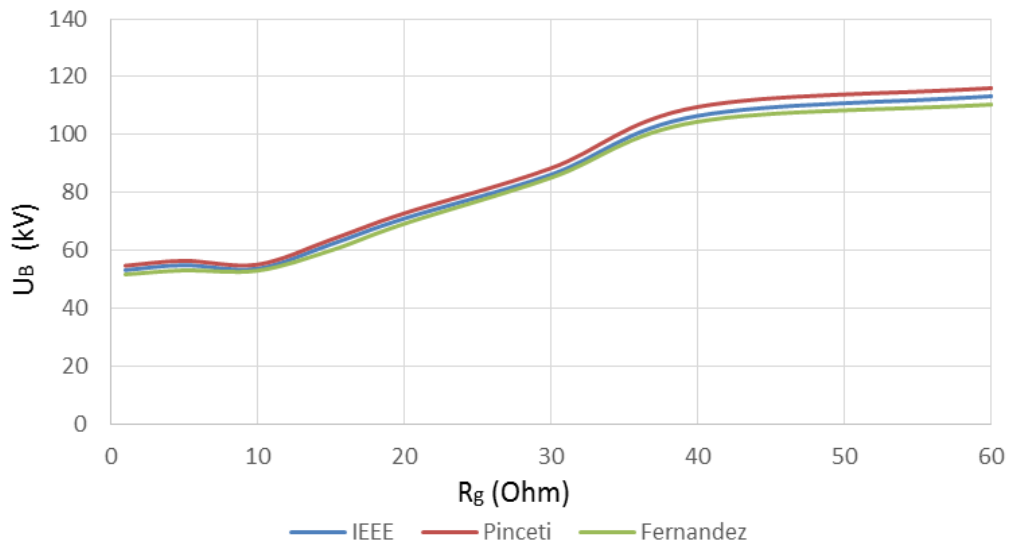


Figure 5.32: Developed overvoltages at position B for different surge arresters models in relation to grounding resistance (no DG).

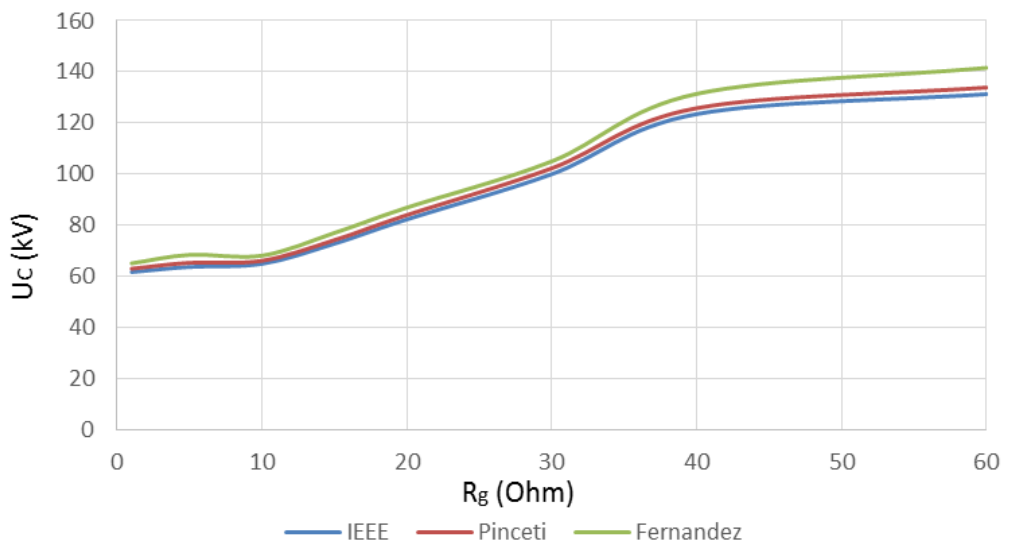


Figure 5.33: Developed overvoltages at position C for different surge arresters models in relation to grounding resistance (no DG).

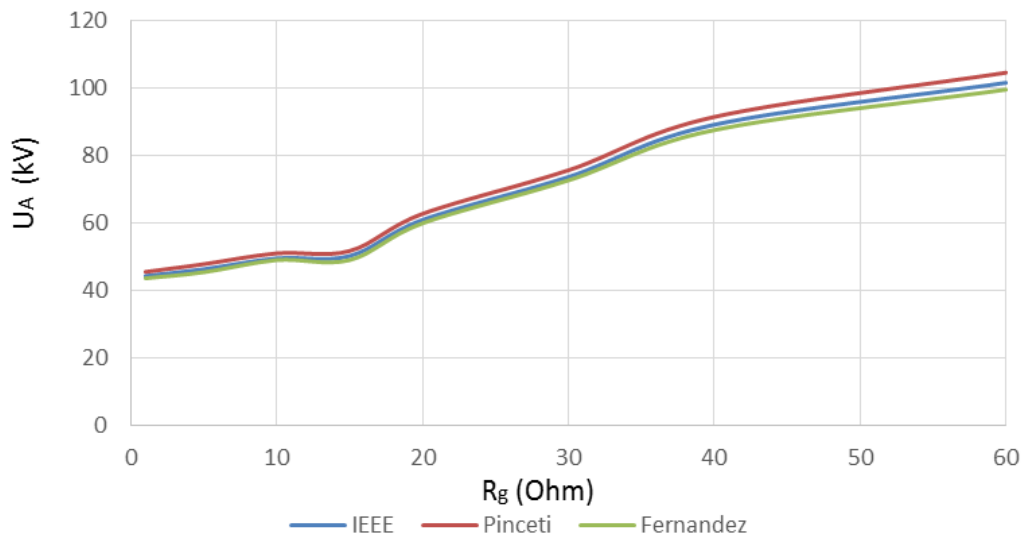


Figure 5.34: Developed overvoltages at position A for different surge arresters models in relation to grounding resistance (with DG).

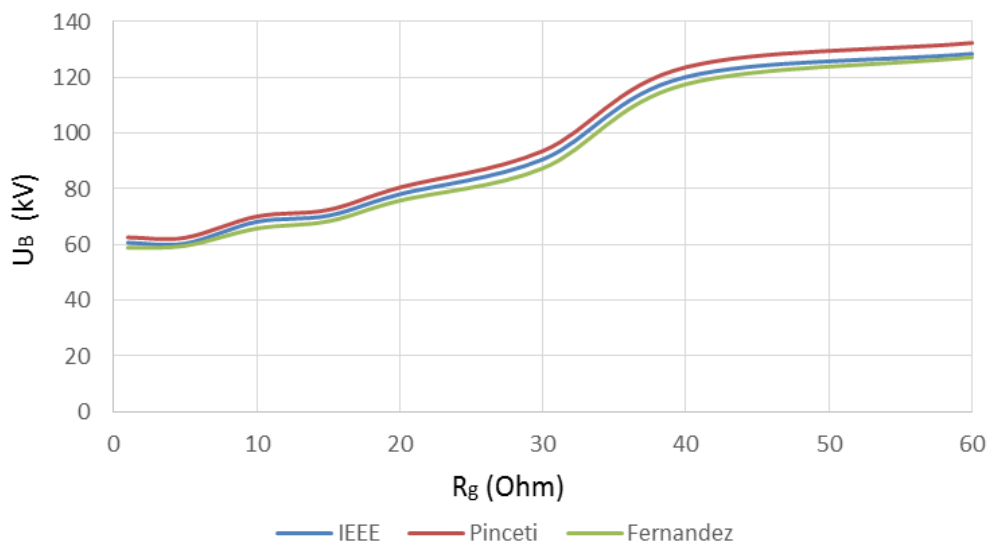


Figure 5.35: Developed overvoltages at position B for different surge arresters models in relation to grounding resistance (with DG).

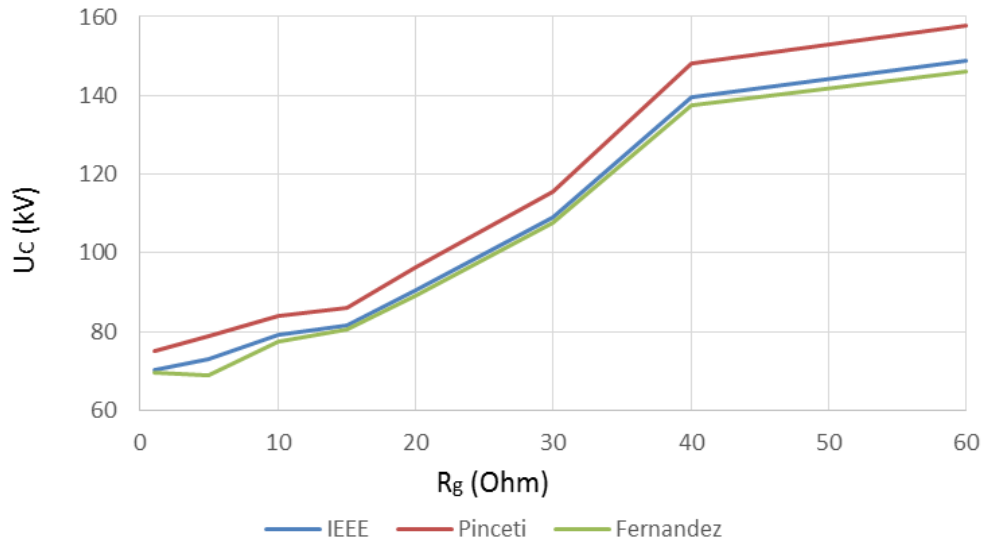


Figure 5.36: Developed overvoltages at position C for different surge arresters models in relation to grounding resistance (with DG).

5.4.5 Sensitivity Analysis for Distributed Generation Sizes

A sensitivity analysis has been conducted to the distribution network for four different combinations of distributed generation sizes, i.e., a) $DG_A=500$ kW - $DG_B=500$ kW - $DG_C=500$ kW, b) $DG_A=500$ kW - $DG_B=1$ MW - $DG_C=500$ kW, c) $DG_A=1$ MW - $DG_B=500$ kW - $DG_C=1$ MW and d) $DG_A=1$ MW - $DG_B=1$ MW - $DG_C=1$ MW. The lightning discharges with lightning current magnitude of 10 kA were applied at position A as shown in Figure 5.9.

Three case studies were considered. In the first case study, arresters were installed at positions A, B, C, D, E. In the second case study, arresters were installed at positions A, C, E and in the third case study no arresters have been installed. The obtained overvoltages for position A and for all four different distributed generation size combinations are shown in Figures 5.37 – 5.40, the obtained overvoltages for position C and for all four different distributed generation size combinations are shown in Figures 5.41 – 5.44, while the obtained overvoltages for position E and for all four different distributed generation size combinations are shown in Figures 5.45 – 5.48.

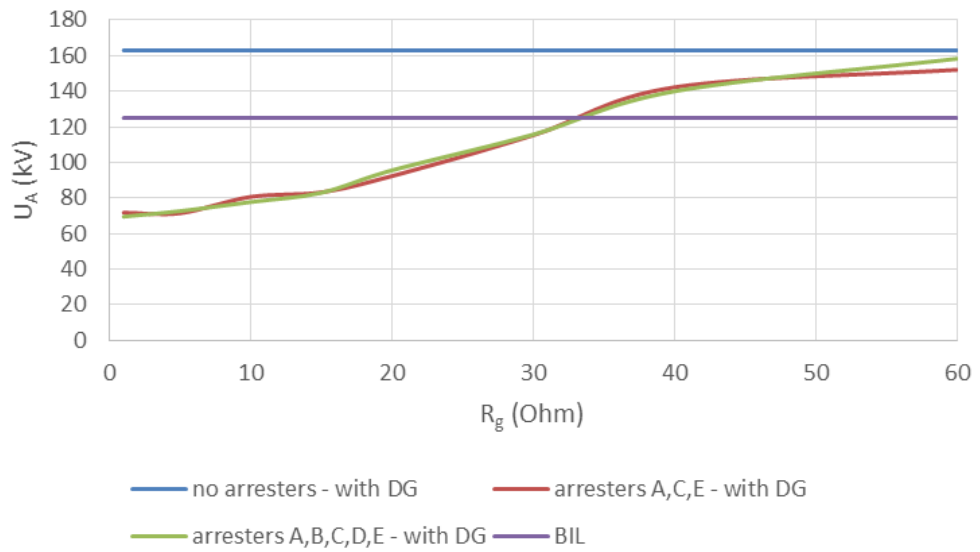


Figure 5.37: Developed overvoltage at position A, for lightning hit at position A, in relation to grounding resistance for DG sizes 500 kW - 500 kW - 500 kW.

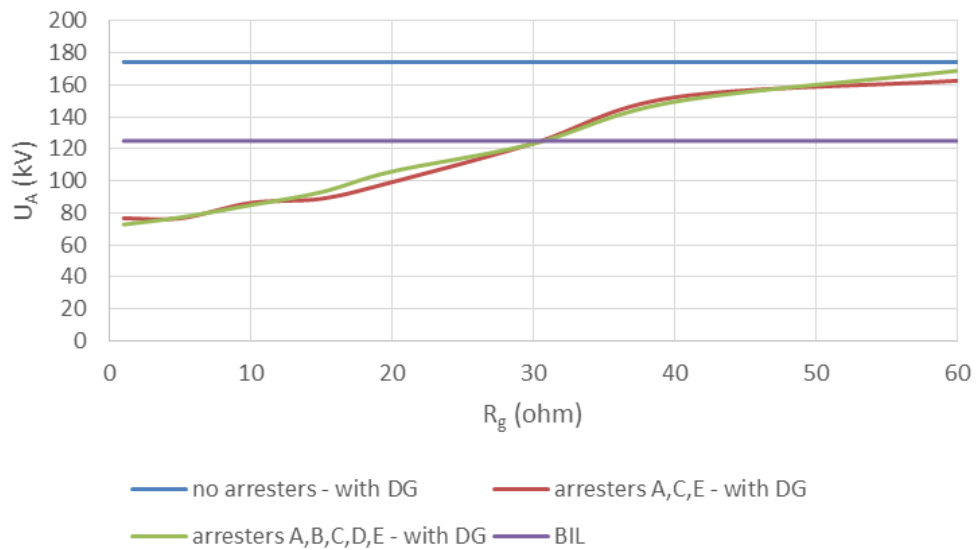


Figure 5.38: Developed overvoltage at position A, for lightning hit at position A, in relation to grounding resistance for DG sizes 500 kW - 1 MW - 500 kW.

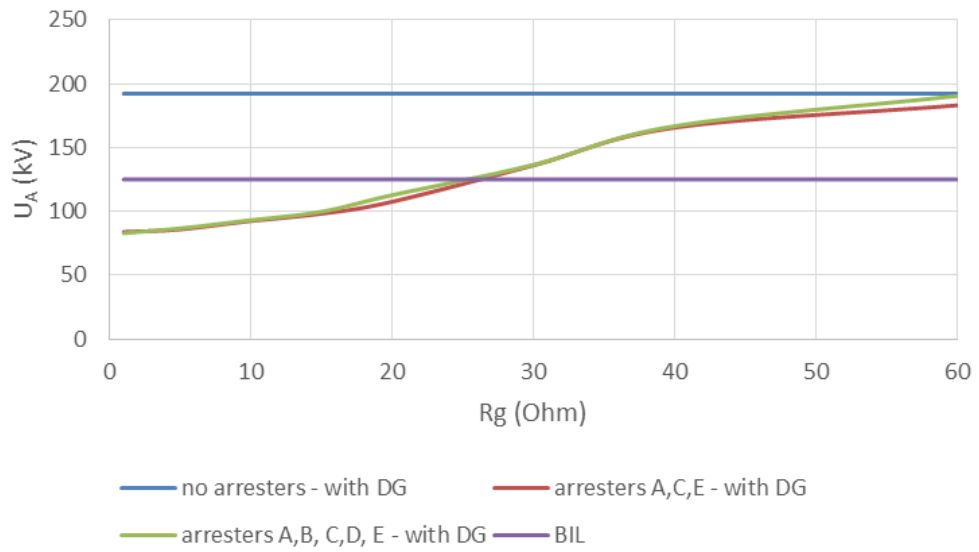


Figure 5.39: Developed overvoltage at position A, for lightning hit at position A, in relation to grounding resistance for DG sizes 1 MW - 500 kW - 1 MW.

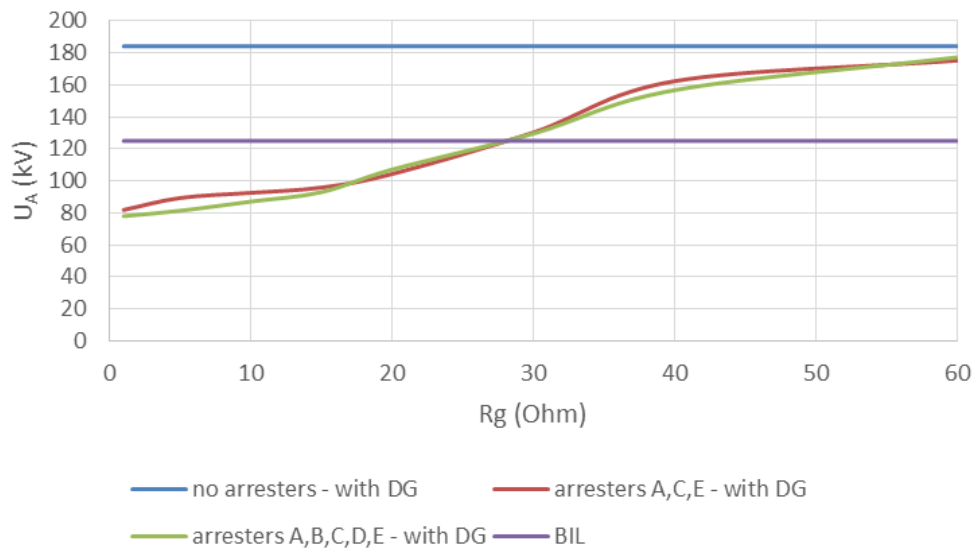


Figure 5.40: Developed overvoltage at position A, for lightning hit at position A, in relation to grounding resistance for DG sizes 1 MW - 1 MW - 1 MW.

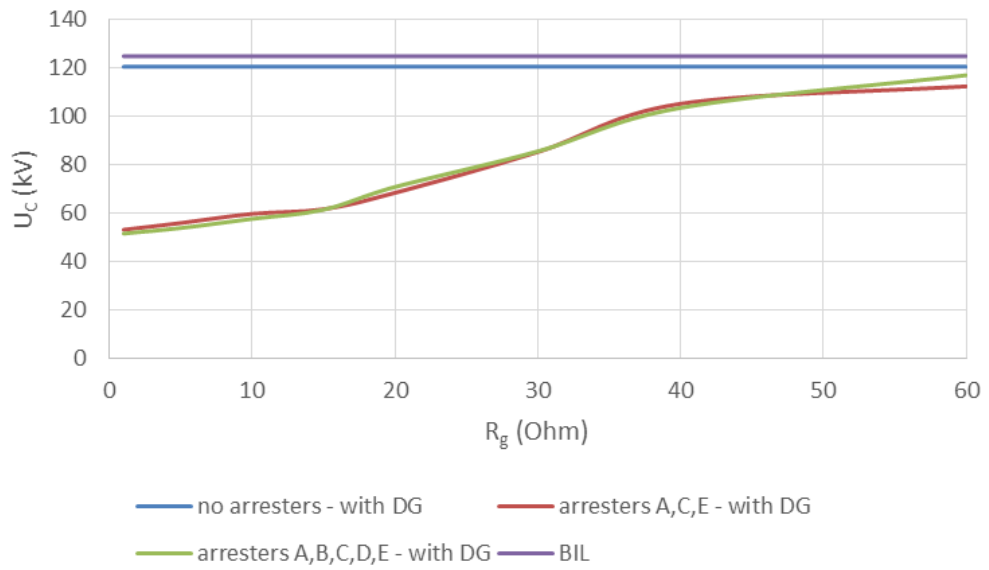


Figure 5.41: Developed overvoltage at position C, for lightning hit at position A, in relation to grounding resistance for DG sizes 500 kW - 500 kW - 500 kW.

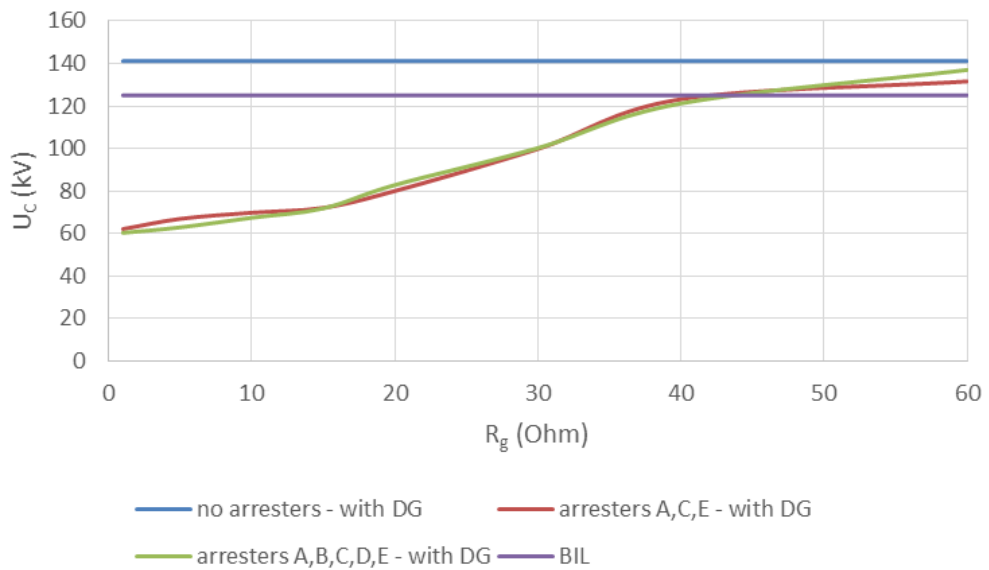


Figure 5.42: Developed overvoltage at position C, for lightning hit at position A, in relation to grounding resistance for DG sizes 500 kW - 1 MW - 500 kW.

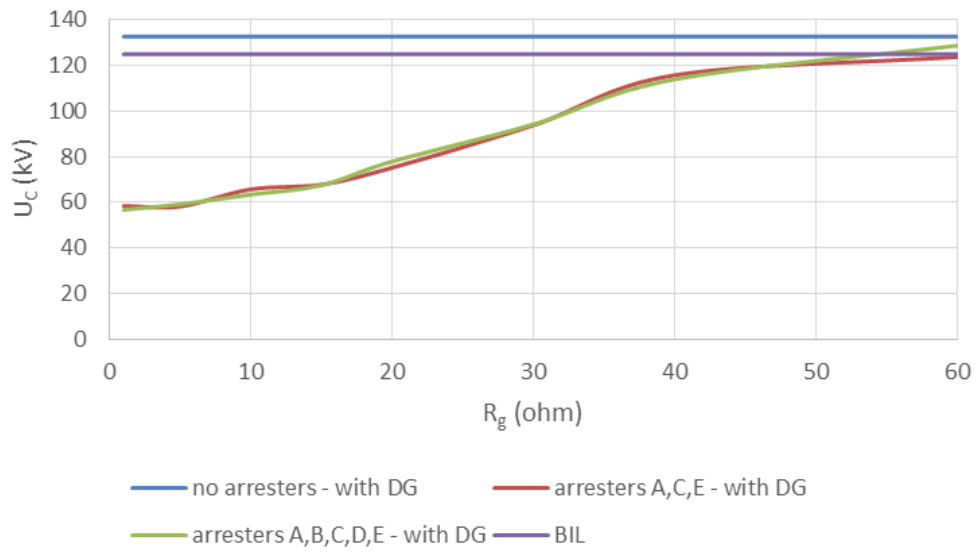


Figure 5.43: Developed overvoltage at position C, for lightning hit at position A, in relation to grounding resistance for DG sizes 1 MW - 500 kW - 1 MW.

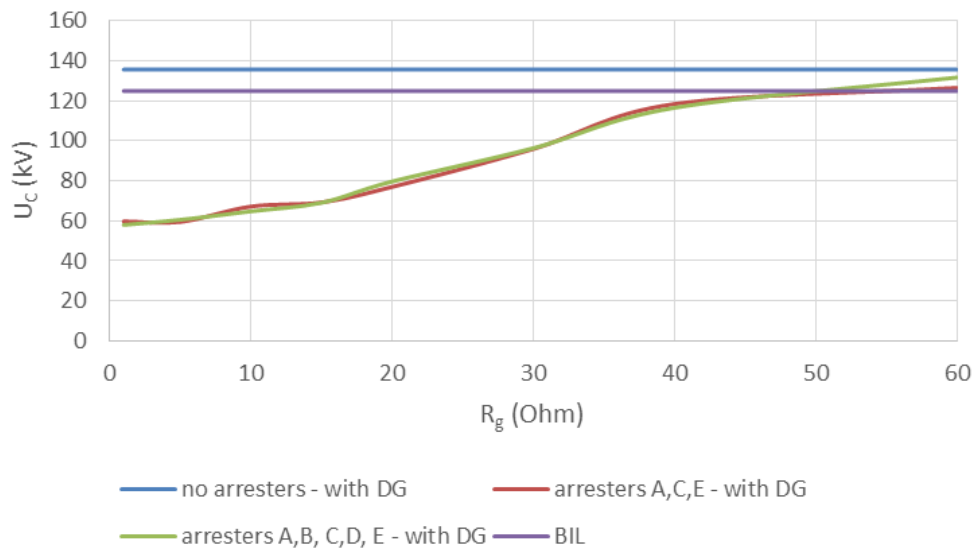


Figure 5.44: Developed overvoltage at position C, for lightning hit at position A, in relation to grounding resistance for DG sizes 1 MW - 1 MW - 1 MW.

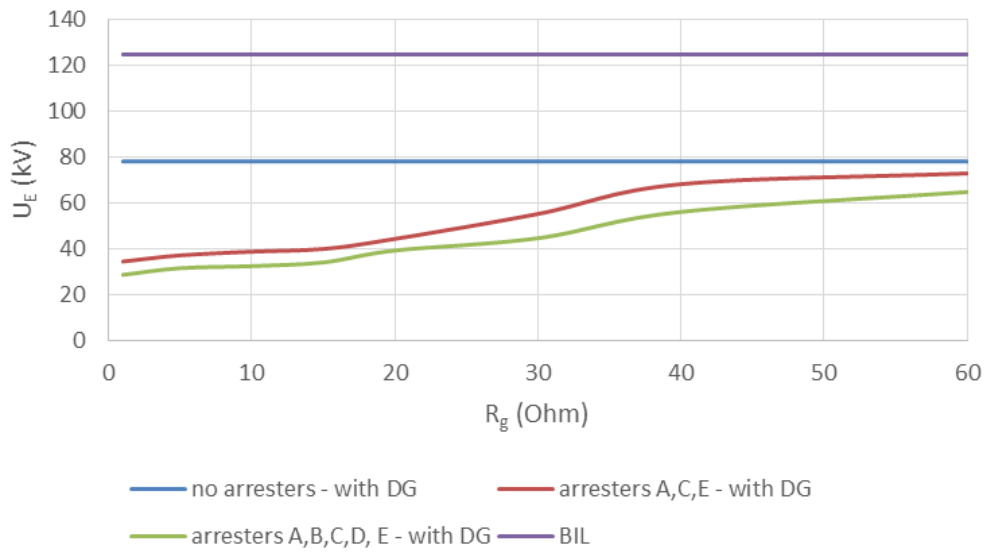


Figure 5.45: Developed overvoltage at position E, for lightning hit at position A, in relation to grounding resistance for DG sizes 500 kW - 500 kW - 500 kW.

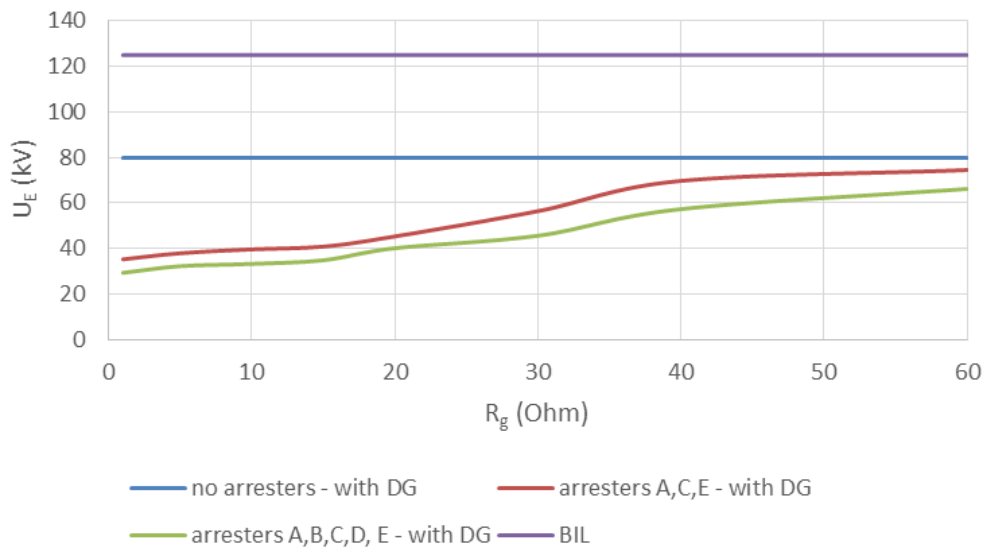


Figure 5.46: Developed overvoltage at position E, for lightning hit at position A, in relation to grounding resistance for DG sizes 500 kW - 1 MW - 500 kW.

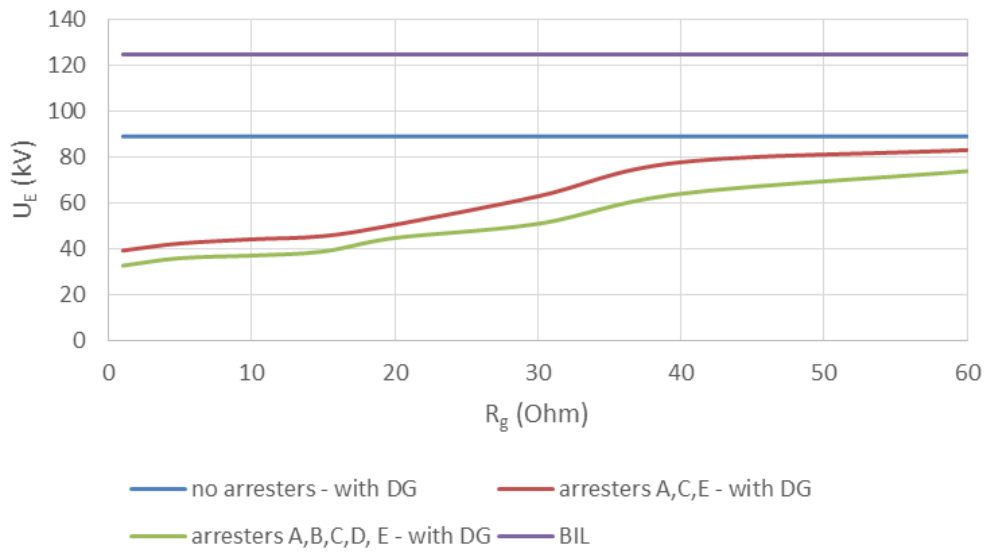


Figure 5.47: Developed overvoltage at position E, for lightning hit at position A, in relation to grounding resistance for DG sizes 1 MW - 500 kW - 1 MW.

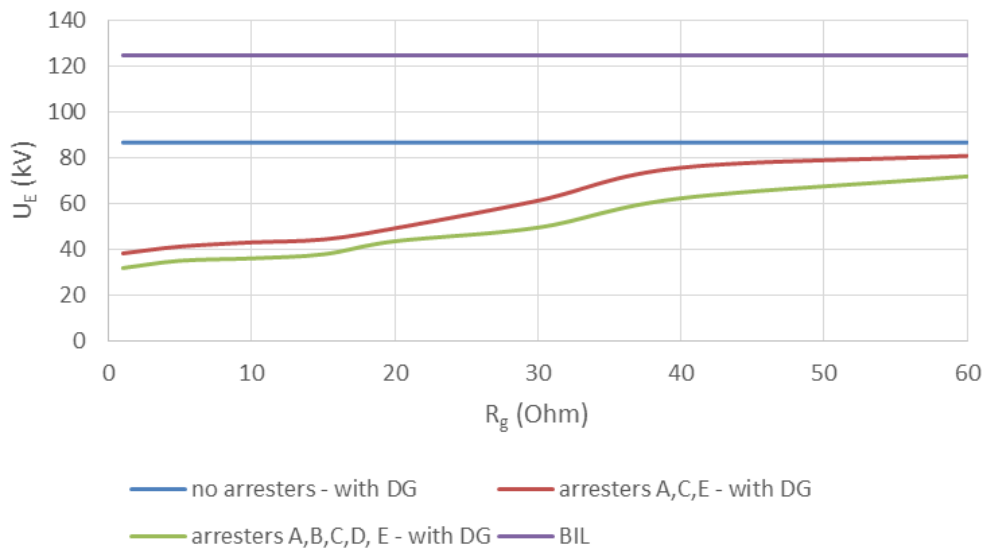


Figure 5.48: Developed overvoltage at position E, for lightning hit at position A, in relation to grounding resistance for DG sizes 1 MW - 1 MW - 1 MW.

The obtained results have shown that the different sizes of the DG units connected with the distribution network produce different overvoltages at different positions of the network that are proportional related to the size of the DG units. The higher the size of the DG, results in higher overvoltages that are abridged as the distance from the lightning hit increases. Moreover, it has been proven that low ground resistance quantities can result in the limitation of produced overvoltages, therefore special attention must be paid while designing a grounding system, since it is the most effective measure for modern distribution networks' lightning protection. Furthermore, it has been presented, that the presence of DGs in distribution networks demonstrates a significant impact in existing lightning protection systems. Thus, novel lightning protection schemes have to be applied, taking into consideration the constant and rising installation of DGs, in the effort to minimize or even eliminate the produced overvoltages caused by lightning strikes which in turn lead to unexpected faults and undesired power supply interruptions.

5.5 Conclusions

In this chapter sensitivity analyses conducted on a distribution network with or without distributed generation (DG) units of different sizes have been presented, in order to study the impact of DGs to lightning protection schemes of modern distribution networks. In all the above studies, real data from a typical distribution line were used. Factors that influence significantly the efficiency of the protection systems towards the developed overvoltages such as: the installation of surge arresters, the surge arresters' installation position, the distribution line's grounding resistance, the lightning current peak magnitude, the position of lightning strike hit, different models of surge arresters and different DG sizes were examined in the conducted analyses. The obtained results can be very useful in electric utilities' design and to researchers in an effort to upgrade/modify the existing lightning protection processes and systems so as to adapt and accommodate the presence of distributed generation.

5.6 References

- [1] IEEE Std 1410-2010, IEEE Guide for improving the lightning performance of electric power overhead distribution lines, 2011.
- [2] Han J, Seo HC, Kim CH, Analysis of lightning overvoltage according to the location of overhead ground wire in Korea distribution system, 2012 IEEE Vehicle Power and Propulsion Conference (VPPC), Seoul, Korea, pp. 1274-1276, 2012.
- [3] Piantini A, Janiszewski JM, The effectiveness of shield wires in reducing induced voltages from lightning electromagnetic fields, 7th Asia-Pacific International Conference on Lightning (APL), pp. 666-672, Chengdu, China, 2011.
- [4] Supanus K, Thansiphraerth W, Rugthaicharoencheep N, Phayomhom A, External grounding design to reduce effects of lightning damage in distribution system, 7th IET International Conference on Power Electronics, Machines and Drives (PEMD 2014), Manchester, United Kingdom, 2014.
- [5] Bhattarai R, Harid N, Griffiths H, Haddad A. Application of surge arresters for lightning protection of 33kV wood pole distribution lines, 20th International Conference and Exhibition on Electricity Distribution, Prague, Czech Republic, Paper 0947, 2009.
- [6] Thanasaksiri T, Improving the lightning performance of overhead distribution lines, IEEE Region 10 Conference TENCON 2004, vol. 3, pp. 369-372, 2004.
- [7] Cabral RJ, Gazzana DS, Leborgne RC, Bretas AS, Dias GAD, Tello M, Analysis of distribution lines performance against lightning using ATP-EMTP, International Symposium on Electromagnetic Compatibility (EMC EUROPE), Rome, Italy, 2012.
- [8] Montanes L, Garcia-Gracia M, Sanz M, Garcia MA, An improvement for the selection of surge arresters based on the evaluation of the failure probability, IEEE Transactions on Power Delivery, vol. 17, no. 1, pp. 123-128, 2002.
- [9] Mikropoulos PN, Tsovilis TE, Statistical method for the evaluation of the lightning performance of overhead distribution lines, IEEE Transactions on Dielectrics and Electrical Insulation, vol. 20, no. 1, pp. 202-211, 2013.

- [10] Busrah AM, Mohamad M, The studies of the line-lightning performance of unshielded distribution lines, International Conference on Electrical, Control and Computer Engineering (INECCE), Pahang, Malaysia, pp. 55-59, 2011.
- [11] Jacob PB, Grzybowski S, Ross ER, An estimation of lightning insulation level of overhead distribution lines, IEEE Transactions on Power Delivery, vol. 6, no. 1, pp. 384-390, 1991.
- [12] Araujo MA, Flauzino RA, Batista OE, Moraes LA, Martins CHR, Protection of the distribution lines with distributed generation against lightning overvoltages in the context of smart grids, 2013 World Congress on Sustainable Technologies (WCST), London, United Kingdom, pp. 36-41, 2013.
- [13] Marti JR, Accurate modeling of frequency-dependent transmission lines in electromagnetic transient simulation, IEEE Transactions on Power Apparatus and Systems, vol. PAS-101, no. 1, pp.147-155, 1982.
- [14] Dommel H, Digital computer solution of electromagnetic transients in single and multiple networks, IEEE Transactions on Power Apparatus and Systems, vol. PAS-88, no. 4, pp. 388-389, 1969.
- [15] IEC 60099-4, Surge Arresters: Part 4: Metal-Oxide surge arresters without gaps for a.c. systems, 2nd edition, 2004-2005.
- [16] Vita V, Mitropoulou AD, Ekonomou L, Panetsos S, Stathopoulos IA, Comparison of metal oxide surge arresters circuit models and implementation on high voltage transmission lines of the Hellenic network, IET Generation, Transmission and Distribution, vol. 4, no. 7, pp. 846-853, 2010.
- [17] Christodoulou CA, Ekonomou L, Mitropoulou AD, Vita V, Stathopoulos IA, Surge arresters' circuit models review and their application to a Hellenic 150 kV transmission line, Simulation Modelling Practice and Theory, vol. 18, no. 6, pp. 836-849, 2010.
- [18] Žitnik B, Žitnik M, Babuder M, The ability of different simulation models to describe the behavior of metal oxide varistors, 28th International Conference on Lightning Protection, Kazanaqa, Japan, pp. 1111-1116, 2006.
- [19] Goedde GL, Kojovic LA, Woodworth JJ, Surge arrester characteristics that provide reliable overvoltage protection in distribution and low voltage systems,

- IEEE Power Engineering Society Summer Meeting, vol. 4, pp. 2375-2380, 2000.
- [20] Christodoulou CA, Ekonomou L, Fotis GP, Karampelas P, Stathopoulos IA, Parameters' optimisation for surge arrester circuit models, IET Science, Measurement and Technology, vol. 4, no. 2, pp. 86-92, 2010.
- [21] IEEE Working Group 3.4.11, Modeling of metal oxide surge arresters, IEEE Transactions on Power Delivery, vol. 7, no. 1, pp. 302-309, 1992.
- [22] Pinceti P, Giannettoni M, A simplified model for zinc oxide surge arresters, IEEE Trans on Power Delivery, vol. 14, no. 2, pp. 393-398, 1999.
- [23] Fernandez F, Diaz R, Metal oxide surge arrester model for fast transient simulations, International Conference on Power System Transients (IPAT'01), Rio De Janeiro, Brazil, Paper 14, 2001.

Chapter 6

Conclusions

6.1 Conclusions

The increasing demand for electric power and the necessity for more efficient and environmental friendly electric power generation resulted in the development of distributed generation (DG) units, using several technologies, and their installation into the electric power systems. The integration of these small scale generation units, which mainly use renewable energy resources, into the traditional and existing electric power system affected primarily the distribution network, since the majority of DG units is coupled close to the load centres. All the above resulted in reassessment and change in: the philosophy, the traditional configuration and the operation of the networks (e.g., bidirectional power flow in contrast to the unidirectional power flow from higher to lower voltage levels) leading in turn to potentially considerable challenges in terms of control, security and protection of the entire electric power system and especially of distribution networks. Additionally, all the above new facts combined with continual modifications of distribution networks brought about a series of other significant problems that must be addressed and further studied in order consumers to continue to be well provisioned with uninterrupted power supply of high quality and at the minimum cost.

The present PhD Thesis contributes in the research conducted worldwide aiming for more efficient and secure electric power systems, focusing on the modern electricity distribution networks with particular references to distributed generation and protection. All through the Thesis, the impact of DG on voltage profiles and power losses in distribution networks is analysed, the decision problem of the optimum size and placement of new DGs in existing distribution networks is studied, while protection related issues were studied, such as: the real-time syntactic pattern recognition of power

system waveforms applied on protective relays and the lightning protection of distribution networks with DGs.

Within the current PhD Thesis the later described structure has been followed. Firstly, the arrangement of electric power systems, the electricity distribution networks and the concept of DG have been presented. The issues and problems that have risen from the installation of DG in existing distribution networks have been examined. Then studies have been conducted on distribution networks in order to identify the impact of DG in voltage profiles and real and reactive power losses, providing very useful inferences and observations relevant to the placement, sizing and type of the interconnected DG. A decision making algorithm has been proposed for the optimum size and placement of DG in existing distribution networks. Following, a novel approach has been presented, designed for tracing power systems signals in a more efficient way that are then applied on protective relays. A hardware implementation for the real-time syntactic pattern recognition of power system waveforms has been executed. Finally, several sensitivity studies were conducted taking into account many crucial parameters that affect vitally the lightning performance of distribution networks in an effort to assist in a more efficient lightning protection of modern distribution networks (connected with DG).

6.2 Contribution

The contribution of the present PhD Thesis are hereupon summarized:

- **A contribution to the improvement of distribution networks' voltage profiles linked with different types of distributed generation has been conducted.**

Thorough studies have been conducted on typical distribution networks (both of network and radial configurations) interconnected with DGs of different types and sizes. Voltage profiles before and after the installation of a DG have been evaluated and useful observations as well as deductions have been extracted that will contribute considerably in the development and design of modern electric power systems.

- **A contribution to the reduction of both real and reactive power losses of distribution networks with different types of distributed generation has been conducted.**

Studies have been conducted on typical distribution networks (both of network and radial configurations) linked with DGs of different types and sizes. The total real and reactive power losses of the network have been calculated and measured and any reduction of losses associated with the installation of DG has been analyzed. Useful observations and deductions have been extracted that will contribute in the development and the design of modern electric power systems.

- **A decision making algorithm for the optimum size and placement of DG in distribution networks has been developed.**

A relative simple decision making algorithm has been proposed that indicates the optimum size and position for a new DG unit to be implemented within an existing distribution network. The algorithm that is implemented in MATLAB and uses NEPLAN power systems software for load flow analysis, is mainly influenced by the improvement in voltage profiles and the reduction of real and reactive power losses.

- **A linguistic representation of power system waveforms has been defined.**

The application of the syntactic methods for the detection and analysis of power system signals and for measuring its parameters is thoroughly examined. Peak has been chosen as primitive pattern because power system signal are mainly sinusoidal. This pattern is that part of a signal which is demarcated by three characteristic points. The first point is called left peak boundary, the second peak extremum, and the third right peak boundary. The left arm of the peak is consisted of all points among the left peak boundary and the peak extremum. The right arm of the peak is consisted of all points among the peak extremum and the right peak boundary. The alphabet of terminal symbols has been selected for modelling the power system waveforms, where p represents a positive peak and n a negative peak. Thus, a string of symbols such as pnpnpn or npnpnp denotes a power system waveform.

- **An attribute grammar capable of modelling power system waveforms has been presented**

Each sample point of a power system signal is presented as a couple (x_i, y_i) , where y_i is the amplitude in volts or amperes of the sample point i and x_i is the corresponding time. A set of attributes is assigned to each primitive pattern. The values of these attributes are calculated during the primitive extraction phase and they are utilized during the recognition process. They contribute both to the recognition of the patterns and to the measurement of their parameters. That is, they are used in a quantitative way for qualitative and quantitative purposes. A set of seven attributes is assigned to each peak.

- **An attribute grammar evaluator based on a parallel parsing algorithm has been designed.**

The proposed attribute grammar evaluator is based upon the methodology presented in a previous study that is capable to achieve the requested performance. Having chosen this system, certain modifications had to be made into the direction of converting it to a suitable parser for the specific application. The main modifications imposed on the parser were focused on the two following tasks: a) extending it in order to recognize the presented grammar AG_{PSW} and b) modifying the architecture so as to cope with such long input strings in real-time.

- **A system for the real-time syntactic pattern recognition of power system waveforms has been implemented on a FPGA reconfigurable board designed to be applied on a protective relay.**

In the case of power systems, large time-series of input data are created due to the high sampling frequency. For example, when the scanning frequency is set to 800 Hz, a new sample is created every 1.25 ms leading to 48,000 samples per second. Given that the frequency of power system signals is 50 Hz (or 60 Hz in some countries), a unique peak is represented every 8 samples and a full period every 16 samples ($800/50$). Consequently, 6,000 sets of 8 samples that each describes a unique peak are created every second. Since every peak is described by a terminal symbol n or p , a powerful parser is needed able to recognize input strings of length 6,000 per second. The proposed system, described in Verilog hardware description language (HDL),

simulated for validation, synthesized and tested on an XILINX FPGA board, is capable to achieve such a performance.

- **The influence of distributed generation in the lightning performance of distribution networks has been analyzed.**

Several studies on the lightning performance of distribution networks with DG coupled have been conducted. The influence of DG in the efficiency of the current protection schemes (e.g., usage of surge arresters) has been acknowledged. Useful remarks and deductions have been extracted, which will significantly assist the challenging task of electric utilities design engineers to preserve the effective lightning protection of distribution networks.

- **Sensitivity analyses of significant parameters affecting the lightning performance of distribution networks, such as grounding resistance, lightning current peak magnitude, position of lightning strike hit, different models of surge arresters and different DG sizes, have been conducted.**

Several extensive sensitivity analyses on the factors that affect the lightning performance of distribution networks with DG coupled have been conducted. From the sensitivity analyses valuable interpretations and deductions have been extracted and attention should be driven upon those conclusions for the design and implementation of a novel distribution system's lightning protection scheme.

6.3 Further Work

Further work of the current PhD Thesis could be the following:

- a) The study of the impact of several network types containing transmission and distribution lines, as well as the study of the impact of different types (e.g., DGs that inject both real and reactive power) and sizes of DG in the improvement of voltage profiles and limitation of real and reactive power losses. Furthermore, the implementation of the developed decision making algorithm for the optimum size and placement of DG units in several distribution networks in

order to evaluate its performance and effectiveness. Finally, the decision making algorithm could be further developed in order to be capable to allocate simultaneously two or even more DG units of different type and size and even be combined with an existing optimization algorithm and/or with a load flow estimation methodology.

- b) The Context Free Grammar formalism can be further extended by adding inexactness to each of the production rules. Some of the most famous inexact models are the probabilistic, the certainty, the possibility-necessity and the fuzzy model. Future work could be the extension of the proposed grammar AG_{PSW} with the probabilistic model and thus forming a Stochastic Context Free Grammar (SCFG). For each non-terminal symbol, a probability will be placed on the set of productions for that symbol. Hence, a rule with probability p is written as $A \rightarrow \gamma [p]$, meaning that p is the probability that the specific production rule is chosen. The addition of probabilities would increase the expressive power of the proposed grammar permitting the evaluation of more useful parameters of the examined waveform.
- c) The sensitivity analyses that have been conducted for the examination of the lightning performance of distribution networks with DG coupled can be further analyzed by taking additional types and parameters under consideration such as: shielded networks, backflashovers, induced overvoltages, different lightning waveforms and insulation levels, etc. The outcomes of these sensitivity analyses could be coded with the help of a user friendly software tool in order to assist the work of electric utilities design engineers for the design of efficient lightning protection schemes for modern distribution networks. Distribution networks are expected to expand immensely in the subsequent years due to the increasing number of DG units installations.